ANL-96/11

ANL Technical Support Program for DOE Office of Environmental Management

Annual Report October 1994–September 1995

by J. K. Bates, E. C. Buck, N. L. Dietz, T. DiSanto, W. L. Ebert, J. W. Emery, J. A. Fortner, L. D. Hafenrichter, J. C. Hoh, J. S. Luo, L. Nuñez, M. T. Surchik, S. F. Wolf, and D. J. Wronkiewicz

Argonne National Laboratory, Argonne, Illinois 60439
operated by The University of Chicago
for the United States Department of Energy under Contract W-31-109-Eng-38

Reproduced from the best available copy.

Available to DOE and DOE contractors from the
Office of Scientific and Technical Information
P.O. Box 62
Oak Ridge, TN 37831
Prices available from (423) 576-8401

Available to the public from the
National Technical Information Service
U.S. Department of Commerce
5285 Port Royal Road
Springfield, VA 22161

Distribution Category:
High-Level Radioactive Waste
Disposal in Tuff
(UC-814)

ANL-96/11

ARGONNE NATIONAL LABORATORY
9700 South Cass Avenue
Argonne, Illinois 60439

ANL TECHNICAL SUPPORT PROGRAM FOR DOE OFFICE OF ENVIRONMENTAL MANAGEMENT

ANNUAL REPORT OCTOBER 1994 - SEPTEMBER 1995

by

J. K. Bates, E. C. Buck, N. L. Dietz, T. DiSanto,
W. L. Ebert, J. W. Emery, J. A. Fortner,
L. D. Hafenrichter, J. C. Hoh, J. S. Luo, L. Nuñez,
M. T. Surchik, S. F. Wolf, and D. J. Wronkiewicz

Chemical Technology Division

July 1996

TABLE OF CONTENTS

TABLE OF CONTENTS (contd)

TABLE OF CONTENTS (contd)

LIST OF FIGURES

LIST OF FIGURES (contd)

LIST OF FIGURES (contd)

LIST OF FIGURES (contd)

LIST OF TABLES

LIST OF TABLES (contd)

This page intentionally left blank.

ANL TECHNICAL SUPPORT PROGRAM FOR DOE OFFICE OF ENVIRONMENTAL MANAGEMENT

ANNUAL REPORT OCTOBER 1994 - SEPTEMBER 1995

by

J. K. Bates, E. C. Buck, N. L. Dietz, T. DiSanto,
W. L. Ebert, J. W. Emery, J. A. Fortner,
L. D. Hafenrichter, J. C. Hoh, J. S. Luo, L. Nuñez,
M. T. Surchik, S. F. Wolf, and D. J. Wronkiewicz

ABSTRACT

A program was established for the DOE Office of Environmental Management (EM) to evaluate factors that are anticipated to affect waste glass reaction during repository disposal, especially in an unsaturated environment typical of what may be expected for the proposed Yucca Mountain repository site. This report covers progress in FY 1995 on the following tasks:

1. Tests are ongoing to evaluate and compare the reactivity of fully radioactive glasses with that of glasses having the same compositions except for the absence of radionuclides under conditions representative of a high-level waste repository environment. Data from these tests will be used to evaluate the effect of radionuclides on the glass corrosion behavior and to determine the disposition of the radionuclides as the glass corrodes. Static dissolution tests and unsaturated tests are being conducted with several Defense Waste Processing Facility (DWPF) and West Valley Demonstration Project (WVDP) glasses.

2. A series of static dissolution tests is being performed to compare the corrosion behavior of nuclear waste glasses made with SRL 131 and SRL 202 frits at different S/V ratios. The S/V ratio affects the extent to which dissolved glass species are diluted; the solution chemistry then affects continued glass dissolution. The solutions generated in tests at high S/V ratios are conducive to the formation of alteration phases that may be deleterious to the glass. After long time periods, the glass dissolution rates of both glasses increase coincidentally with the formation of analcime and other alteration phases. However, the release of radionuclides from the glasses into solution is controlled by their individual solubilities.

3. A series of static dissolution tests is being performed with West Valley Reference 6 (WV6) glass under conditions previously shown to promote the formation of alteration phases during the corrosion of other glasses. These tests are being conducted to characterize the corrosion behavior of the WV6 glass and to support the design of a

test matrix to be used for evaluating the corrosion behavior of the fully radioactive West Valley reference glass (WVSG 2) that will be tested at Argonne National Laboratory (ANL) in the future. Vapor hydration tests conducted at 200°C show WV6 glass to be unstable with respect to an assemblage of alteration phases. However, the WV6 glass dissolves slowly in dissolution tests conducted at 90°C, and alteration phases have not formed through 600 days.

4. A series of static dissolution tests is being conducted with the Environmental Assessment (EA) glass to characterize its corrosion behavior. This glass will be used as a benchmark for the consistency of waste glasses to be produced at the DWPF. The results of these tests will address the following question: if a glass performs better than the EA glass in a 7-day PCT, does that result indicate that the long-term performance of the glass will also exceed that of the EA glass? In addition, these tests permit direct comparison of the measured long-term corrosion behavior of the EA glass and of other waste glasses.

5. Vapor hydration tests are being conducted at several temperatures with the EA glass to determine the corrosion rate and identify alteration phases. Reacted samples are being examined with electron microscopy and diffraction methods.

6. Tests with the actinide-doped West Valley glass ATM-10 have been in progress for over seven years as a part of work for the Yucca Mountain Site Characterization Project. During the first year of testing, eight tests were terminated, but the glass and metal components of the tests were never analyzed, so solution and component analyses could not be fully correlated. We have analyzed the glasses from these tests and found that the actinide-bearing phase, brockite, which was previously found in solution, actually forms as part of the reacted glass.

7. Synthetic basalt and waste glasses that have reacted with water vapor for up to nine years are being examined and compared with naturally reacted Hawaiian basalt to determine whether laboratory test methods can be used to reproduce the long-term corrosion of glass. The reacted glasses are being examined with electron microscopy.

8. Analytical electron microscopy (AEM) is being used to characterize the reacted glass surface and identify alteration phases formed during glass corrosion. Colloids filtered from test solutions are also being examined with AEM.

9. Critical Reviews of important parameters that affect the reactivity of glass in an unsaturated environment are being prepared. A Critical Review was published this year on the effect of glass surface area-to-liquid volume (S/V) ratio on glass reaction. Critical reviews of glass weathering in unsaturated environments and the use of natural analogues are being prepared. Data Reports are also being prepared to cover the experimental work ongoing in the program.

EXECUTIVE SUMMARY

This report is an overview of the progress during FY 1995 for the High-Level Nuclear Waste Technical Support Program that is part of the ANL Technology Support Activity for the DOE Office of Environmental Management (EM). The purpose is to evaluate, before hot start-up of the Defense Waste Processing Facility (DWPF) and the West Valley Demonstration Project (WVDP), factors that are anticipated to affect glass reaction in an unsaturated environment typical of what may be expected for the candidate Yucca Mountain repository site. Specific goals for the testing program include the following:

- reviewing and evaluating available data on parameters that will be important in establishing the long-term performance of glass in a repository environment,
- performing tests to further quantify the effects of important variables where there are deficiencies in the available data, and
- initiating long-term tests to determine glass performance under a range of conditions applicable to repository disposal.

The progress made in FY 1995 on each of the technical tasks is summarized below.

Long-Term Testing of Fully Radioactive Glass

Three types of tests are ongoing to evaluate the long-term behavior of glass made from tank sludge from the Defense Waste Processing Facility (DWPF). These include (1) dissolution tests done under static conditions and a range of surface area-to-volume (S/V) ratios with various SRL compositions, (2) drip tests done with as-cast glass and with glass aged by reaction with water vapor, and (3) laboratory analogue tests wherein the glass is encased in a tuff core to closely simulate reactions that may occur in an unsaturated environment.

Static dissolution tests are being conducted to compare the reactivity of radioactive glasses and glasses having the same composition except without the radionuclides. Radioactive glasses made at the Savannah River Technology Center (SRTC) with actual tank wastes and SRL 131, SRL 165, and SRL 200 frits and their nonradioactive counterparts are being reacted in a tuff groundwater solution at 90°C and at S/V ratios of 340, 2000, and 20,000 m^{-1}. Tests have been in progress for about five years.

Similar tests are being conducted with a radioactive glass made at SRTC with Tank 51 sludge and a nonradioactive glass at S/V ratios of 2000 and 20,000 m^{-1}. These tests were started this year. The corrosion behavior of both the radioactive and nonradioactive glasses observed so far is similar to that of other DWPF glasses.

Drip tests with as-cast and vapor-hydrated SRL 200R glass have been in progress for more than four years. In tests conducted with as-cast glass, a reactive layer has formed on the glass surface that spalls from the glass as the water flows over the glass surface. The layer is mainly clay that contains transuranic elements. In the tests performed with vapor-hydrated glass, the release of anions is initially fast but decreases with time. Likewise, the release of Li and B is initially fast but decreases to a nearly constant rate. A fibrous white alteration product is forming on the glass and metal components of the test. This phase is likely a calcium silicate mineral.

The laboratory analogue tests have been in progress for over four years. The tests are working as expected, in that water is passing through the cores, and no radioelements have been detected with gross counting methods, although more extensive analysis of the condensed solution

will be needed to confirm this preliminary result. The tests will continue, with periodic monitoring of the effluent, and the solutions will be subjected to extensive analysis.

Relationship between High S/V Experiments and MCC-1

A series of static dissolution tests is being performed to compare the corrosion behavior of nuclear waste glasses at different S/V ratios. Glasses made by doping SRL 131 and SRL 202 frits with radionuclides were reacted with tuff groundwater at 90°C at S/V ratios of 10, 340, 2000, and 20,000 m^{-1} for up to five years. The S/V ratio affects the extent to which dissolved glass species are diluted; the solution chemistry then affects continued glass dissolution. The solutions generated in tests at high S/V ratios were conducive to the formation of alteration phases that were deleterious to the glass. After long time periods, the glass dissolution rates of both glasses increased coincidentally with the formation of analcime and other alteration phases. However, the release of radionuclides from the glasses into solution was controlled by their individual solubilities. Glass dissolution results in a decrease in the surface area available for reaction as the test proceeds, which complicates the calculation of the dissolution rate. A simple method for adjusting the measured rates to take into account the decrease in the surface area is being devised.

Laboratory Testing of West Valley Reference 6 Glass

A laboratory testing program was initiated to characterize the corrosion behavior of a nonradioactive homologue of the high-level waste glasses to be produced by the West Valley Demonstration Project (WVDP). Tests are being conducted according to the MCC-1, Product Consistency Test (PCT), and vapor hydration test protocols to measure the corrosion rates under various conditions. The MCC-1 and PCT tests indicate that the WV6 glass is a relatively durable high-level waste glass, compared to other reference glasses. Dissolution is measurably affected by the level of silicon in the leachant groundwater, which is about 46 mg/L, and the dissolution rate is low in all MCC-1 and PCT tests. In vapor hydration tests, several alteration phases are shown to form as the glass corrodes, and the formation of certain phases increases the glass dissolution rate. However, such phases have not yet formed in PCT tests in progress for about two years.

Static Dissolution Tests with SRL EA Glass

Static dissolution tests are being conducted with the DWPF Environmental Assessment (EA) glass to characterize its long-term corrosion behavior. Tests are being conducted at 90°C and at S/V values of 2000 and 20,000 m^{-1}. These tests will allow the behavior of the EA glass to be compared to the behavior of other glasses reacted under the same conditions. These tests show that corrosion of the EA glass results in the formation of smectite clay and several precipitated alteration phases after only a few weeks. Various zeolite and calcium-silicate phases have been identified. Similar phases form in tests with other glasses. The dissolution rate of EA glass increases significantly when these phases form.

Vapor Hydration Testing with SRL EA Glass

Vapor hydration tests are being conducted with the EA glass at several temperatures to measure the corrosion rate and to identify alteration phases that are formed. Reacted samples are being examined with optical and electron microscopy. Alteration phases, including analcime and calcium-silicates, formed after short reaction times in tests conducted at elevated temperatures (>90°C). The similarity of the alteration phases formed in vapor hydration and PCT tests indicates that the same reaction mechanism is operative in both tests. In tests at 70°C, a layer of smectite clay was observed to form on the glass surface, but no precipitated alteration phases were found through 91 days of reaction.

Components from Drip Tests with ATM-10 Glass

Components of actinide-doped West Valley ATM-10 reference glass and sensitized 304L stainless steel were reacted with liquid groundwater using the Unsaturated Test Method. Surface corrosion and reaction products, resulting from tests of up to one year on these components, were analyzed. These tests, initiated in 1987 and still ongoing for several other samples, were designed to determine the suitability of glass waste forms for the proposed high-level repository at the Yucca Mountain Site. While elemental release rates to solution have been reported for these tests, an analysis of reaction products and surface corrosion of the waste form components is important for a more complete understanding of reaction mechanisms and dynamics. Together, these data will provide constraints on long-term geochemical modeling of waste form performance in the repository.

Mechanistic Validation through Natural Analogues

Ten naturally reacted basaltic glasses collected from Hawaii have been characterized by using scanning electron microscopy with energy dispersive X-ray spectroscopy (SEM/EDS) and analytical electron microscopy (AEM). A layer consisting of an amorphous gel phase plus a small amount of clay was present on the surface of all the glasses. The nature of corrosion seems to depend strongly on the local environmental conditions to which the glass has been exposed. Consequently, the time dependence of alteration (i.e., the reaction kinetics) could not be well established by measuring the thickness of alteration rims, because of the limited knowledge of the likely natural environments for waste disposal and because the alteration layers may have spalled during the course of alteration.

Thirteen long-term tests with synthetic basalt and simulated waste glasses were terminated during FY 1995. These tests had been ongoing in water vapor at 75°C for the past seven to nine years. The reacted glasses are being examined, and the results will be compared with those from naturally altered glasses. These studies will be used to evaluate the applicability of laboratory test methods in reproducing the long-term reaction of waste glasses.

Analytical Electron Microscopy Support

The surfaces of glasses reacted in tests in other Tasks have been studied by using AEM. These characterization studies provide information that advances our understanding of glass reaction and that may be used in performance assessment models. This year, analysis of samples from the Long-Term Testing of Fully Radioactive Glass, Relationship between High S/V Experiments and MCC-1, Dissolution Tests with SRL EA Glass, and Laboratory Testing of West Valley Reference 6 Glass Tasks continued.

Research highlights this year include the detection of transuranic elements in alteration phases and the development of techniques to obtain chemical state data from rare earth elements. These advances have been of interest to the Nuclear Waste Management Section of ANL and the electron microscopy community in general.

Critical Review of Parameters Affecting Glass Reaction in an Unsaturated Environment

The repository environment at Yucca Mountain has been predicted by the Yucca Mountain Site Characterization Project (YMP) to be hydrologically unsaturated and to have possible air exchange with the neighboring biospheres. We have identified several environmental conditions that can affect the durability of waste emplaced in such an unsaturated environment over repository-relevant time periods. To date, much of the information regarding what is known about these conditions has not been compiled for use within the waste glass research community. While the document *High-Level Waste Borosilicate Glass: A Compendium of Corrosion Characteristics*

discusses some of the effects of unsaturated conditions on glass performance, we identified the need for a critical review of important parameters that would affect the reactivity of glass in an unsaturated environment. This task is currently underway.

The Critical Review reports provide more detail than the *Compendium*, contain more subjective judgments on the literature data than presented in the *Compendium*, and contain experimental data, either as part of the Reviews or as separate Data Reports, collected during this program that address each parameter studied.

This year, a report was completed on the *Effects of the Glass Surface Area/Solution Volume Ratio on Glass Corrosion* and work has continued on the effects of an unsaturated environment on glass corrosion and on the use of natural analogues in interpreting glass reaction processes.

I. INTRODUCTION

The High-Level Nuclear Waste Technical Support Program at Argonne National Laboratory (ANL) is part of a continuing activity performed for the U.S. Department of Energy (DOE) Office of Environmental Management (EM). The purpose of the program is to evaluate factors likely to affect glass reaction in an unsaturated environment to support hot start-up of the Defense Waste Processing Facility (DWPF) and the West Valley Demonstration Project (WVDP), and to provide input that may prove useful in developing and evaluating the behavior of glasses that could be used to immobilize high-level waste (HLW) at Hanford and Idaho. Past progress is given in the annual reports for FY 1990 through FY 1994 [1-5]. The program is based on determining the long-term glass behavior under conditions that may simulate an unsaturated repository environment and studying the release of radionuclides from a glass waste package. Such tasks will not be completed until the application for a repository license occurs, which will be several years after the production of waste for storage and disposal begins. The Technical Support Program at ANL also recognizes that the modeling and performance assessment programs must have a firm basis that (1) accounts for important physical parameters that will affect glass reaction in an unsaturated environment and (2) relates the mechanistic basis of glass reaction to conditions that will exist in an unsaturated environment.

The goals of the ANL Technical Support Program are to (1) review parameters that will be important in evaluating glass behavior, (2) perform testing to further quantify the effects of important variables, (3) perform long-term testing that will examine glass behavior under a range of conditions that may be important to storage of waste in an unsaturated environment, and that can be used to confirm models developed to calculate long-term performance, and (4) identify mechanisms that control glass reaction, thereby providing input to models that calculate glass behavior. The information developed in this program, when combined with data generated by the waste glass producers and by the Yucca Mountain Site Characterization Project (YMP), will form the scientific basis for a well-founded program that will ultimately qualify vitrified high-level waste for repository disposal.

The parameters that are important for controlling glass reaction in an unsaturated environment include (1) glass composition, (2) radiation, (3) temperature, and (4) ratio of surface area of glass to volume of liquid (S/V). Also being studied are the effects of unsaturated conditions (weathering) on glass reaction and modeling of glass behavior. Prior to hot facility start-up, these items will be critically evaluated such that their role in glass performance will be established. Results will be presented in Critical Reviews and Data Reports.

This page intentionally left blank.

II. BACKGROUND

Work in each area is governed by a Task Plan, which enables the work to be planned according to the quality guidelines of the ANL Technical Support Program and allows all program activities to be coordinated. The Task Plans outline work to be done in an activity, but they do not restrict the flexibility to make adjustments based on knowledge gained as the test results are evaluated. Plans are in place for the following tasks:

(1) Long-Term Testing of Fully Radioactive Glass,

(2) Relationship between High S/V Experiments and MCC-1,

(3) Laboratory Testing of West Valley Reference 6 Glass,

(4) Static Dissolution Tests with SRL EA Glass,

(5) Vapor Hydration Testing of SRL EA Glass,

(6) Components from Drip Tests with ATM-10 Glass,

(7) Mechanistic Validation through Natural Analogues,

(8) Analytical Electron Microscopy Support, and

(9) Critical Review of Parameters Affecting Glass Reaction in an Unsaturated Environment.

While these Task Plans are not formally published documents, copies of them are available upon request. Ongoing work in each of these tasks is described in later sections of this report.

An integral part of the testing program is the identification and preparation of glasses to be used. Several factors are considered in choosing glass compositions, including the following: (1) the composition of "fully" radioactive glasses* available for testing; (2) the need to test a range of compositions based on glass durability, which may be a function of the test conditions; (3) the desire to use compositions similar to those already in use so that a comparative data base can be developed; (4) the necessity to test both radioactive and nonradioactive compositions (for comparative and technique-development purposes); and (5) minimization of testing time and cost.

The compositions of fully radioactive glasses are set by glass availability and include several glass produced by Westinghouse Savannah River Company (WSRC) over the past several years: (1) 165 sludge-only-based glass, designated 165/42 (the glass frit is 165 type and the sludge is from tank 42 at the Savannah River Site); (2) 131 sludge-only-based glass, designated 131/11 (the glass frit is 131 type and the sludge is from tank 11); and (3) 200 frit-based glass, 200R (the glass frit is 200 type, the sludge is from tanks 8 and 12, and the precipitate hydrolysis aqueous [PHA] feed is simulated). Glasses represent compositions developed as the process engineering matured. The base frits used in these glasses (131, 200, and 165) represent the expected durability range from least to most durable based on hydration theory [6]. The sludge from tanks 11 and 42 is rich in aluminum, and the final compositions of the 131/11 and 165/42

*The term "fully radioactive glass" is used to designate glasses containing actual waste taken from the waste storage tanks at the Westinghouse Savannah River Site. The glass may not contain the complete complement of radionuclides anticipated to exist in the final DWPF product because the glass contains only radionuclides contained in the sludge component of the waste.

glasses do not represent glasses expected to be produced by the DWPF. However, the composition of 200R glass was expected to be similar to that of the blend identified in the Waste Compliance Plan (WCP) [7] and, therefore, similar to a production glass. However, the composition of the test glass differed from that of the WCP blend and was close to a bounding composition. Bounding in this context means that the calculated free energy of hydration of the glass is near the limit of acceptability for the DWPF, and the bounding composition is predicted to be more reactive than the blend composition.

The extent to which a glass composition falls within the range of production compositions influences the use of the glass in testing. The 131/11 and 165/42 compositions, although they may not be produced, are useful for comparative testing with a simulated nonradioactive glass of the same composition to demonstrate whether any differences in reactivity exist between production and simulated glasses. The 200R glass is also useful for comparative testing, but because its composition is closer to that of the production glass, it is used in a more extensive test matrix to assess glass behavior under unsaturated conditions. (See Sec. III for details of testing these glasses.) For each of these fully radioactive glasses, simulated glasses were produced with the same composition. Simulated glasses are designated as "S" glasses (e.g., 131/11S).

Because none of the fully radioactive glasses are exact representations of glasses identified in the WCP, we felt that another set of glasses should be produced for testing done in other tasks in this program and in other testing performed by the YMP. Concurrence of glass compositions to be tested was obtained from Lawrence Livermore National Laboratory, the agency responsible for the YMP Glass Task. The compositions chosen were 131-, 165-, and 202-based DWPF glasses, WV6 reference glass identified by the WVDP, and the Environmental Assessment (EA) glass used by all U.S. vitrification facilities. To arrive at the actual compositions, bulk frits were used as starting frits and were modified to match WCP glasses as closely as possible. Thus, the "base 131 frit" is 131 frit produced in the semiworks at WSRC, the "base 165 frit" is 165 black frit manufactured by Ferro Corp., the base 202 frit is based on DWPF start-up frit, WV6 glass was produced by The Catholic University of America (CUA), and the EA glass was produced by the Corning Glass Works. Each base frit was modified, if required, by the addition of chemical additives, including zeolite and actinide elements, to produce the glasses used in testing. If a glass contains uranium but no transuranic elements, it is designated U (e.g., 131U). If a glass contains transuranic elements, it is designated A (e.g., 131A).

At this time, testing has been initiated on all of the fully radioactive (R) and simulated (S) glasses. The starting glasses have been analyzed several times over the past few years to obtain the most reliable values to be used in data assimilation. The compositions are shown in Table 1 and may vary slightly from compositions given in previous annual reports [1-5]. This is especially true for the radionuclide content of the glasses that were analyzed with inductively coupled plasma-mass spectrometry (ICP-MS) and alpha counting combined with electroplating. The data presented in the subsequent sections of this report are based on the values in Table 1. A standard leachate, which is based on the equilibration of well water J-13 with tuff rock, was used throughout the testing program. The resulting water is termed "EJ-13 water," and its general composition is listed in Table 2. The composition of EJ-13 water varies slightly between batches, and the composition used in more recent tests has a slightly higher pH.

The above information provides a background on the materials used in the testing program. Enough information has been collected to provide in addition a general approach for use in interpreting the results from each of the Tasks. This approach is presented in terms of a general reaction progress pathway for the glass (Fig. 1). In a thermodynamic sense, the reaction of glass with water proceeds to minimize the free energy of the system and also to minimize the chemical potential gradients between the solution and the glass. When the gradients are steep, particularly for major glass-forming components such as SiO_2, the rate of reaction will be relatively high, whereas when the gradients are comparatively shallow, the rate of reaction will be relatively low.

Table 1a. Composition of Nonradioactive Glasses Used in Testing.[a] Compositions are reported in units of oxide wt %.

Element	131/11S	165/42S	200S	EA[b]	WV 6[c]	51S
Al	9.1	9.2	5.4	3.6	6.0	4.99
B	9.3	7.9	9.5	11.1	12.9	7.08
Ba	0.05	0.36	0.03	N.D.[d]	0.16	—
Ca	2.9	0.31	0.86	1.2	0.48	1.33
Ce	N.D.	N.D.	N.D.	N.D.	0.16	—
Cr	0.69	0.50	0.28	N.D.	0.14	0.42
Cu	0.04	0.02	0.18	N.D.	0.03	—
Fe	5.2	6.51	9.1	9.1	12.0	11.71
K	0.16	0.05	3.2	0.04	5.0	1.33
La	N.D.	N.D.	0.02	0.28	0.04	0.52
Li	3.2	4.7	3.3	4.2	3.7	4.34
Mg	1.6	0.96	1.7	1.8	0.89	1.96
Mn	1.7	1.7	1.5	1.4	1.0	1.35
Mo	N.D.	N.D.	0.02	N.D.	0.04	—
Na	17.5	10.0	15.3	16.8	8.0	9.18
Nd	N.D.	N.D.	N.D.	N.D.	0.14	—
Ni	0.56	0.70	0.91	0.53	0.25	0.26
P	—	—	—	—	—	0.54
Pb	0.13	N.D.	0.43	N.D.	N.D.	—
Rh	N.D.	N.D.	N.D.	N.D.	N.D.	—
Ru	N.D.	N.D.	N.D.	N.D.	N.D.	—
Si	45.8	55.4	46.1	48.6	41.0	53.81
Sr	0.02	0.01	0.02	N.D.	0.02	—
Th	N.D.	N.D.	0.01	N.D.	N.D.	0.02
Ti	1.7	0.07	0.13	0.65	0.80	—
U	0.26	0.13	1.9	N.D.	0.59	1.05
Zn	0.05	0.02	0.04	0.26	0.02	0.11
Zr	0.12	1.4	0.09	0.48	1.32	—

[a]Results were obtained by analyzing dissolved, cleaned, 100-200 mesh glass. Values are typically mean values from multiple analyses. Analyses were performed using inductively coupled plasma-atomic emission spectroscopy (ICP-AES) and ICP-MS.

[b]Compositions reported are from C. M. Jantzen, et al. [8]. Values have been normalized to 100% oxide wt %.

[c]The compositions reported are from Catholic University of America. Values have been normalized to 100% oxide wt %.

[d]N.D. = no data exist for that element.

Table 1b. Composition of Radioactive Glasses Used in Testing.[a]
Compositions are reported in units of oxide wt %.

Element	131/11R	131U/A	165/42R	165U/A	200R	202U/A	51R[b]
Al	9.9	3.3	11.1	4.5	6.3	3.9	4.82
B	10.5	9.8	9.9	6.7	10.7	8.0	6.41
Ba	0.02	0.02	0.05	0.03	0.02	0.21	—
Ca	3.8	0.94	0.40	1.6	0.92	1.3	1.38
Ce	0.05	0.06	0.06	<0.01	0.04	<0.01	—
Cr	0.34	0.13	0.33	0.02	0.30	0.12	0.44
Cu	0.02	0.02	0.03	N.D.[c]	0.10	0.41	—
Fe	5.9	12.8	6.3	12.2	9.1	11.9	13.10
K	0.18	3.9	0.05	0.20	3.4	3.7	1.56
La	0.01	0.02	0.03	<0.01	0.05	0.11	0.55
Li	3.1	3.0	4.7	4.5	3.1	4.4	4.50
Mg	1.3	1.3	0.99	0.73	1.4	1.4	2.05
Mn	1.8	2.5	2.2	2.8	1.7	2.2	1.54
Mo	0.01	<0.01	<0.01	0.01	0.01	0.05	—
Na	15.8	12.2	11.1	11.4	14.1	7.8	9.35
Nd	0.04	0.09	0.09	N.D.	0.07	<0.01	—
Ni	0.51	1.2	0.69	0.85	1.0	0.85	0.29
P	—	—	—	—	—	—	0.60
Pb	0.01	<0.01	0.04	0.01	0.02	0.01	—
Rh	<0.01	<0.01	<0.01	<0.01	<0.01	<0.01	—
Ru	<0.01	<0.01	0.02	0.01	<0.01	<0.01	—
Si	44.3	44.3	50.4	52.4	45.7	50.2	52.16
Sr	0.02	0.01	0.04	0.11	0.01	0.03	0.0060
Th	0.40	0.01	0.50	N.D.	0.03	0.28	0.02
Ti	1.5	0.66	0.12	0.15	0.08	0.93	—
U	0.21	3.0	0.13	1.1	1.7	2.0	1.09
Zn	0.03	0.02	0.02	0.02	0.02	0.29	0.14
Zr	0.07	0.22	0.72	0.70	0.04	0.06	—
^{241}Am	9.1E-5	4.5E-4	8.1E-5	1.8E-4	2.8E-4	4.4E-4	7.4E-5
^{244}Cm	1.2E-6	N.D.	2.1E-6	N.D.	2.1E-5	N.D.	1.1E-5
^{60}Co	4.1E-8	N.D.	1.9E-7	N.D.	3.6E-7	N.D.	NR[d]
^{137}Cs	6.6E-4	N.D.	9.9E-5	N.D.	6.5E-5	N.D.	2.2E-5
^{154}Eu	8.5E-6	N.D.	1.3E-5	N.D.	3.8E-6	N.D.	NR
^{155}Eu	1.1E-6	N.D.	1.5E-6	N.D.	1.2E-6	N.D.	NR
^{237}Np	5.6E-4	1.3E-2	8.0E-4	1.4E-2	2.1E-4	1.4E-2	4.2E-4
^{238}Pu	5.7E-4	N.D.	2.7E-4	N.D.	2.8E-4	N.D.	1.1E-4
^{239}Pu	1.6E-3	1.2E-2	1.5E-3	8.7E-3	2.0E-3	1.3E-2	2.2E-3
^{240}Pu	3.1E-5	N.D.	1.7E-4	N.D.	2.7E-4	N.D.	3.0E-4
^{125}Sb	7.5E-8	N.D.	1.0E-7	N.D.	1.0E-7	N.D.	NR
^{99}Tc	2.9E-4	3.5E-3	1.6E-5	1.5E-3	3.3E-5	3.0E-3	3.8E-4

[a]Results were obtained by analyzing dissolved, cleaned, 100-200 mesh glass. Values are typically mean values from multiple analyses. Stable element analyses were performed using ICP-AES and ICP-MS. Radionuclide content was measured using a combination of ICP-MS, gamma spectrometry.

[b]From N. E. Bibler [9].

[c]N.D. = no data exist for that element.

[d]NR = Not reported.

Table 2. Typical Composition of EJ-13 Leachate at a pH of 8.1

Major Components	mg/L
Al	1.1
B	0.17
Ca	5.4
Li	0.050
Mg	0.4
Na	53.9
Si	46.4
K	7.3
NO_3^-	11
F^-	2.3
HCO_3^-	100
Cl^-	8.4

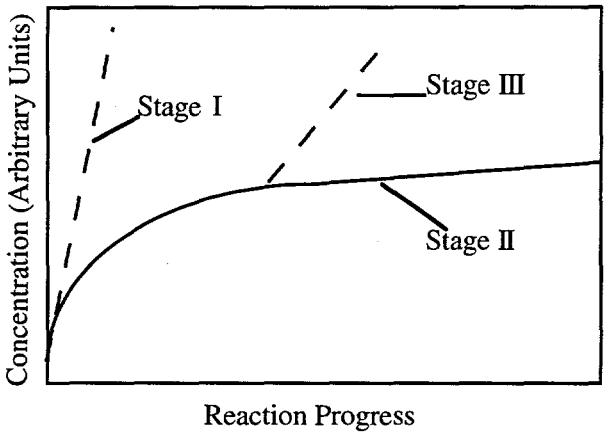

Fig. 1

Schematic of the Reaction Progress Pathway for Glass (Reaction Stages Defined in Text)

The slope of the chemical potential gradients and the activation energy of the rate-limiting reaction are controlling factors in determining the rate of glass corrosion. The hydrolysis reaction that results in the extraction of silicic acid from the glass is usually assumed to be the rate-limiting step [10]. The chemical potential gradients between the glass and water are initially large (Stage I) because the leachant is dilute, and the reaction proceeds at a maximum rate that depends only on the temperature and solution pH. This rate is sometimes called the forward rate. As the silicic acid concentration in solution increases, the chemical potential gradient and the reaction rate decrease (Stage II). Glass reaction during Stages I and II usually results in the formation of a reacted layer, which may or may not be crystalline, but does not result in an increase in the glass reaction rate. However, the glass may be unstable with respect to certain alteration phases that nucleate during glass corrosion. These phases can serve as sinks for glass components. When this occurs, the rate of glass corrosion is controlled not by the chemical potential gradient between glass and solution, but by the gradient between the glass and alteration phases. This relationship, in turn, may accelerate the rate of glass corrosion (Stage III). Glass corrosion observed in laboratory tests that are conducted in this program can be related to the behavior depicted in Fig. 1. Tests conducted under different conditions may result in glass corrosion in Stages I, II, or III.

III. LONG-TERM TESTING OF FULLY RADIOACTIVE GLASS

A. Introduction and Background

The source term for the release of radionuclides from a nuclear waste repository is the corrosion of the waste form. Evaluation of the performance of the repository and the engineered barrier system (EBS) against regulations established by the Nuclear Regulatory Commission and the Environmental Protection Agency requires that either (1) expert judgment be used to identify parameters that control waste form (glass) reaction and radionuclide release, and bounding limits placed on the role of the source term in calculating release from the EBS and the boundary of the repository; or (2) a predictive model be developed, based on a mechanistic interpretation of the radionuclide release as a function of reaction progress, and confirmed by using tests done under potential reaction conditions.

The problem with the first approach is that there is little experience to draw upon when evaluating glass waste form reaction under unsaturated conditions, such that the error in applying expert judgment to the problem may be unacceptably large. The alternative approach, testing and modeling the glass reaction progress, is a more defensible means of providing input to the prediction of radionuclide release and performance of the repository, because information related to the source term has a technical basis and will provide an essential starting point to make more reasonable assumptions regarding the remainder of the EBS and repository performance. Keys to obtaining the necessary input are in establishing and understanding the reaction progress, that is, the corrosion rate as a function of time and reaction conditions and the manner in which the radionuclides are released to solution.

Many evaluations of the behavior of high-level waste glass have used the results from tests based on simulated, nonradioactive analogs of the same nominal composition as the radioactive glass. To apply the knowledge gained in those studies to understanding the behavior of the fully radioactive production glass, it must be demonstrated that experiments with simulated glasses are an adequate representation of the reaction that will occur with the actual production glasses. Also, to obtain information regarding the performance of radionuclides, tests must be done with radioactive glasses. To fully assess glass behavior it is necessary to address the following:

1. Do both the radioactive and simulated glasses react through the same controlling mechanism, thereby producing the same secondary phases in the same sequence?

2. Is there an effect due to the radioactivity, which is not adequately simulated when using the nonradioactive glass?

3. What is the relevance to the actual production process of using glass that may not contain all the nonradioactive components present in the sludge, supernate, and frit feeds? (Simulated glasses are generally produced with pure starting materials and the minor components are ignored.)

4. Is there a difference in reactivity between the two glass types?

Comparison studies on the performance of fully radioactive and simulated nuclear waste glasses [10-16] assessed these questions. Most of the studies [10-13] were performed at low to intermediate S/V ($\leq$1100 m^{-1}) in static batch tests for periods of less than one year. The general conclusion from these studies is that there is little difference in the reactivity between the two glass types. The comparison study reported here reinvestigates that conclusion by evaluating glass behavior under conditions that are more applicable to the prediction of long-term behavior, and which built on previous testing of radioactive glasses by WSRC [17-21]. The studies reported

here are done in the batch mode for longer time periods at higher S/V values, such that the reaction process is accelerated, and also in a dripping water mode to evaluate conditions that are more relevant to an unsaturated repository.

B. Objectives

The objective of this task is to evaluate the behavior of fully radioactive glasses, similar to those that will be produced by the DWPF, with emphasis on studying glass reaction during Stages II and III in the reaction progress plot (Fig. 1). Specifically, long-term data will be generated such that (1) reaction of fully radioactive glass can be compared with that of nonradioactive glass with a similar nominal composition; (2) interactions between waste package components that must be accounted for in independent reaction path models are identified; and (3) the long-term behavior of glass is established under anticipated disposal conditions, such that glass performance models can be validated.

To meet the above objectives, we evaluated (1) how the glass reaction progressed along its long-term reaction path as predicted by models of glass reaction (Fig. 1), and (2) the release of radionuclides from the glass. To evaluate radionuclide release, we measured the amount of an isotope released from the glass and determined its distribution between dissolution, suspension in solution as colloidal material, and sorption onto metal components of the test. The fractional solution components together make up the total release of radioactivity and can be used as input to evaluate the release of radionuclides from glass under a repository setting.

C. Technical Approach

To provide information that can be fully used in evaluating the performance of glass throughout its reaction progress, tests must cover a range of conditions and times. The goal is to provide information regarding the "final" portion of the reaction progress, since that information is most relevant to long-term performance, and to evaluate factors that can be used as source term input for EBS design and repository assessment. An unsaturated environment presents a challenge in performing long-term testing because the conditions, in particular the amount of water available to react with the glass and to transport radionuclides, are expected to change, perhaps significantly, over the duration of storage.

Tests to evaluate the performance of glass in an unsaturated environment must address the unique features of such an environment and must be performed for time periods long enough so that the stage is reached where alteration phase formation (as opposed to supersaturated solution concentrations) controls the glass reaction. Relevant tests include static and intermittent-flow tests performed at high S/V ratios to simulate the waste package environment. The information obtained from these tests must include the solution composition as a function of time, combined with a description of the glass alteration. To meet these goals, three types of tests are being performed:

(1) Long-term static tests (i.e., no water flow) with monoliths and crushed glass. These tests provide temporal solution trends, plus easy identification of alteration phases combined with the distribution of radionuclides in the reacted glass layers.

(2) Long-term static dissolution tests at high S/V with crushed glass.

(3) Long-term intermittent flow tests at high S/V following a modified version of the Unsaturated Test Procedure [22] as applied to "aged" and fresh glass monoliths.

(4) Long-term repository environment tests following the laboratory analog procedure as applied to "aged" and fresh glass monoliths [23].

The tests are being performed with the three different general groups of glass compositions: 165-, 200-, and 131-frit based glasses (Table 1). The tests in each test category are described below, including status, results, and discussion.

D. Results and Discussion

The tests with radioactive glasses are discussed in four sections: (1) long-term static tests; (2) long-term static dissolution tests; (3) long-term intermittent flow tests; and (4) long-term repository environment tests.

1. Long-Term Static Tests with SRL 200R, SRL 165/42, and SRL 131/11 Glasses

To date, 159 of the planned 212 long-term tests have been terminated. The longest test has been in progress for more than 65 months. For a complete test matrix of long-term static tests and the status of the tests, refer to Table 3. The solution analyses of all the terminated tests, which include analyses of leachant pH values, cations, selected anions, total carbon, and actinides, are about 95% completed. The surface analyses on the terminated samples are also nearly complete and include optical microscopy (OM), scanning electron microscopy with dispersive X-ray spectroscopy (SEM/EDS), and transmission electron microscopy (TEM) with associated analytical electron microscopy (AEM).

a. Blank Tests

A series of blank tests is currently in progress. The purpose of these tests is to monitor the changes in the EJ-13 solution (Table 2) in a stainless steel vessel as a function of test duration. The major elements, Si, Na, K, B, and Li, are monitored and have remained constant through test durations of 1820 days. Additionally, elements such as Fe, Ni, Cr, and Cu have shown a slight increase; this change has been attributed to the dissolution of the stainless steel vessel and copper gaskets.

b. Tests with SRL 200 Glasses

The reaction progress of SRL 200 glasses was measured at S/V values of 340, 2000, and 20,000 m^{-1}. These tests provide information on the different stages of glass corrosion. The dissolution of the glass is monitored by the solution concentrations of matrix elements.

The normalized mass losses, $(NL)_i$, of Bi, Li, Na, and Si and the solution pH as a function of test duration for 340, 2000, and 20,000 m^{-1} are shown in Figs. 2, 3, and 4. The results for both the 200R and 200S glasses at 340 m^{-1} are shown in Fig. 2. The largest difference in the $(NL)_i$ values is less than 30%, with the values for the 200S glass being greater than those for the 200R glass. The pH values of tests with 200R glass are about 0.5 pH units lower than those for S glass. The lower pH is attributed to both the effects of radiolysis and small differences in the composition of the glasses. Evidence for a radiation effect in the tests with 200R glass is the formation of NO_2^-, oxalate, and formate.

Overall, tests at 340 m^{-1} with both the 200R and 200S glasses demonstrate behavior characteristic of Stages I and II of the reaction progress. For both glasses, the solution concentration of silicic acid increases, and at approximately 200 days of test duration, the reaction rate starts to plateau as it reaches Stage II. Surface analysis of these glasses shows the formation of a clay layer, but no evidence of the more mature alteration phases that are typical of the Stage III reaction.

Table 3. Test Matrix[a] for Long-Term Static Tests at High S/V Ratios (duration in days)

Reaction Progress,[b]	131 Glass Type[c]				200 Glass Type[d]						165 Glass Type[d]				
	131/11R		131/11S		200R			200S			165/42R		165/42S		
day•m^{-1}	340	2000	340	2000	340	2000	20,000	340	2000	20,000	340	2000	340	2000	Blank[c]
1,020															3
2,380															7
4,760					14[e]			14							14
6,000						3			3						28
9,520	28		28								28		28		56
14,000															70
19,040					56			56							91
28,000						14			14						98
30,940	91		91								91		91		140
60,000		30		30								30		30	182
61,880					182			182							238
123,760	364		364		364			364			364		364		280
140,000		70		70		70			70			70		70	364
247,520	728		728		728			728			728		728		546
280,000		140		140			15			15		140		140	728
495,000	1456		1456		1456			1456			1456		1456		980
560,000		280		280		280			280			280		280	1456
990,080	2912		2912		2912			2912			2912		2912		1820
1,120,000		560		560		560	56		560	56		560		560	2912
1,960,000		980		980		980	98		980	98		980		980	TBD
3,649,000		1820		1820		1820	182		1820	182		1820		1820	TBD
7,280,000							364			364					TBD
10,920,000							546			546					TBD
14,560,000							728			728					
					TBD[f]	TBD	TBD	TBD	TBD	TBD[g]	TBD	TBD	TBD	TBD	
					TBD	TBD	TBD	TBD	TBD	TBD					

[a]The tests done at 340 m^{-1} used monoliths; the tests done at 2000 and 20,000 m^{-1} used powder.
[b]Reaction progress in terms of S/V•t (units of day•m^{-1}). No significance is attached to the use of this reaction progress indicator.
[c]Tests are single tests.
[d]Tests are duplicate.
[e]The underlined tests are terminated.
[f]TBD = to be determined.
[g]TBDs were terminated at 330, 390, and 1095 days.

(a)

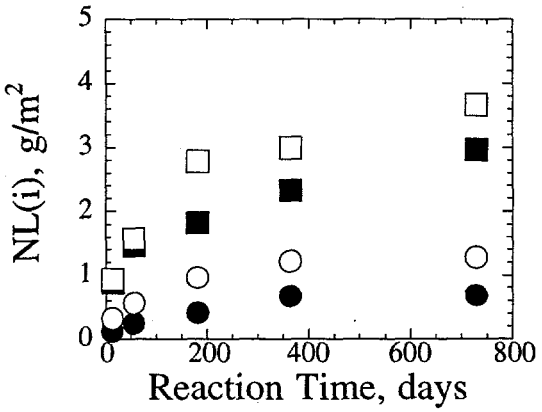

(b)

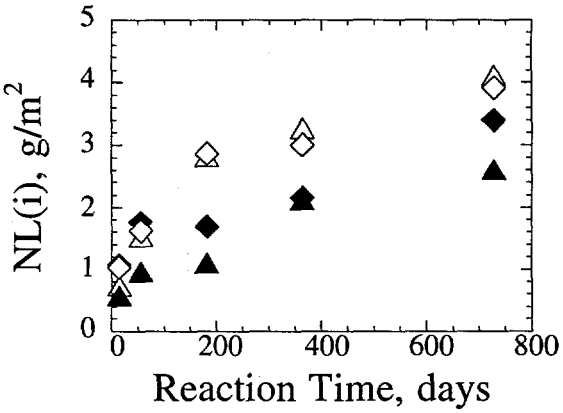

(c)

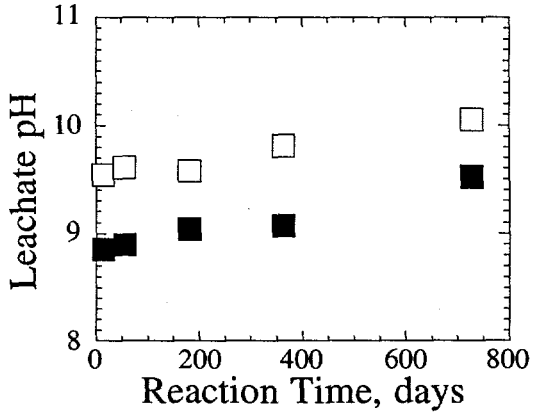

Fig. 2. Normalized Mass Losses of (a) Li (■ and □) and Si (● and ○) and (b) B (▲ and Δ) and Na (◆ and ◊) from SRL 200 Glasses Reacted in Static Tests at 90°C and 340 m^{-1}. In (c) the solution pH is shown. The filled symbols represent the results of tests with the fully radioactive glass; the open symbols represent the results of tests with the simulated glass.

(a)

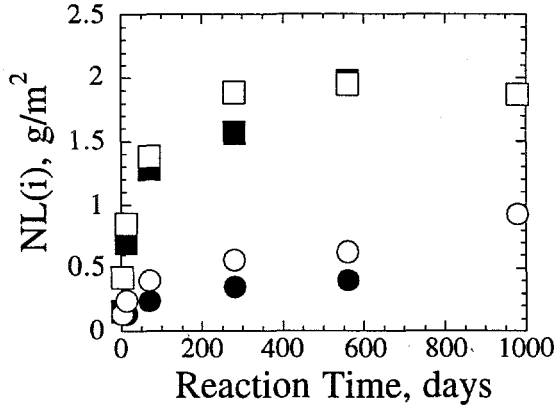

(b)

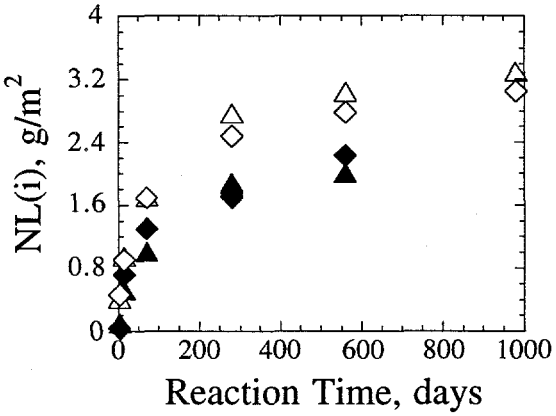

(c)

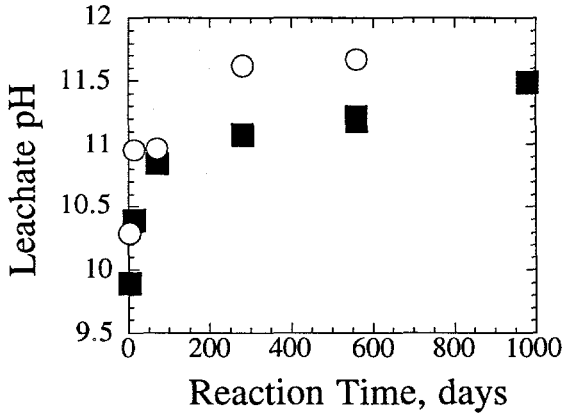

Fig. 3. Normalized Mass Losses of (a) Li (■ and □) and Si (● and ○) and (b) B (▲ and Δ) and Na (◆ and ◊) from SRL 200 Glasses Reacted in Static Tests at 90°C and 2000 m^{-1}. In (c) the solution pH is shown. The filled symbols represent the results of tests with the fully radioactive glass; the open symbols represent the results of tests with the simulated glass.

(a)

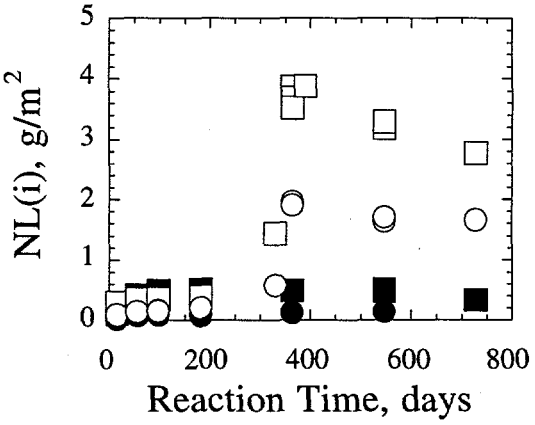

(b)

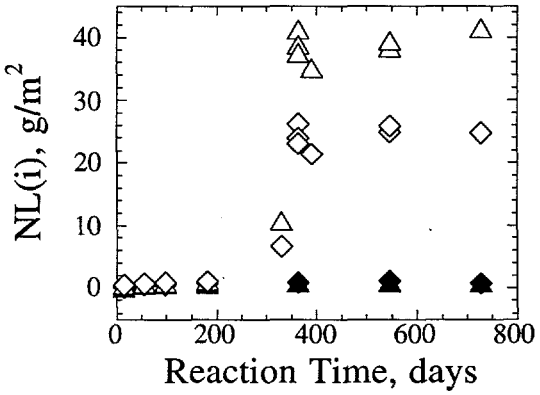

(c)

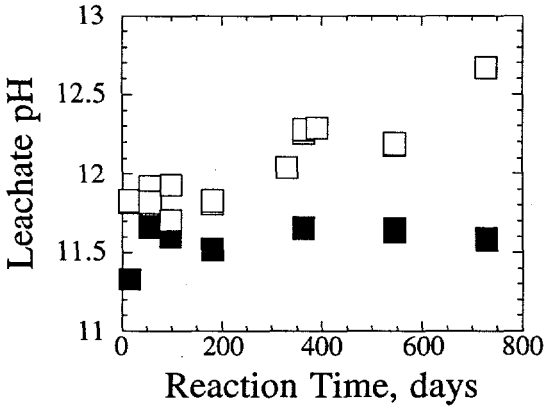

Fig. 4. Normalized Mass Losses of (a) Li (■ and □) and Si (● and ○) and (b) B (▲ and Δ) and Na (◆ and ◊) from SRL 200 Glasses Reacted in Static Tests at 90°C and 20,000 m^{-1}. In (c) the solution pH is shown. The filled symbols represent the results of tests with the fully radioactive glass; the open symbols represent the results of tests with the simulated glass.

Glass dissolution at 2000 m^{-1} (Fig. 3) shows behavior similar to that of glasses tested at 340 m^{-1}. The 200R glass corrodes less than the 200S glass throughout the 560-day test duration. Surface analysis (Fig. 5) demonstrates that the glass had formed a clay layer; however, no other phases were observed. The solution and solid phase results suggest that the glasses are corroding by the same mechanism at S/V ratios of 340 and 2000 m^{-1}.

The glass reaction at 20,000 m^{-1} is shown in Fig. 6. The general observation that 200R glasses react at a lower rate than the 200S glasses still holds for these tests. The results show that corrosion of 200S glass occurs at Stage II through about 282 days and at Stage III at longer times. The change from Stage II to Stage III results in a large increase in $(NL)_{B,Li,Na,Si}$. The 200R glass continues to corrode at Stage II at all times tested. The pH values of tests with 200S glass are consistently higher than those of tests with 200R glass. The pH of the 200S tests increased slightly when the rate increased, at about 300 days. Additional evidence for Stage III reaction for 200S glass is that solids analyses showed the glass to have transformed into alteration phases at reaction times of 330 days and longer. Very little unreacted glass remained after one year. This is why $(NL)_B$ reached a maximum of ~40 g/m^2 after one year, because almost all of the glass had dissolved. The reported $(NL)_i$ values are based on the initial surface area. The solid analyses indicate the surface area has decreased significantly during Stage III reaction, and the effect of this change on normalized reaction rates is currently being evaluated (see Sec. IV).

c. Tests with SRL 165/42 Glasses

The solution data from testing SRL 165/42 glasses on the monolithic samples at S/V = 340 m^{-1} and on the powder samples at S/V = 2000 m^{-1} are presented in Figs. 6 and 7, respectively. Testing at 20,000 m^{-1} for this glass was not done because a limited amount of glass was available and because the composition is not within the envelope of glasses expected to be produced at the DWPF.

The $(NL)_i$ values for Li, Si, B, and Na for the fully radioactive and simulated 165/42 glass are similar in both magnitude and trend. The largest differences in $(NL)_i$ are factors of 2.0 and 1.7 for $(NL)_B$ and $(NL)_{Na}$, respectively. The leachate pHs in tests with the 165/42S glass were slightly higher than those of the 165/42R glass. The $(NL)_i$ values increase through 1465 days, with the 165/42R and 165/42S glasses reacting at about the same rate.

The results of tests with SRL 165/42 glasses at 2000 m^{-1} are shown in Fig. 7. Within the precision of the data, the results of the 165/42R and 165/42S glasses are the same, and the reaction has reached Stage II. The leachate pH values are also similar for both glass compositions. The surface analyses show no evidence of the zeolite and other crystalline phases expected in Stage III. The solid phase analyses shown in Fig. 8 represent reacted layers becoming progressively thicker as the reaction time increased to 140 and 980 days. Etch pits were also observed under the layers for the longer-duration samples. Because of the fine-grained nature of the clay phases, an exact identification of the clay has not been made.

d. Tests with SRL 131/11 Glasses

Figure 9 shows the solution data from tests with SRL 131/11 glass at S/V = 340 m^{-1}. These data show that the 131/11R and 131/11S glasses initially react at nearly the same rate, but after about 500 days, the two diverge, with the 131/11S glass reacting faster. The leachate pH is similar in the nonradioactive and radioactive glass tests.

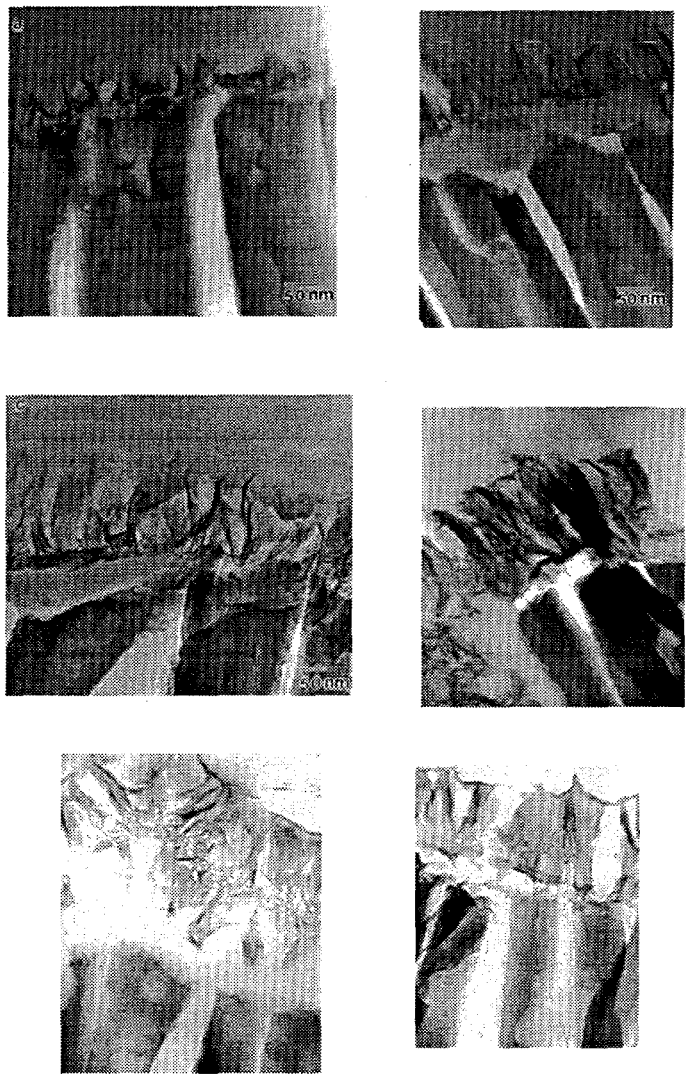

Fig. 5. Transmission Electron Microscopy Photomicrographs of Cross Sections of SRL 200S Glass Reacted at 2000 m^{-1} for (a) 3 Days, (b) 14 Days, (c) 70 Days, (d) 280 Days, (e) 560 Days, and (f) 980 Days.

(a)

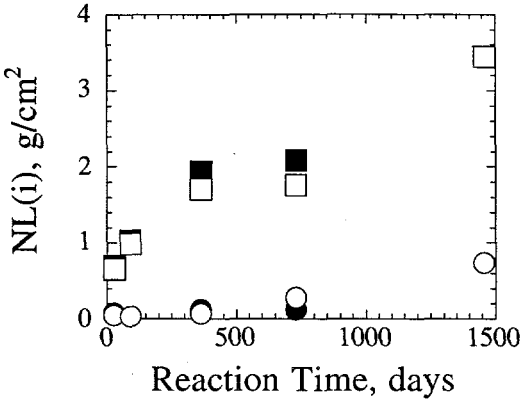

(b)

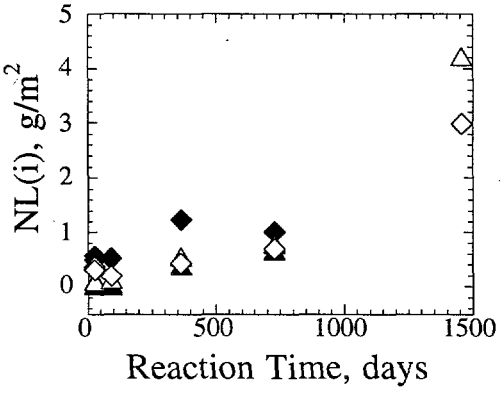

(c)

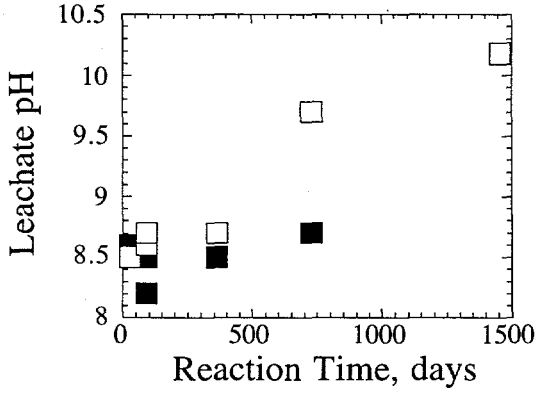

Fig. 6. Normalized Mass Losses of (a) Li (■ and □) and Si (● and ○) and (b) B (▲ and Δ) and Na (◆ and ◊) from SRL 165/42 Glasses Reacted in Static Tests at 90°C and 340 m^{-1}. In (c) the solution pH is shown. The filled symbols represent the results of tests with the fully radioactive glass; the open symbols represent the results of tests with the simulated glass.

(a)

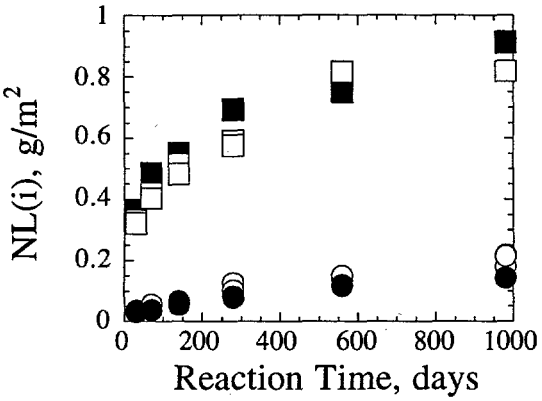

(b)

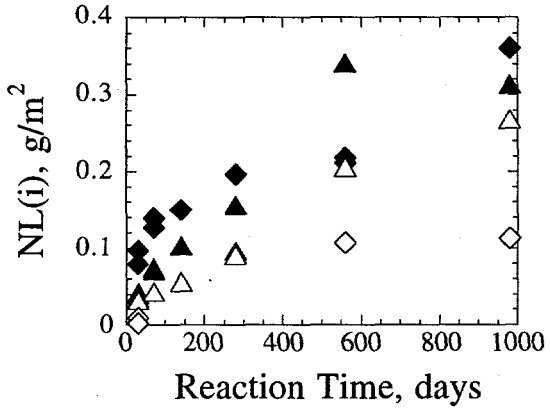

(c)

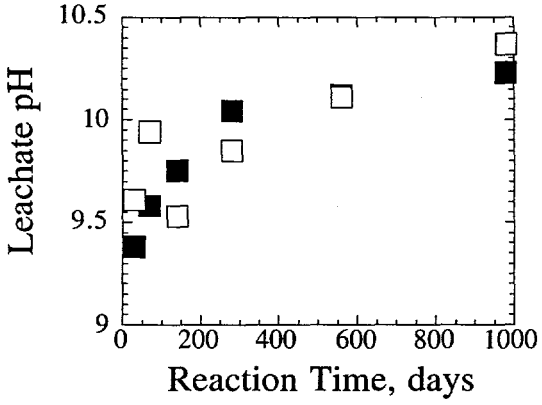

Fig. 7. Normalized Mass Losses of (a) Li (■ and □) and Si (● and ○) and (b) B (▲ and Δ) and Na (◆ and ◊) from SRL 165/42 Glasses Reacted in Static Tests at 90°C and 2000 m^{-1}. In (c) the solution pH is shown. The filled symbols represent the results of tests with the fully radioactive glass; the open symbols represent the results of tests with the simulated glass.

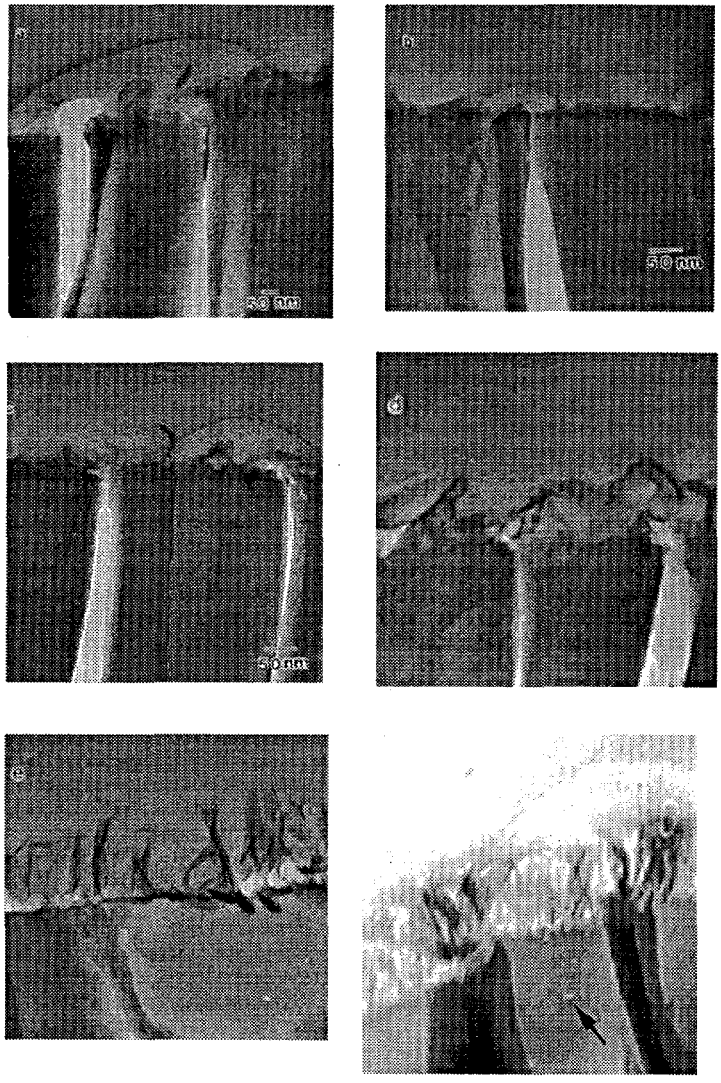

Fig. 8. Transmission Electron Microscopy Photomicrographs of Cross Sections of SRL 165/42S Glass Reacted at 2000 m^{-1} for (a) 30 Days, (b) 70 Days, (c) 140 Days, (d) 280 Days, (e) 560 Days, and (f) 980 Days. This sequence shows the thickening of the reacted layer. The arrow in (f) shows an etch pit. All the micrographs have the same magnification.

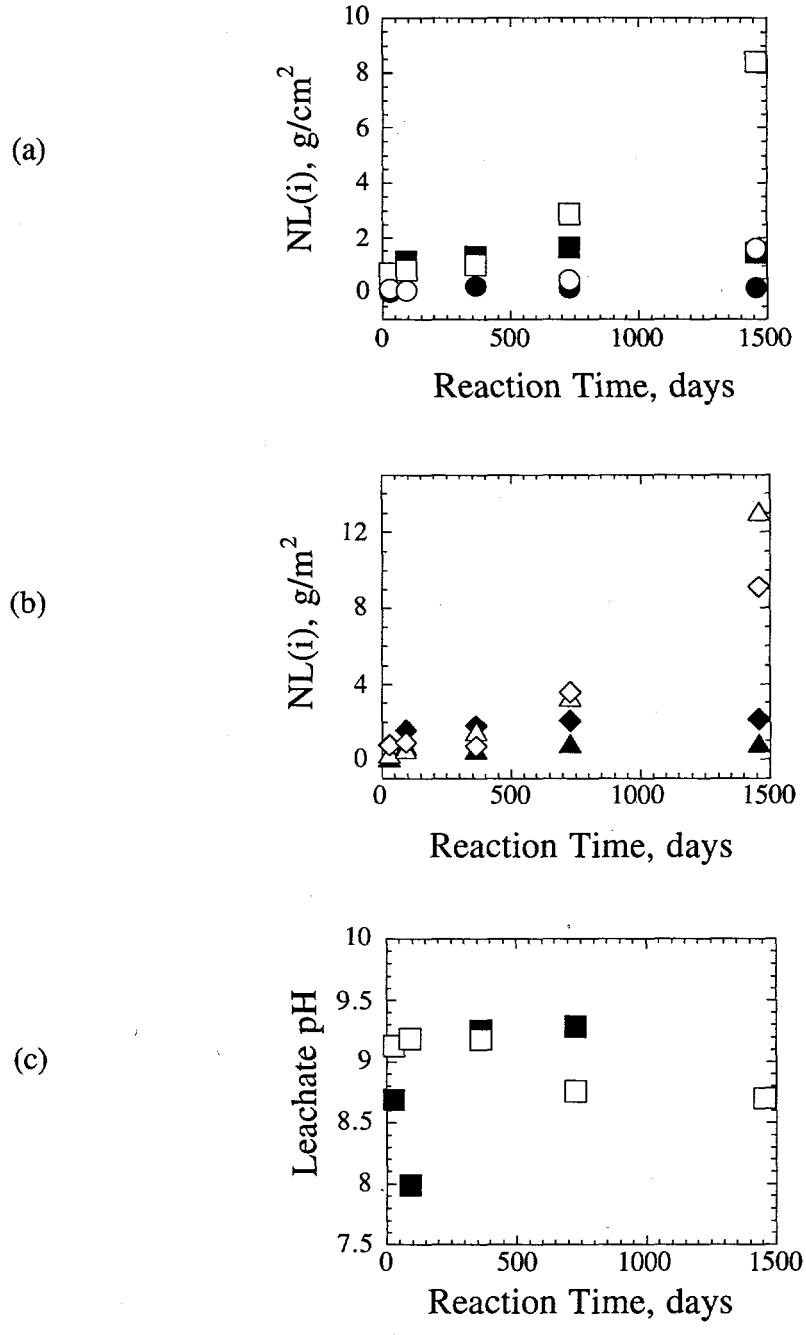

Fig. 9. Normalized Mass Losses of (a) Li (■ and □) and Si (● and ○) and (b) B (▲ and Δ) and Na (◆ and ◊) from SRL 131/11 Glasses Reacted in Static Tests at 90°C and 340 m^{-1}. In (c) the solution pH is shown. The filled symbols represent the results of tests with the fully radioactive glass; the open symbols represent the results of tests with the simulated glass.

The glass corrosion behavior of SRL 131/11 glasses at 2000 m^{-1} is shown in Fig. 10. For the 131/11R and 131/11S glasses, similar trends and magnitudes of normalized release were observed for lithium and silicon throughout the 980-day test duration. However, boron and sodium are released faster from 131/11S than from 131/11R. The corrosion behavior of SRL 131/11 at 2000 m^{-1} is similar to the corrosion behavior of SRL 200 glasses at 2000 m^{-1} in that the simulated nonradioactive glass corrodes faster than its radioactive counterpart. The leachate pH values for the tests with 131/11S glass are always higher by about 0.2 pH units than those for the 131/11R glass, as shown in Fig. 10.

The solid state data suggest the glass has reached Stage II of the reaction progress curve. Figure 11 shows TEM images of 131/11S samples reacted for 30, 70, 140, 280, 560, and 980 days at S/V = 2000 m^{-1}. Each sample displays an outer reaction layer made up of wisps of clay-like material. In general, this clay layer is continuous, but the fringes are observed only periodically because of a sample orientation effect. This clay layer becomes thicker as the reaction duration progresses from 30 to 980 days, increasing from 30 to about 160 nm thick. Beneath the clay layer, voids or etch pits are observed on all samples; these pits are typically 30 to 100 nm in diameter. As the etch pits form, sections of glassy-looking materials or "stringers" remain as a bridge between the glass and the clay layer. Analysis of these stringers reveals that they are composed primarily of Si, Al, and Fe. In general, layers that form on samples that undergo reaction for the longer periods of time are more crystalline. The composition and spacing data are consistent with nontronite or Na-montmorillonite. The iron concentration observed is intermediate between these two minerals. Brindley [24] points out that intermediate compositions are quite common. A Ca-montmorillonite exists that has similar spacings. Both Na and Ca are taken up into the clay structure in the d-spaces between silicate layers, where these elements are readily substituted for each other; therefore, a range of intermediate compositions is possible. Formation of this clay layer is representative of Stage II reaction. The absence of additional alteration phases indicate Stage III reaction has not been reached.

e. Future Studies

The ongoing static tests are scheduled to continue to investigate the approach to Stage III reaction. Data generated from solution analyses will be combined with surface layer studies to compare more completely the reactivity of the radioactive and simulated waste glasses and to provide a data base for validation of glass performance models. Several tests of to-be-determined duration will be terminated to confirm the observed trends. A draft version of a report on the long-term static testing is currently being reviewed internally.

2. Laboratory Testing of SRL Tank 51 Sludge-Based Glass

a. Introduction and Background

Static dissolution tests are being used to characterize the long-term corrosion behavior of a radioactive glass produced at SRTC during vitrification of sludge from Tank 51 at the Savannah River Site. This glass is being tested in parallel with a nonradioactive glass produced at ANL having the same composition as the sludge glass, except for fission products and transuranic elements. The radioactive and nonradioactive glasses are referred to as 51R and 51S, respectively. The 51R glass was made during a demonstration of the DWPF process control for remote vitrification using a 1/100th scale melter. The sludge used to make this glass is similar to the first batch of sludge that will be sent to the DWPF for vitrification. The compositions of the 51R and 51S glasses are given in Tables 1a and 1b. The compositions are very similar to the SRL 202 glass that is being characterized in the ongoing Task "Relationship Between High S/V Experiments and MCC-1." Alteration phases formed during Stage III of the corrosion of SRL 202 glass have been observed to increase the dissolution rate of that glass in long-term static dissolution tests. The same suite of tests used to characterize the corrosion of the SRL 202 glass is being conducted with

(a)

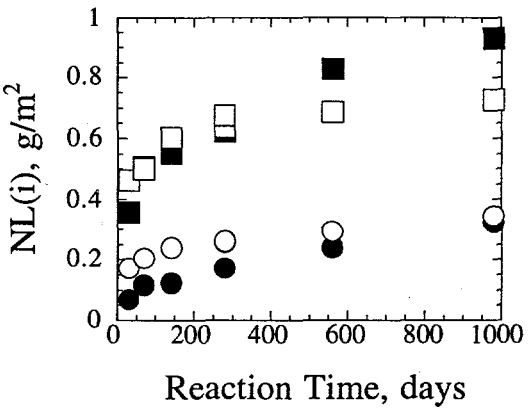

(b)

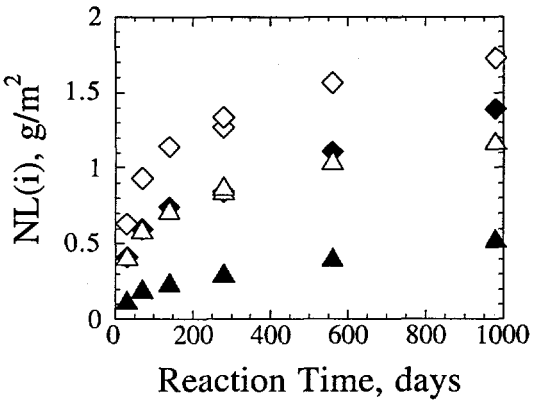

(c)

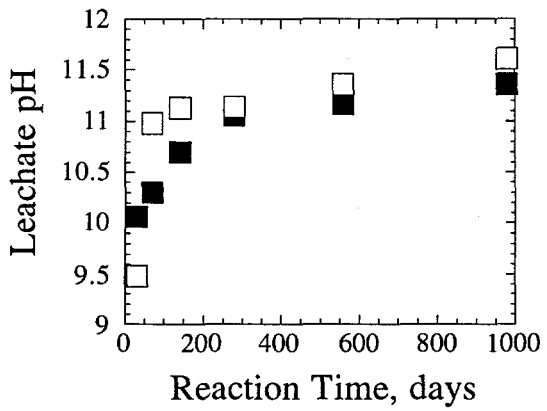

Fig. 10. Normalized Mass Losses of (a) Li (■ and □) and Si (● and ○) and (b) B (▲ and Δ) and Na (◆ and ◊) from SRL 131/11 Glasses Reacted in Static Tests at 90°C and 2000 m^{-1}. In (c) the solution pH is shown. The filled symbols represent the results of tests with the fully radioactive glass; the open symbols represent the results of tests with the simulated glass.

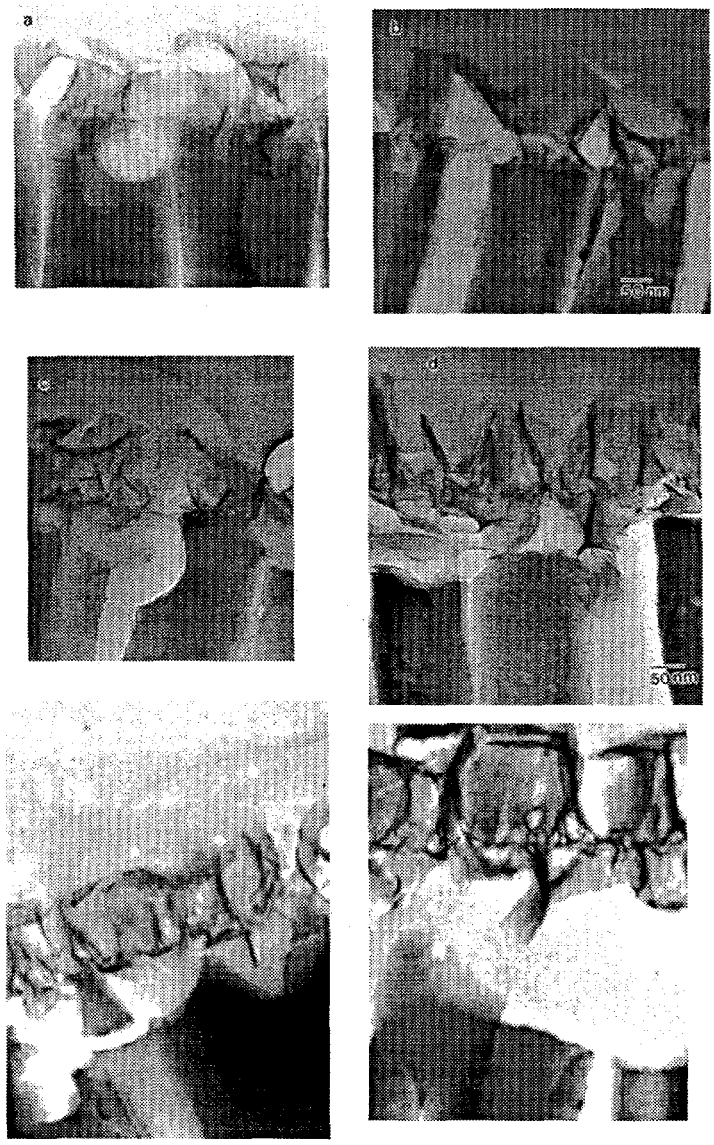

Fig. 11. Transmission Electron Microscopy Photomicrographs of Cross Sections of SRL 131/11S Glass Reacted at 2000 m^{-1} for (a) 30 Days, (b) 70 Days, (c) 140 Days, (d) 280 Days, (e) 560 Days, and (f) 980 Days. The 30-day sample highlights the developing clay layer seen as wisps of parallel fringes. A lattice spacing of 13-14 Å is observed.

the 51R and 51S glasses to determine if the formation of certain alteration phases increases the glass corrosion rate, to identify the phases that form, to measure the dissolution rates before and after these alteration phases form, and to determine the disposition of released radionuclides. These test results will provide information pertinent to assessing the long-term durability of glasses made during the initial DWPF campaigns.

b. Objectives

The objectives of this Task are to characterize the corrosion behavior of the 51R and 51S glasses, to determine how the radionuclides affect the corrosion behavior, to determine if alteration phases formed during Stage III will increase the glass corrosion rate, and to determine the disposition of radionuclides as the glass dissolves.

c. Technical Approach

The 51R glass was supplied by SRTC, and the 51S glass was made at ANL from reagent-grade chemicals. The composition of the 51S glass was measured at ANL, and the composition of the 51R glass was measured at SRTC [26]. The difference in the concentration of each element in the glasses is within the combined analytical uncertainties for analyses of 51R and 51S glasses, which is assumed to be about ±15% for the analysis of each glass. Samples of both glasses were prepared for testing at ANL by crushing and sieving to isolate the -100+200 mesh fraction. The crushed glass was washed with deionized water to remove fines and then dried in a 90°C oven. Static dissolution tests are being conducted at S/V ratios of 2000 and 20,000 m^{-1} in EJ-13 water at 90°C for reaction times between 7 days and longer than 2 years. Both the solutions and reacted solids will be analyzed to characterize the corrosion behaviors of the two glasses. Standard 7-day PCT tests in deionized water were also conducted for comparison with other glasses.

d. Results and Discussion

Tests with 51R and 51S glasses have been completed through 14 and 182 days, respectively. (The tests with 51S have progressed to longer times because that glass was available for testing before the 51R glass.) Table 4 summarizes the normalized solution concentrations of B, Na, and Si in three 7-day PCT tests conducted in deionized water at 2000 m^{-1}. The average results of triplicate 7-day PCT tests conducted at SRTC using samples of 51R glass taken from the top and the bottom of the pour canister are included for comparison. The normalized solution concentrations were calculated by dividing the measured solution concentrations by the mass fraction of B, Na, or Si in each glass so that the numbers in the table can be compared directly.

Table 4. Results of 7-Day PCT Test in Deionized Water with 51R Glass

Glass	Test	pH	[B], mg/L	[Na], mg/L	[Si], mg/L
51R	51R-0	9.82	9.1	31	95
	51R-1	9.92	9.0	27	96
	51R-2	9.91	8.8	28	94
	SRTC-top[a]	10.3	14	44	102
	SRTC-bottom[a]	10.3	16	49	111

[a]Average of triplicate tests. From Ref. 27.

Consider first the tests with 51R glass conducted at ANL and SRTC. More 51R glass is measured to have dissolved in tests conducted at SRTC than in tests conducted at ANL. Higher pH values were also attained in the tests conducted at SRTC than at ANL. The differences in these results may be due to differences in the amounts of remaining fines of the crushed glass tested, despite the fact that the same cleaning procedure was followed. They may also be due to small differences in the oven temperatures (the PCT procedure calls for temperatures of 90±2°C) and in testing parameters and analytical methods.

We now compare the results of tests with 51R and 51S glasses conducted at ANL. The pH values attained in tests with the 51R glass are the same as those measured in tests with the 51S glass, within experimental uncertainty. The higher normalized concentrations of B and Na indicate that the 51S glass has reacted to a greater extent than the 51R glass. Although the normalized Si concentrations are higher in tests with 51R glass than in tests with 51S glass, it is likely that Si is being incorporated into alteration phases (see below) so that the solution concentration of Si does not provide a reliable measure of the extent of glass dissolution.

The results of tests conducted with 51S glass at 2000 and 20,000 m^{-1} are plotted in Fig. 12 as the normalized mass loss based on the B, Li, Na, and Si concentrations. The glass dissolution is nonstoichiometric at both S/V ratios, with B, Li, and Na being released preferentially to Si. The same behavior has been seen in tests with other DWPF glasses [28]. Notice that the normalized mass losses are consistently higher in tests conducted at 2000 m^{-1} than in tests conducted at 20,000 m^{-1}. This occurs because the dissolution rate decreases with increasing Si concentrations, and the Si concentration is higher in tests at 20,000 m^{-1} than in tests at 2000 m^{-1}. Notice also that NL(B) values increase with the reaction time at a rate of about 0.002 g/(m^2•d) at 2000 m^{-1} and at a rate of about 0.001 g/(m^2•d) at 20,000 m^{-1} over the time range tested.

Analyses of the reacted 51S glass showed a small amount of clay-like material to have formed as a surface layer. While the layer material has not yet been analyzed, it has the same appearance as smectite clay that forms upon corrosion of the SRL 202 glass [28]. The glass dissolution rate, as measured by the release of B, has not been significantly affected by the formation of alteration phases through 182 days, and the glass is still reacting in Stage II. An estimate of when alteration phases might be expected to form and drive the corrosion into Stage III can be obtained by considering the results of tests with SRL 202 glass. Phases that affected the dissolution rate of SRL 202 glass formed between 182 and 364 days [28]. The time at which such phases may form in tests with 51S (and 51R) glass can be estimated based on the solution chemistries in tests with the different glasses. Table 5 summarizes the solution concentrations measured in tests with SRL 202 and SRL 51S glasses for tests conducted at an S/V ratio of 20,000 m^{-1} through 182 days. The formation of analcime, which is an alteration phase known to affect the dissolution rates of several glasses, depends on the concentrations of Na, Al, and Si and on the pH. For tests conducted for the same time period, tests with the 51S glass attain higher pH values but lower silicon concentrations than tests with SRL 202 glass. Therefore, the solutions generated during dissolution of 51R glass are probably more undersaturated with respect to analcime than solutions in tests with SRL 202 glass, and analcime will require longer to form in tests with 51S glass than in tests with SRL 202A glass, that is, longer than about 182 days. The evolution of the solution chemistry in tests with 51S glass will be tracked using a geochemical equilibration code when more data become available. However, this simple analysis provides some insight into when alteration phases may form.

a.

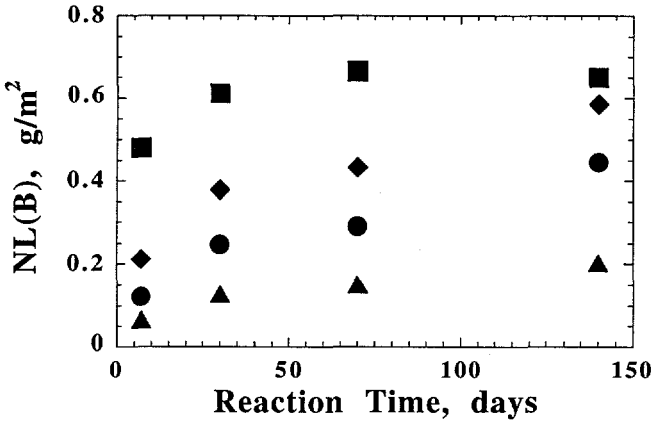

b.

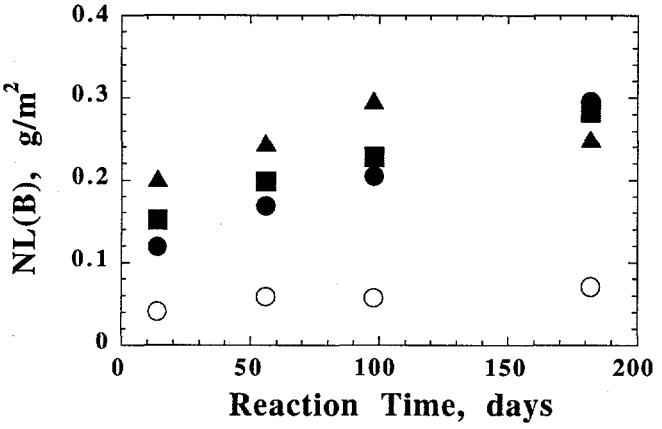

Fig. 12. Normalized Mass Loss for PCT Tests with 51S Glass in EJ-13 at (a) 2000 m^{-1} and (b) 20,000 m^{-1} Based on B (●), Li (■), Na (▲), and Si (○). Results are the average of duplicate tests.

Table 5. Results of Tests with 51R, 51S, and SRL 202 Glasses at 20,000 m^{-1} in EJ-13 Water

			Concentration, mg/L			
Glass	Time, days	pH	[Li]	[B]	[Na]	[Si]
51R	14	11.18	5.26	53.6	162	327
	14	11.24	4.80	52.0	152	315
51S	14	11.18	3.85	53.9	309	275
	14	11.22	4.10	54.9	292	257
	56	11.42	4.53	76.0	327	322
	56	11.51	5.48	77.6	354	351
	98	11.30	2.24	93.8	441	381
	98	11.34	2.78	94.3	427	341
	182	11.42	1.73	135	315	383
	182	11.46	1.87	136	360	413
SRL 202[a]	14	10.98	11.6	97.6	336	325
	14	11.01	11.3	99.9	336	331
	56	11.24	1.82	155	510	388
	56	11.33	2.29	155	505	394
	98	11.26	1.45	190	593	526
	98	11.43	1.51	177	561	530
	182	10.92	<1.99	260	747	508
	182	11.29	<1.68	287	774	532
	364	12.03	1.61	3220	6790	1400
	364	12.02	1.38	2606	5590	1350

[a]From Ref. 28.

e. Future Studies

A total of 13 tests with 51S glass and 22 tests with 51R glass remain in progress. Three tests with 51S and 10 tests with 51R are scheduled to be completed during FY 1996. The solutions and reacted solids will be analyzed to characterize the corrosion mechanism, measure the dissolution rate, and determine the dispositions of radionuclides. The remaining tests will continue beyond FY 1996. The evolution of the solution chemistry and the formation of alteration phases will be modeled using geochemical equilibration codes when more data become available. The dissolution rates will be calculated as corrosion progresses for comparison to the long-term corrosion rates of other glasses.

3. Long-Term Intermittent Flow Tests with SRL 200 Glass

The long-term intermittent flow tests are being conducted using a modified version of the Unsaturated Test Method, or drip test procedure, developed by the YMP, to assess glass performance in an unsaturated environment [29,30]. The standard drip test matrix was modified to include effects of aging both the glass and metal components to make the results more relevant to an actual storage environment. The tests are being performed with 200R glass, and the objectives of the tests are to provide (1) data that describe the release of radionuclides from a specifically designed waste package under strictly controlled test conditions and (2) information concerning synergistic effects that may occur between waste package components. Radionuclide release is evaluated as both the amount dissolved in solution and the fraction associated with particles

suspended in solution. Data from these tests provide bounding values for radionuclide release from glass under conditions of slow water ingress; the test mimics such conditions because the water flow path is relatively constrained from input to when it drips from the waste package.

a. Status

The test matrix is shown in Table 6. There are two sets of five replicate tests and one blank test. The test periods have been modified from the matrix presented in the FY 1991 report [31] to collect more solution for analyses and to allow for more flexibility in hot-cell operations.

The first set of five tests (N4-1 to N4-5) is being done with aged components. The glass was aged by contact with water vapor at 200°C. This reaction accelerated hydration of the glass such that the outer surface of the glass was transformed into stable crystalline phases. Two degrees of hydration aging were obtained by reacting the glass samples for two and four weeks. Two tests (one batch and one continuous) are being done with the four-week hydrated glass, and three tests (one batch and two continuous) are being done with the two-week hydrated glass. The hydration of glass in a vapor environment is not only a process that can be used to age the glass in the laboratory, but also a process that likely will occur in the repository. Glass aging could occur in a steam environment if containment breach occurs before the temperature of the waste package cools below 95°C. However, the rate of aging is expected to be low under these conditions because, while the atmosphere is steam saturated, the relative humidity drops below 100% because the pressure remains at ambient. Glass reaction in vapor where the relative humidity is less than 80% is known to be quite slow.

Glass aging could also occur in a vapor environment if a breach occurred at a temperature below ~95°C prior to ingress of liquid water. This case is the expected environment for the unsaturated repository; thus, the present tests are being done to induce a degree of vapor hydration aging that likely will occur in the repository. However, a direct relationship between temperatures and the aging rate for 200R glass has not been established, so the relative aging imparted to the glass is not known with certainty. It is anticipated that the relationship between time, temperature, and extent of vapor hydration will be developed by the YMP.

The second set of five tests (N4-6 to N4-10) is being performed with unaged or as-cast glass, and the results will be comparable with previous test series using the Unsaturated Test Method [30]. These tests represent the scenario in which the container and pour canister are breached at a time after liquid water has penetrated the waste package environment and liquid water immediately passes through one breach, contacts and reacts with the glass, and passes out through a second breach. This scenario is unlikely; nevertheless, it represents a bounding condition with fresh glass, and the results will form a basis for comparison with tests done with aged components.

There has been some variance from the matrix in that sampling was done at the 85- and 114-week periods, and two tests (N4-3 and N4-7) were terminated at the 114-week period. The sampling periods were adjusted from the original matrix to allow more water to be collected for analysis. This change was required because a series of solution filtrations was added to investigate particle size distribution in solution, and these filtrations required ideally 1-2 mL of solution.

Table 6. Test Matrix for Long-Term Intermittent Flow Tests at High S/V Ratios

Test No.	Test Type[a]	Components[b,c]	Test Duration, weeks 0	18	55	85	114	143	169	195	221	247
N4-1	Batch	4-week-aged glass & 304L SS holder	———									
-2	Continuous	4-week-aged glass & 304L SS holder	———	√	√	√	√	√	√	√	√	→
-3	Batch	2-week-aged glass & 304L SS holder	———									
-4	Continuous	2-week-aged glass & 304L SS holder	———	√	√	√	√	√	√			→
-5	Continuous	2-week-aged glass & 304L SS holder	———	√	√	√	√	√	√			→
-6	Batch	glass, 304L SS holder	———									
-7	Batch	glass, 304L SS holder	———									
-8	Continuous	glass, 304L SS holder	———	√	√	√	√	√	√			→
-9	Continuous	glass, 304L SS holder	———	√	√	√	√	√	√			→
-10	Continuous	glass, 304L SS holder	———	√	√	√	√	√	√			→
-11	Continuous	blank	———	√	√	√	√	√	√			→

[a]The continuous tests are sampled approximately every 26 weeks after the 143-week period.

[b]In tests 6-10, the 304L SS holder is partially sensitized; in tests 1-5, the 304L SS holder is partially sensitized and then subjected to an aging process along with the glass.

[c]In tests 6-10, the glass is unaged (as-cast). In tests 1-5, the glass is aged as indicated in the text.

b. Results and Discussion

The tests were sampled at six-month intervals during FY 1995, in March and September. After the September sampling, the tests had been in progress for 221 weeks. At each sampling period, the solutions were analyzed for cations, anions, total and organic carbon, pH, and radioelements, and the distribution of radioelements between dissolved, suspended (colloidal), and precipitated (sorbed) fractions was evaluated. The size distribution of the colloids was obtained via a sequential filtering technique, whereby an aliquot of the test solution was passed through a relatively coarse filter (1 μm) and then centrifuged through a 30,000 MW polysulfane membrane with a nominal port size of ~4 nm. Any material that passed through the membrane was considered to be dissolved. Material trapped on the 1 μm filter is colloidal and will be investigated after dissolution of the filter. To further evaluate the colloidal fraction, a small portion of the test solution was passed through a perforated carbon grid. The colloidal material retained on the grid can be studied using TEM (see Sec. X).

The results of the solution analyses are shown in Table 7. Initially, there was a significant difference in the reaction and subsequent solution composition for the aged and as-cast glass. The solution pH values for the aged glass were consistently in the 11.0 to 11.7 range, while the as-cast glass solutions had pHs of about 8. With continued testing, however, the differences in solution chemistry are diminishing.

Major glass cations (such as Li, B, Na, and Si) were initially detected in solution at levels several hundred times greater for the aged glass than for as-cast glass [13]. This probably occurs because not all of the major elements are incorporated into stable alteration products as the glass is aged and forms a hydrated layer; thus, they are readily rinsed from the surface during initial contact with liquid water. As with other indicators of solution chemistry (see above), the amounts of the major elements in solution have been steadily decreasing throughout the duration of the test. The results for Li and B, two elements that are normally released most rapidly from glass, are shown as total elemental release in Tables 8 and 9.

While normalized release values could be calculated for the as-cast glass by employing the rationale used in analyzing the long-term test results of drip tests on SRL 165 [IV-18], a normalized release from the hydrated glass was more difficult to determine because of the unknown surface area that contacts the test solutions. For the as-cast glass tests (N4-8 and N4-9), the release trends were similar in that the release was initially small and then increases by about an order of magnitude (B release) for several years. The release of Li was less than B, which is to be expected based on the compositions shown in Table 1; however, the ratio of B release to Li release suggests that Li may be incorporated to a small extent into a secondary phase. This phase is probably the clay phase that forms on the surface of the glass. Evidence of the clay phase is shown in Fig. 13, which is an optical image of the reacted glass surface after the last sampling period. The spallation of the reacted layer is clearly marked by the patches of black glass visible beneath the layer. The micrographs are taken from a video image, so the normal sampling routine could continue. That is, the samples did not dry and crack because they were out of the reactive environment for only about two minutes.

The releases from the tests with the vapor-hydrated glasses were at least three orders of magnitude greater than from the as-cast glass (note that the values in Table 9 are in milligrams). The trend in all of these tests is for declining releases, essentially for the entire test period. The release of Li was significantly less than that of B, suggesting that during the hydration process Li was incorporated into a secondary phase and was not as readily rinsed from the

Table 7a. Analyses of pH, Carbon, and Anions in Leachates from the Drip Tests with As-Cast Glass

Test No.	Sampling Period[a]	pH	Carbon (ppm)		Anions (ppm)							
			Organic	Inorganic	F^-	CHO_2^-	Cl^-	NO_2^-	NO_3^-	HPO_4^{2-}	SO_4^{2-}	$C_2O_4^{2-}$
8	10/31/91	7.97	15	15	4.6	<0.5	7.5	5.2	3.3	<1	104	2.8
	7/16/92	8.26	8	25	7.6	b	14	15	2.5	<1	38	11
	2/11/93	6.73	13	5	2.0	14	1	3	2.1	<1	6	11
	9/2/93	7.40	9	4	4.0	13	29	1	3.5	<1	23	6
	3/24/94	7.80	3	10	41.0	18	10	24	9.1	<0.5	48	14
	9/22/94	7.75	2	11	12.0	19	8	11	7.2	<0.5	22	<1
	3/23/95	8.05	20	10	10	<5	29	22	44	<10	86	20
	9/21/95	8.20	13	21	18	14	13	21	7.2	3.2	42	—
9	10/31/91	8.12	10	20	9.3	<0.5	9.4	9.0	4.0	<1	10	<0.7
	7/16/92	7.94	13	13	8.5	b	20	23	4.3	<1	60	11
	2/11/93	5.61	10	3	1.2	b	1.5	2	2.8	1.0	13	11
	9/2/93	7.94	27	149	61	188	73	11	184	<1	294	332
	3/24/94	7.58	3	5	34	14	6	44	28	<0.5	28	8.8
	9/22/94	7.60	0	2	<0.2	<0.5	1.6	0.4	2.9	<0.5	3.3	<1
	3/23/95	8.29	21	17	20	<5	25	16	23	<10	67	8.9
	9/19/95	8.56	11	27	63	<10	52	20	76	5	175	—
10	10/31/91	8.60	20	25								
	7/16/92	8.55	13	35	5.3	b	5.2	6.7	2.4	<1	18	10
	2/11/93	6.42	12	3	1.5	12	1.4	2.1	2.5	<1	11	9.2
	9/2/93	8.72	25	32	20	30	20	5.3	6.2	<1	31	2
	3/24/94	8.03	5	12	32	10	13	53	65	<0.5	39	5.2
	9/22/94	8.65	2	33	24	25	25	33	11	<0.5	62	<1
	3/23/95	8.16	18	10	25	<5	39	21	24	<10	79	17
	9/19/95	8.22	8	17	13	12	16	26	5.6	<0.5	49	—
6	terminated	8.45	11	36	5.7	b	10	13	1.9	<1	81	7.8
7	terminated	9.14	32	33	4.4	4.6	11	3.1	4.3	<1	55	3.8

contd.

Table 7b. Analyses of pH, Carbon, and Anions in Leachates from the Drip Tests with Aged Glass

Test No.	Sampling Period[a]	pH	Carbon (ppm)		Anions (ppm)							
			Organic	Inorganic	F^-	CHO_2^-	Cl^-	NO_2^-	NO_3^-	HPO_4^{2-}	SO_4^{2-}	$C_2O_4^{2-}$
2	11/4/91	11.28	145	20			167	<15	<25	193	5660	<50
	7/20/92	11.27	108	6	11	b	71	<15	42	169	781	56
	2/15/93	11.26	140	77	6	<1	7	30	8	135	171	61
	9/7/93	11.68	28	141	12	79	25	5.5	31	274	151	<30
	3/28/94	11.48	12	134	6	35	13	53	56	149	60	35
	9/26/94	11.50	7	135	20	<1	14	20	17	141	52	<1
	3/27/95	10.93	50	97	26	59	85	39	252	50	239	213
	9/25/95	10.91	32	80	9	21	14	21	12	19	56	—
4	11/4/91	11.37	21	4			211	<15	<25	397	9870	<50
	7/20/92	11.13	113	210	11	b	47	<15	40	168	815	60
	2/15/93	11.62	52	77	11	22	11	22	7	147	162	69
	9/7/93	11.48	29	90	16	74	31	3.4	20	150	175	<30
	3/28/94	11.48	7	93	19	<10	11	30	26	70	53	18
	9/26/94	11.50	6	107	17	<1	13	18	20	78	47	<1
	3/27/95	11.39	32	64	24	45	73	32	203	48	196	33
	9/25/95	11.17	41	96	9	18	12	16	9.1	26	44	—
5	11/4/91	11.33	35	0			256	<15	<25	334	8840	66
	7/20/92	11.43	96	6	13	b	36	<15	44	197	886	<50
	2/15/93	11.27	44	90	8	24	14	23	7	140	209	80
	9/7/93	11.38	33	79	12	86	31	3.7	20	78	137	<30
	3/28/94	11.19	12	108	11	<10	10	39	68	24	65	18
	9/26/94	11.34	10	144	12	<1	11	17	16	25	51	<1
	3/27/95	11.39	21	79	15	<5	28	26	42	39	83	16
	9/25/95	11.36	32	89	11	23	13	16	14	44	46	—
1	terminated	11.09	125	15	29	b	58	<15	74	286	2376	59
3	terminated	11.11	212	11	12	117	38	5.4	9.3	138	87	<30

[a]Tests 6-10 were initiated on 6/23/91 and tests 1-5 on 7/1/91.

[b]The F^- and CHO_2^- peaks were not resolved; thus, the values reported for F^- include a factor due to CHO_2^-. Because the starting concentration of F^- in the EJ-13 water is ~3 ppm, the contribution due to CHO_2^- is significant.

Table 8. Elemental Release, As-Cast Glass

Test #	Sampling Period	Elemental Release, μg[a] B	Li
8	10/31/91	2	9
	07/16/92	33	17
	02/11/93	17	2
	09/02/93	18	2
	03/24/94	59	22
	09/22/94	15	6
	03/23/95	39	8
	09/21/95	57	4
9	10/31/91	3	6
	07/16/92	29	8
	02/11/93	24	3
	09/02/93	NR[b]	NR
	03/24/94	65	19
	09/22/94	4	1
	03/23/95	30	4
	09/20/95	30	2
10	10/31/91	81	21
	07/16/92	60	28
	02/11/93	20	3
	09/02/93	17	17
	03/24/94	56	17
	09/22/94	16	4
	03/23/95	3	17
	09/21/95	3	38
6	07/16/92	46	52
7	09/07/93	139	66

[a]Amount of each element detected in the leachate for the designated sampling period.

[b]No solution remained in the test vessel at the end of the sampling period. The vessel was rinsed and the rinse solution was analyzed but no data are reported.

Table 9. Elemental Release, Aged Glass

Test #	Sampling Period	Elemental Release, mg[a] B	Li
2	11/04/91	41.6	2.3
	07/20/92	22.1	1.6
	02/15/93	8.4	0.7
	09/07/93	0.4	0.7
	03/28/94	2.2	0.7
	09/26/94	0.5	0.3
	03/23/95	0.3	0.5
	09/21/95	0.2	0.2
4	11/04/91	39.4	2.2
	07/20/92	19.4	1.2
	02/15/93	7.7	0.5
	09/07/93	4.1	0.5
	03/28/94	1.5	0.3
	09/26/94	0.6	0.3
	03/23/95	0.4	0.3
	09/21/95	0.3	0.3
5	11/04/91	32.6	1.6
	07/20/92	24.8	1.4
	02/15/93	9.3	0.7
	09/07/93	4.2	0.5
	03/28/94	2.2	0.3
	09/26/94	0.8	0.2
	03/23/95	0.8	0.3
	09/21/95	0.6	0.3
1	07/20/92	53.6	3.4
3	09/07/93	6.3	0.3

[a]Amount of each element detected in the leachate for the designated sampling period.

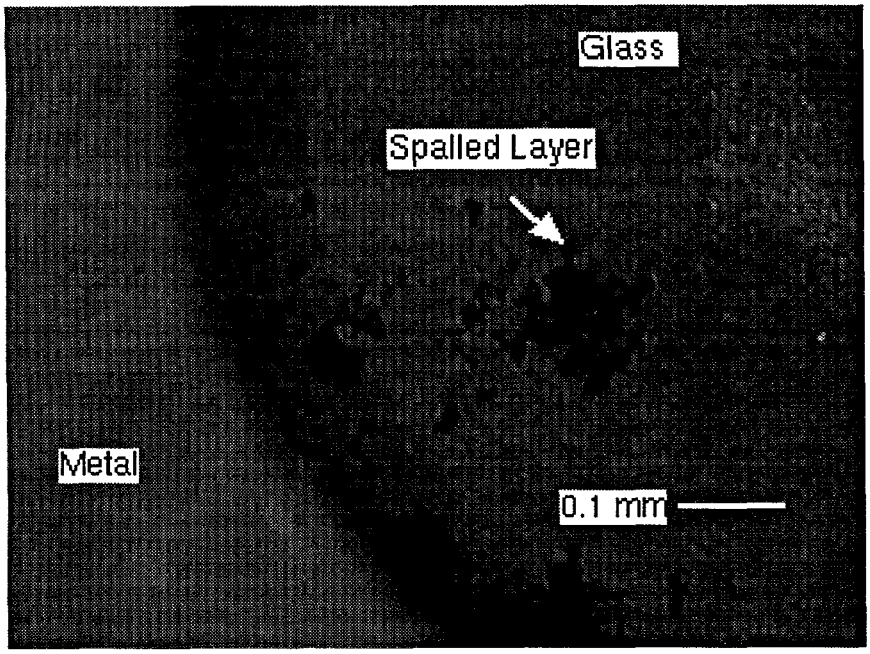

Fig. 13. Optical Micrograph of a Portion of the Top Glass Surface of Test N4-9 Showing Where the Reacted Layer is Spalling from the Glass

hydrated glass as B. An image from the surface of test N4-5 is shown in Fig. 14. This image shows that the glass is covered with alteration phases that formed during the initial hydration but that a large amount of a white, fibrous material is also forming. This fibrous material also formed on the metal surfaces.

Anion release provides perhaps the most striking and significant difference in the solution chemistries between the two test types. Anion concentrations in starting glasses are generally not reported because they are minor components (<0.1 wt %), are difficult to analyze, and are thought to have little effect on glass reactivity when present in low levels. However, the potential for anions to complex radionuclides [13] adds significance to their concentrations in the leachates. As is presented in Table 7, the concentrations of SO_4^{2-}, Cl^-, and HPO_4^{2-} in the leachates from the aged glass tests (1-5) were initially in the 150 to 10,000 ppm range, which is significantly larger than the concentrations in the starting EJ-13 water or in the leachates from the as-cast glass tests. As the tests continued, the concentration of anions in solution decreased, suggesting that these elements are rapidly rinsed from the hydrated glass surface. The release of anions has stabilized over the past year, suggesting that much more of these components has been rinsed from the hydrated glass.

To report accurate and consistent actinide release values for these tests, the leachates must be analyzed by a combination of analytical techniques. The results from different techniques are being compared to deconvolute isobaric interferences in ICP-MS measurements and to deconvolute alpha spectra for which the energy resolution is not sufficient to quantify certain radionuclides. We calculate the ^{238}Pu concentration of each sample by subtracting the ^{241}Am activity contribution to the $^{238}Pu+^{241}Am$ peak measured using alpha spectrometry. Leachate solutions have been analyzed using alpha spectrometry of aliquots prepared by electrodeposition or evaporation. Results from analyses of individual samples prepared by both methods are being

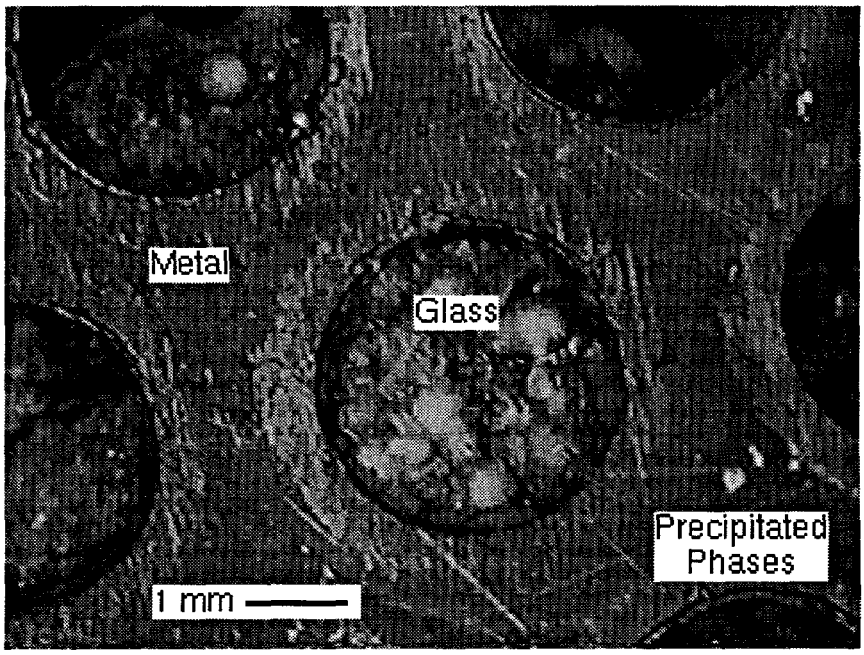

Fig. 14. Optical Micrograph of the Center Section of the Top of Test N4-5, Showing a Fibrous, White Precipitate That Forms on Both the Hydrated Glass (Center Circular Region) and on the Metal Surface

compared to assess each method of preparation and interpret any differences. Additionally, filters of decreasing pore size, which were used to sequentially filter leachate solutions, have been analyzed by alpha spectrometry. Leachate solutions have also been analyzed using ICP-MS and gamma spectrometry. Samples generated from the March and September 1995 sampling periods have been analyzed and are being compiled and reviewed along with data from all previous sampling periods.

Data from all samples analyzed using gamma spectrometry are currently being verified. To calculate normalized release rates for a given radionuclide, the concentration of that radionuclide in the glass must be determined. If the half-life of the radionuclides is on the same order as the test duration, it may be necessary to correct for changing concentration in the glass. This correction is necessary for all of the radionuclides measured by gamma spectrometry with the possible exception of ^{241}Am. A spreadsheet has been generated that calculates the concentration of ^{241}Am, ^{60}Co, ^{134}Cs, ^{137}Cs, ^{152}Eu, ^{154}Eu, ^{155}Eu, and ^{125}Sb in 200R glass at any given time. The concentration of these radionuclides calculated at the midpoint of each sampling period will be used to calculate normalized release for that sampling period. Total releases and normalized releases are currently being calculated for radionuclides determined by gamma spectrometry using this correction.

Some indication of the distribution of radionuclides and species in solution can be obtained by examining particles isolated on perforated-carbon TEM grids. The solutions from tests N4-6 and N4-10 wicked easily through the grid and produced good samples for analysis. The solutions from the aged glass reaction had a large salt content and were wicked with more difficulty through the grid. While the salt content disrupts the clear distinction of colloidal particles, some discrete colloids were identified. A full discussion of the examination of colloids

from these tests is given in Sec. X, but in test N4-9, which is shown in Fig. 13, a large amount of colloidal material was detected on the grids; this observation corresponds to the observed spallation of the clay layer from the glass.

c. Future Studies

The ongoing drip tests will be sampled according to the schedule in Table 6. The components (glass and metal) from the terminated tests will be analyzed to determine the mass balance of the reaction progress. The data collected through the scheduled March 1996 sampling period will be compiled into an ANL topical report.

4. Long-Term Repository Environment Tests

The "laboratory analog" test [32] was developed to relate the performance of glass as observed in the Unsaturated Test with a more repository-relevant environment. In the laboratory analog test, the waste package assemblage (WPA), like that used in the Unsaturated Test, is placed within a bored-out cavity in a tuff core. The dimensions of the WPA and the cavity are similar to those used in the Unsaturated Test. A sketch of the apparatus can be found in previous reports in this series [1-5]. The tuff core and WPA are assembled, and an unsaturated flow of water is forced through the core by using a vapor pressure slightly above ambient.

The objective of this test is to evaluate glass performance in an environment that closely matches that expected in the repository. Emphasis is placed on measuring glass reaction by examining the reacted glass and surrounding tuff rock at the test termination and by monitoring the radionuclide content of the groundwater as it is released from the test vessel. The tuff used in these tests is an outcrop sample taken from the same location as will be used for the large-scale block tests currently planned by the YMP. Thus, while not from the repository horizon, the tuff is similar to that expected for the repository site. The rock was conditioned by pouring water through it prior to testing to rinse out surface deposits; however, the focus of our analyses will be the radionuclide content of the effluent, not the chemical composition.

a. Status

On December 19, 1991, two analog tests were started using 200R glass. One test uses unaged glass and a sensitized 304L stainless steel retainer; the other uses three-week-aged glass and stainless steel. The tests have been ongoing for 208 weeks, and the water that passes through the cores is collected at selected intervals. The tests are being run at two different flow rates: the unaged glass has a flow rate of 0.02 mL/h, and the aged glass a flow rate of less than 0.005 mL/h. The effluent has been collected and periodically checked for gross radioactivity. To date, no indication of activity in the solution has been detected.

b. Results and Discussion

The tests are working as expected, in that water is passing through the cores, and no radioelements have been detected with gross counting methods. A more extensive analysis of the condensed solution will be needed to confirm this preliminary result.

c. Future Studies

The tests will continue, with periodic monitoring of the effluent, and the solutions will be subjected to extensive analysis.

IV. RELATIONSHIP BETWEEN HIGH S/V EXPERIMENTS AND MCC-1

A. Introduction and Background

Static dissolution tests are being conducted to characterize the long-term corrosion behavior of two borosilicate glasses representative of glasses that may be produced during operation of the DWPF. The glasses are being tested at four different S/V ratios to assess the effect of this parameter on the corrosion mechanism, glass dissolution rate, and disposition of radionuclides. Tests are being conducted at the S/V ratios specified by two standardized tests and at two higher S/V ratios. The MCC-1 Static Leach Test [33] specifies the use of monolithic samples and an S/V ratio of 10 m^{-1}. Tests are being conducted following the MCC-1 procedure at 10 m^{-1} and also at 340 m^{-1}. The Product Consistency Test (PCT) Method A [34] specifies the use of crushed samples and an S/V ratio of 2000 m^{-1}. Tests are being conducted following the PCT procedure at 2000 m^{-1} and also at 20,000 m^{-1}. The higher-than-specified S/V ratios that are used are the highest practical values for tests with monoliths and for crushed glass of the -100 +200 mesh size fraction that provide enough solution for complete analysis.

This Task was initiated to study how the S/V ratio used in a static dissolution test affects the corrosion rate and mechanism of glass dissolution and the release of radionuclides from vitrified high-level waste forms. Variation of the S/V in static dissolution tests can be used to simulate conditions in which the waste form is contacted by large or small volumes of groundwater during storage, to determine the corrosion mechanism under different environmental conditions, and to accelerate the corrosion process to provide insight regarding the durability of high-level waste forms over geologic time periods relevant to repository isolation. In addition, these tests will provide insight into whether the results of short-term tests, including MCC-1 and PCT, can be used to infer long-term behavior.

Tests have shown the major effect of the S/V ratio on the glass reaction to be through dilution of the corrosion products. Since the rate of glass reaction is known to depend on the solution chemistry (particularly the silicic acid concentration and the pH), differences in dilution of dissolved corrosion products in tests at different S/V ratios will affect the reaction response of a particular glass. Both the rate-controlling process and the rate of glass reaction may change as the S/V ratio is varied. Under the dilute conditions that are maintained in tests at low S/V ratios, ion exchange reactions dominate the observed corrosion behavior. Under conditions attained in short-term tests conducted at high S/V ratios, hydrolysis reactions generally dominate the observed corrosion behavior. At advanced stages of corrosion, alteration phases may affect the dissolution rate. To project the long-term glass durability, it is important to understand how the results of specific tests relate to the overall glass corrosion process.

The effect of the S/V ratio on the behavior of individual radionuclides must also be known to assess the performance of a waste form and a waste disposal system. While much is known about the chemistries of various radionuclides in aqueous solutions, little is known regarding the effects of glass corrosion on the disposition of radionuclides between the solution and reacted glass. Glass corrosion will affect the pH and Eh of the solution, will supply species that may complex actinide species and form solubility-controlling phases, and will generate colloids and secondary phases that may sorb actinides. The effects of glass corrosion on the disposition of radionuclides must be taken into account when assessing the long-term behavior of high-level waste glasses during repository storage. Other studies have characterized the disposition of radionuclides under highly dilute conditions in which the buildup of glass corrosion products in the solution has no significant effect on the disposition. Tests in this Task allow direct comparison of the disposition of radionuclides under the dilute conditions maintained in tests at low S/V ratios to that under highly concentrated conditions attained in tests at high S/V ratios. Tests were conducted using glasses doped with Tc, U, Np, Pu, and Am to measure their disposition between the glass,

leachate, the reaction vessel, and alteration phases in tests at different S/V ratios and at different stages of the corrosion process.

B. Objectives

The primary objective of this Task is to assess the effects of the S/V ratio used in a static dissolution test on the mechanism and rate of the glass reaction over both short test periods relevant to testing product consistency and long test periods relevant to projecting long-term glass stabilities. Tests in this Task have been designed to monitor changes in both the leachate composition and the reacted glass surface as a function of the S/V ratio, the reaction time, and the initial leachant solution composition. Tests were performed with glasses doped with radionuclides having long half-lives to monitor their disposition as the reaction proceeds. In addition, the results of these tests provide insight regarding how tests performed at different S/V ratios are related, whether the S/V ratio can be used as an accelerating parameter for static dissolution tests, how the S/V ratio influences the assemblage of alteration phases that forms, and what the long-term glass reaction rate is under the conditions attained in the different tests.

An additional objective is to describe the corrosion mechanism of glass compositions relevant to high-level waste disposal. These tests generate corroded glass samples that show the glass alteration during all stages of the corrosion process, that is, both when corrosion is controlled by dilute and concentrated solution conditions and when it is affected by alteration phases. Detailed analysis of the reacted solids provides a valuable description of the process by which the alteration layers form on the glass surface and how they interact with radionuclides.

C. Technical Approach

Tests were performed with glasses made at ANL from frits SRL 131 and SRL 202 that were supplied by the SRTC. The SRL 202 composition is a reference composition for blended tank wastes at the Savannah River Site [35], while the SRL 131 composition was developed as a reference glass based on earlier estimates of tank waste compositions at the Savannah River Site. The SRL 131 glass is known to be less durable than the SRL 202 glass in short-term tests, and tests were conducted using SRL 131 to assure that advanced stages of corrosion would be attained within the testing program. Both glasses were doped at ANL with Tc-99, natural U, Np-237, Pu-239, and Am-241 at levels of about 0.003, 2, 0.01, 0.01, and 0.0004 elemental mass %, respectively. These glasses are referred to as SRL 131A and SRL 202A. Another glass was prepared by doping SRL 202 frit with uranium only. This glass is referred to as SRL 202U. The glass compositions are presented in Table 1b. (The SRL 202U composition is the same as the SRL 202A composition, except it does not contain Tc, Np, Pu, or Am.)

Monolithic disk samples about 10 mm in diameter and 1 mm thick were prepared for use in the tests at 10 and 340 m^{-1}. All surfaces were polished to a 600-grit final finish with SiC paper and water lubrication. The fraction of crushed glass that passed through a 100 mesh (140 μm) sieve but was retained by a 200 mesh (74 μm) sieve was separated for use in the tests at 2000 and 20,000 m^{-1}. The glass was washed per the PCT procedure [34].

The leachant was prepared by reacting tuff groundwater from well J-13 with pulverized tuff rock for about 28 days at 90°C to simulate interaction between the rock and groundwater in a repository. The resulting solution was cooled and filtered to remove any suspended tuff particles, and is referred to as EJ-13 water. The composition is given in Table 2. Some tests with SRL 202U glass were conducted using deionized water.

Tests were conducted at 10 and 340 m^{-1} following the MCC-1 protocol [33] by reacting one or four monolithic samples with about 17 or 2 mL of EJ-13 water, respectively. Tests were conducted with crushed glass at 2000 and 20,000 m^{-1} following PCT method B [34] by reacting

either 1 or 5 g of crushed glass with either 10 or 5 mL of EJ-13 water, respectively. Tests with SRL 202A and SRL 131A glasses were conducted in 304L stainless steel reaction vessels at 90°C. Tests with SRL 202U glass were conducted in Teflon reaction vessels at 90°C.

After the scheduled test duration, the vessels were removed from the oven and opened. The leachate solutions and reacted glasses were removed for analysis. The leachates were removed while still hot to avoid thermal effects, such as precipitation of solids or flocculation of colloids. Small portions of some solutions were filtered through holey carbon grids used for TEM to isolate suspended solids for later analysis. Aliquots were also removed for analysis of transuranic. The remaining solution was then filtered through a preheated 450-nm pore size cartridge filter. A portion of the filtrate solution from some tests was additionally filtered through an Amicon model CF50A filter, which has an effective pore size of about 6 nm. Solutions were analyzed for pH (with a combination electrode), anions (with ion chromatography), Tc and U (with ICP-MS), and transuranics (with alpha spectroscopy). Aliquots of the unfiltered leachates or the 450-nm filtrate solutions were retained for analysis of radionuclides.

The reacted glass was gently rinsed with deionized water and then removed from the vessel and allowed to dry. The vessel was then filled with a nitric acid solution and placed in a 90°C oven for about 16 hours to dissolve any transuranics that had become fixed to the stainless steel surface. An aliquot of this solution was analyzed with alpha spectroscopy. Some solutions were also analyzed with ICP-MS.

Some of the reacted solids were analyzed with an optical microscope, SEM, and AEM. Both the SEM and AEM are equipped with X-ray spectrometers for compositional analysis, and the AEM provides selected area electron diffraction (SAED) for structural analysis. Alteration phases found distributed among the reacted grains were isolated and analyzed separately.

D. Results and Discussion

Results of testing and analyses have been published elsewhere [36-49]. In this report, we focus on the dissolution rates that have been measured in these tests, and on the effect that the decrease in the surface area of the glass samples as the glass dissolves has on the calculated rate. The dissolution rate of a waste glass is important because it is the maximum rate at which radionuclides can be released from the glass into the groundwater, although most radionuclides will be released into solution at rates that are significantly less than the dissolution rate of the glass because of their solubility limits and retention in reaction products.

According to the DWPF Glass Product Control Program, glasses produced at the DWPF must consistently perform better than the SRL EA glass when measured in a PCT Method A test (i.e., a 7-day test in deionized water at an effective S/V ratio of 2000 m^{-1} and at 90°C). "Performance" in the PCT Method A test refers to the concentrations of boron, alkali metals, and silicon measured in the solution after the test; the concentrations of these elements in tests with any product glasses must be less than their concentrations in tests with the EA glass.

The dissolution rate calculated from the PCT test is an average rate over the 7-day test period. Different rates are calculated for tests conducted for different time periods. A general expression for the normalized dissolution rate can be written as

$$NR(B) = \frac{\{NL(B)_{t2} - NL(B)_{t1}\}}{(t_2 - t_1)} \quad (1)$$

or

$$NR(B) = \frac{\{C_{Bt2} - C_{Bt1}\}}{\left\{\left(\frac{S}{V}\right) \bullet f_B \bullet (t_2 - t_1)\right\}} \quad (2)$$

where $NL(B)_{t1}$ and $NL(B)_{t2}$ are the normalized mass losses based on the boron concentrations at reaction times t_1 and t_2, respectively. The concentrations of boron (in mg/L) at times t_1 and t_2 are given as C_{Bt1} and C_{bt2}, and f_B is the mass fraction of boron in the glass. For a PCT Method A test, t_1 is 0 days and t_2 is 7 days.

We have calculated the average dissolution rates based on the boron concentrations attained in 7-day PCT and long-term PCT for comparison. The results are presented in Table 10 in three groups: 7-day PCT rates, rates representing Stage II reaction under "saturated" conditions, and rates representing the long-term dissolution rate in Stage III after alteration phases that increase the rate have formed. The rates in Stages II and III were calculated from the values of NL(B) measured at two reaction times deemed to represent the beginning and end of that Stage. The calculated rates are the average rates over the specified time periods. The times in Table 10 refer to the test durations used to calculate the accompanying rates and the times over which the rates were averaged. The final pH of the test with the longest duration is included in the table.

The dissolution rates of the SRL EA glass measured in other tasks are included in Table 10 for comparison. The rate is lower in EJ-13 water than in deionized water because of the approximately 40 mg/L of silicon in the EJ-13 water. The dissolution rate of SRL EA glass decreases significantly in Stage II as the silicic acid concentration increases, but increases significantly after zeolite alteration phases form (see Sec. VI). The results of long-term tests with SRL EA glass that were conducted at 20,000 m^{-1} are included for comparison. Note that the dissolution rates in Stage III are about the same for tests conducted at S/V ratios of 2000 and 20,000 m^{-1}. This occurs because similar pH values are attained in tests at both S/V ratios and the same alteration phases are formed (see Sec. VI).

The dissolution rate of SRL 131A glass measured in a 7-day PCT in EJ-13 water is 0.16 g/(m^2•d). This is about 13 times less than the dissolution rate of SRL EA. The dissolution rate in a PCT conducted at 20,000 m^{-1} is 0.69 g/(m^2•d). The rate is higher in the test conducted at 20,000 m^{-1} than in the test at 2000 m^{-1} because of the higher pH value that is attained. The dissolution rates of several waste glasses are known to increase by a factor of about 2.5 for each unit increase in the pH value [50-52]. Likewise, the rate in Stage III is slightly higher in tests conducted at 20,000 m^{-1} than in tests conducted at 2000 m^{-1} because of the higher pH attained in the tests at 20,000 m^{-1}. The long-term dissolution rate of SRL 131A glass is about four times less than the rate of SRL EA glass, at similar pH values.

The compositions of the SRL 202A and SRL 202U glasses differ only in that minor amounts of doped radionuclides are included in the SRL 202A glass. As expected, the dissolution behavior of the two glasses is identical, within experimental uncertainty. In PCT conducted at 2000 m^{-1}, the dissolution rate of SRL 202U in deionized water and the dissolution rate of SRL 202A in EJ-13 water are much lower than the corresponding dissolution rates of SRL EA. Also, the dissolution rate of SRL 202U in deionized water is about twice the dissolution rate of SRL 202A in EJ-13 water. The dissolution rates of SRL 202U and SRL 202A in 7-day PCT at 20,000 m^{-1} in deionized water and in EJ-13 water are all about the same, within experimental uncertainty. Likewise, the long-term rates in Stage III are also about the same. The rates are about five times lower than the long-term rate of the SRL EA glass, although part of the difference (as much as a factor of about 1.3) is due to the lower pH attained in tests with the SRL 202A and SRL 202U glasses. Note that the difference between the rates measured in deionized water and in EJ-13 water is greater in short-term tests than in long-term tests. This is because the solution becomes

Table 10. Dissolution Rates, NR(B), Measured in Tests with SRL EA, 131A, and 202A Glasses[a]

Test Conditions			PCT			Stage II			Stage III		
Glass	S/V, m^{-1}	Leachant	Time, days	Rate, $g/(m^2 \cdot d)$	pH	Time, days	Rate, $g/(m^2 \cdot d)$	pH	Time, days	Rate, $g/(m^2 \cdot d)$	pH
SRL EA[b]	2000	DIW	0-7	1.2[b]	10.3						
SRL EA	2000	EJ-13	0-7	0.65	11.8	7-131	0.0043	12.1	>313	0.18	12.1
SRL EA	20,000	EJ-13							>56	0.19	12.0
SRL 131A	2000	EJ-13	0-7	0.16	10.3	70-140	0.0063	10.7	>70	0.021	11.5
SRL 131A	20,000	EJ-13	0-7	0.69	12.0	56-182	0.015	12.1	>182	0.051	12.2
SRL 202A	2000	EJ-13	0-7	0.025	9.5	280-980	0.00040	10.5			
SRL 202A	20,000	EJ-13	0-7	0.024	10.7	28-182	0.0020	11.3	>200	0.034	11.9
SRL 202U	2000	DIW	0-7	0.055	10.0	140-560	0.00017	10.3	—	—	—
SRL 202U	20,000	DIW	0-7	0.027	11.2	28-182	0.0017	11.5	>200	0.037	11.7
SRL 202U	20,000	EJ-13	0-7	0.028	11.0	28-182	0.0021	11.4	>200	0.044	11.7

[a]All rates were calculated using initial surface area. Stage III rates were calculated from data in which the loss of surface area can be considered to be negligible.

[b]Calculated from Jantzen et al. [8].

dominated by dissolved glass components after very little glass reacts, and the effects of the starting composition of the leachant become negligible. Also note that the Stage III reaction rate of SRL 202 glass is similar to the rate measured in a 7-day PCT Method A test.

1. Accounting for the Loss of Surface Area as Glass Dissolves

The normalized mass loss and normalized dissolution rates are usually calculated using the initial surface area of the crushed glass. The rates given in Table 10 were calculated in this way. However, the surface area of any finite sample will decrease as the glass dissolves. In short-term tests, such as a 7-day PCT, the loss of surface area is usually negligible. However, the surface area will decrease significantly if the glass is highly corroded or if the glass dissolves at a high rate, as it does in Stage III. In that case, the normalized mass loss calculated using the initial surface area of the sample will not correctly reflect the corrosion rate. Instead, the normalized mass loss should take into account the decrease in the available surface area as the glass dissolves.

The effect of the decreasing surface area on the solution concentrations in static dissolution tests can be estimated by assuming that boron released from the glass is totally soluble. An expression for the remaining surface area after glass dissolution based on the measured boron concentration is derived in Appendix A. If the crushed glass is approximated as spherical particles, then the remaining surface area after a reaction time t is

$$S_t = \frac{\left(6 m_o^{1/3}\left(m_o - \frac{m_B}{f_B}\right)^{2/3}\right)}{\rho d_i} \qquad (3)$$

where S_t is the surface area at time t, m_o is the initial mass of glass, m_B is the mass of boron in solution at time t, f_B is the mass fraction of boron in the glass, ρ is the density of the glass, and d_i is the initial diameter of the glass spheres. Figure 15 shows the remaining surface area as 5 g of glass dissolves into 5 mL of solution, based on Eq. 3, for m_o = 5 g, f_B = 0.03, ρ = 2.7, and d_i = 112 μm. The initial surface area is 0.10 m^2. About 80% of the initial surface area remains after about 25% of the glass has corroded.

The loss of available surface area as the glass dissolves can be taken into account in several ways when calculating the dissolution rate. Several variations of the NL(B) results for tests with SRL 202A glass conducted at 20,000 m^{-1} are displayed in Fig. I6. The filled circles give the NL(B) values calculated based on the initial surface area. These values are not adjusted for the effects of the decreasing surface area. The values shown by the diamond symbols were calculated from the measured boron concentration at time t and the calculated surface area at time t-1. The triangles give the values calculated from the measured boron concentration at time t and the arithmetic average of the surface area calculated at times t-1 and t. The open circles give the values of NL(B) calculated using the boron concentration measured at time t and the surface area calculated to remain at time t.

Several points can be made based on the results as plotted in Fig. 16. First, the difference in the NL(B) values adjusted for the loss of surface area is within the uncertainty for solution analysis (which is about ±15%) until NL(B) is greater than about 20 g/m^2. Second, the values calculated using the boron concentration measured at time t and the surface areas at t = 0 and at t are upper and lower bounding values, respectively. The values of NL(B) calculated using the initial surface area are too low, since the surface area must decrease as glass dissolves. However, the NL(B) calculated using the surface area at t = t are too high because the surface area was greater than it is at times prior to time t. In addition, the maximum possible value of NL(B) is 50 g/m^2, assuming the specific surface area of -100+200 mesh glass is 0.02 m^2/g. The value of NL(B)

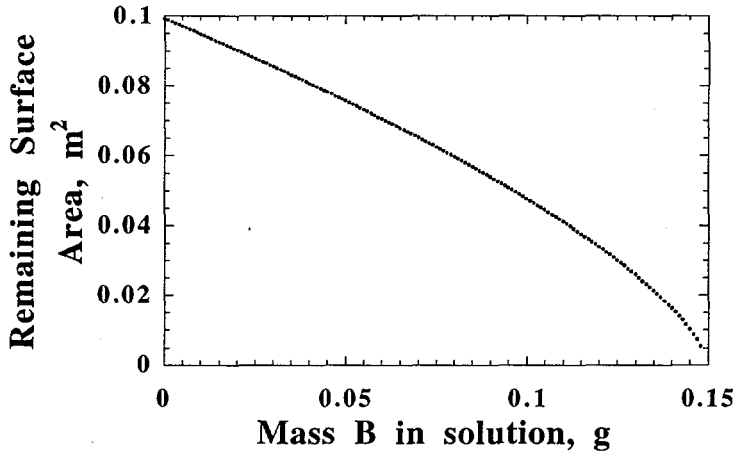

Fig. 15. Calculated Surface Area vs. Amount of Boron in Solution (initial mass of glass, 5 g; solution volume 5 mL; mass fraction of boron, 0.03; glass density, 2.7; assumed initial diameter of glass spheres, 112 μm)

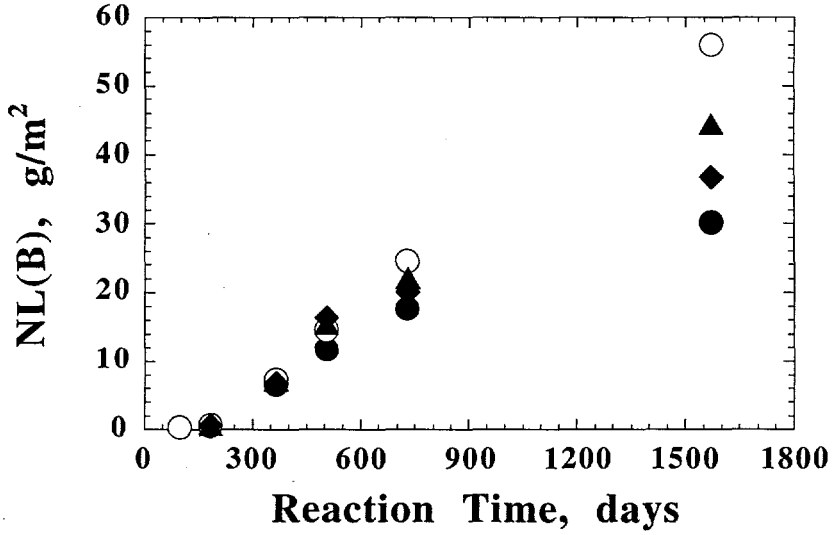

Fig. 16. Values of NL(B) for Tests with SRL 202A Glass at 20,000 m^{-1} Calculated Using Different Surface Areas: Initial Surface Area (●), Surface Area at t (○), Surface Area at t-1 (◆), and Surface Area at (t+(t-1)/2) (▲).

calculated using t = t at about 1600 days is greater than 50 g/m^2. We believe the NL(B) values calculated for time t using the average surface area between times t and t-1 provide the best simple adjustment for the effects of decreasing surface area. The dissolution rate calculated from consecutive test data and with the average surface area is 0.034 ± 0.009 $g/(m^2 \cdot d)$, which is the long-term dissolution rate. As shown in Fig. 16, the rate is only weakly affected by the scheme used to adjust for the loss of surface area for values of NL(B) less than about 20 g/m^2.

That the adjustment of NL(B) to account for the loss of surface area gives a nearly linear fit also indicates that the dissolution rate is nearly constant after formation of zeolite phases between 182 and 364 days. This means that the clay layer that forms at the glass surface has only a minor affect on the glass dissolution rate.

E. Future Studies

Several long-term tests remain in progress. The results of those tests will be used to determine whether the trends observed in tests completed to date continue for longer times. Work is in progress to determine whether an analytical expression for the loss of surface area can be used to adjust the results of tests with crushed glass to account for the loss in surface area as the glass dissolves. Alteration phases generated in tests with the actinide-doped glasses will be examined to identify the phases and determine whether they contain radionuclides.

V. LABORATORY TESTING OF WEST VALLEY REFERENCE 6 GLASS

A. Introduction and Background

The WVDP will vitrify high-level wastes generated during the reprocessing of nuclear fuels. A target composition has been identified by the WVDP for glass to be produced by vitrification. Argonne National Laboratory is assisting the WVDP by conducting laboratory tests using both the fully radioactive glass and a nonradioactive homologue to determine its long-term corrosion behavior. The fully radioactive reference glass has been produced at the Material Characterization Center but has not yet been shipped to ANL. The nonradioactive glass was provided by the Catholic University of America and is referred to as West Valley Reference 6 (WV6) glass. The results of tests performed with WV6 glass will provide insight regarding the corrosion behavior of the fully radioactive glass, since reacted nonradioactive WV6 glass samples can be analyzed more completely. The results of tests with WV6 glass will be used to define the testing matrix for the radioactive glass.

Three types of tests are being conducted: the MCC-1 static leach test, the PCT, and the Vapor Hydration Test. The PCT was developed to verify the consistency of glasses produced by the DWPF. The PCT may also be used by the WVDP to verify product consistency. The PCT is a highly interactive test that measures the extent of glass corrosion in a solution that becomes highly concentrated in glass components as the test proceeds.

While the PCT provides information regarding the consistency of the glass produced, no single test can characterize the corrosion behavior of a waste glass over long time periods. The long-term durability of vitrified waste forms emplaced in a repository can only be projected based on a mechanistic understanding of the corrosion processes. Previous studies conducted by DOE-EM have shown that glass corrosion slows as glass components build up in the solution, but may increase after certain alteration phases form [53]. In this Task, we will identify the alteration phases that form during the corrosion of WV6 glass and evaluate how their formation affects the dissolution rate.

B. Objectives

The purpose of this Task is to characterize the corrosion behavior of the WV6 glass when the corrosion is controlled by the intrinsic durability of the glass (Stage I), by the dissolved glass components (Stage II), and by the formation of alteration phases (Stage III). Tests are being performed to measure the glass corrosion rate as the corrosion progresses, to assess the long-term stability of the glasses, and to identify stable alteration phases that form as the glasses corrodes. These corrosion characteristics are required input parameters for computer simulation models that will be used to calculate the glass corrosion behavior over long time periods as a part of repository performance assessment. In addition, the results of these tests will provide insight into the corrosion behavior and alteration phases formed during the corrosion of the radioactive West Valley sludge-based reference glass that will be tested in another Task (see Sec. II).

C. Technical Approach

Separate test methods designed to access the different stages of the corrosion process are being used to characterize the corrosion behavior of WV6 glass. The glass composition is given in Table 1a. We performed tests using a modified MCC-1 procedure in which a monolithic sample was immersed in solution to achieve a low S/V ratio. Short-term tests are used to characterize the corrosion behavior in highly dilute solutions. These tests were conducted in a tuff groundwater solution. Other tests are being conducted at high S/V ratios and for long time periods following

PCT Method B to measure the corrosion rate as glass components build up in solution and, eventually, after alteration phases form.

Alteration phase formation was achieved in vapor hydration tests conducted at 200°C for times up to 55 days. Glass corrosion is accelerated by the high temperature and the high S/V achieved in these tests. The alteration phases formed in these tests were also isolated for detailed analysis and identification. The alteration phases must be known to calculate the long-term corrosion behavior using geochemical codes such as EQ3/6 [54].

D. Results and Discussion

1. MCC-1 Tests in EJ-13

Tests with WV6 glass were conducted at 10 m^{-1} following the MCC-1 static leach test procedure in EJ-13 water for periods of 3, 7, and 14 days to measure the initial corrosion rate. The corrosion rate will be less than the intrinsic dissolution rate because the silicon present in the EJ-13 water (about 40 mg/L) slows the glass dissolution. In fact, the concentrations of all glass components after 3, 7, and 14 days of corrosion were only slightly above their concentrations in the EJ-13 water. The (background-subtracted) normalized mass loss values based on boron, NL(B), after 3, 7, and 14 days were all about 0.07 g/m^2, corresponding to corrosion rates of about 0.02, 0.01, and 0.005 $g/(m^2 \cdot d)$, respectively. The MCC-1 test run for 91 days had NL(B) values of 0.28 g/m^2 and an integrated corrosion rate of about 0.003 $g/(m^2 \cdot d)$. For comparison, a different West Valley glass, the WV-205 glass, had a measured corrosion rate of about 0.6 $g/(m^2 \cdot d)$ in deionized water over 28 days in an MCC-1 test [55]. These results suggest that silicic acid present in the EJ-13 or released as the glass corrodes slows the corrosion rate significantly, and that the intrinsic dissolution rate is greater than 0.02 $g/(m^2 \cdot d)$.

2. PCT Tests in Deionized Water

The PCT has been used to study a wide range of waste forms and compare the performance of glasses having different compositions. Replicate PCT tests conducted in deionized water for 7 days gave an average NL(B) value of about 0.3 g/m^2 for WV6. For comparison, the reported NL(B) values in PCT tests with other glasses are 0.4 g/m^2 for SRL 202, a reference glass for the DWPF [8]; about 5 g/m^2 for the DWPF EA glass [42]; and about 0.4 g/m^2 for HW-39 glass, a reference glass for the Hanford Waste Vitrification Plant (HWVP) [56]. Thus, the WV6 glass has a slightly lower average dissolution rate through 7 days than these reference glasses for the DWPF and the HWVP.

3. PCT Tests in EJ-13

Several PCT tests were conducted in EJ-13 water at 90°C and at S/V ratios of 2000 and 20,000 m^{-1} with crushed glass of the -100+200 mesh (74-140 μm) size fraction. Tests were also conducted at 20,000 m^{-1} with crushed glass of the -200+325 mesh (43-74 μm) fraction to assess the effects of the initial size of glass particles on the dissolution behavior. The solution concentrations of major glass components in tests with these fractions are presented in Fig. 17 as the normalized mass losses. The average values of duplicate tests are plotted and the precision is ±10%. The results show that alkali metals and boron are released faster than silicon, while uranium and silicon are released stoichiometrically. All solution concentrations increase with the reaction time; this indicates that the solutions have not become saturated. Note that Li and Na are released to a greater extent than B in tests at 2000 m^{-1}, but that B is released to a greater extent than Li and Na in tests at 20,000 m^{-1}. This occurs because Li and Na are being incorporated into alteration phases to a greater extent in the tests at 20,000 m^{-1} than in tests at 2000 m^{-1}. The similarity in the results of tests conducted at 20,000 m^{-1} with both size fractions of crushed glass indicates that there is not a significant effect of particle size. The buildup of corrosion products in

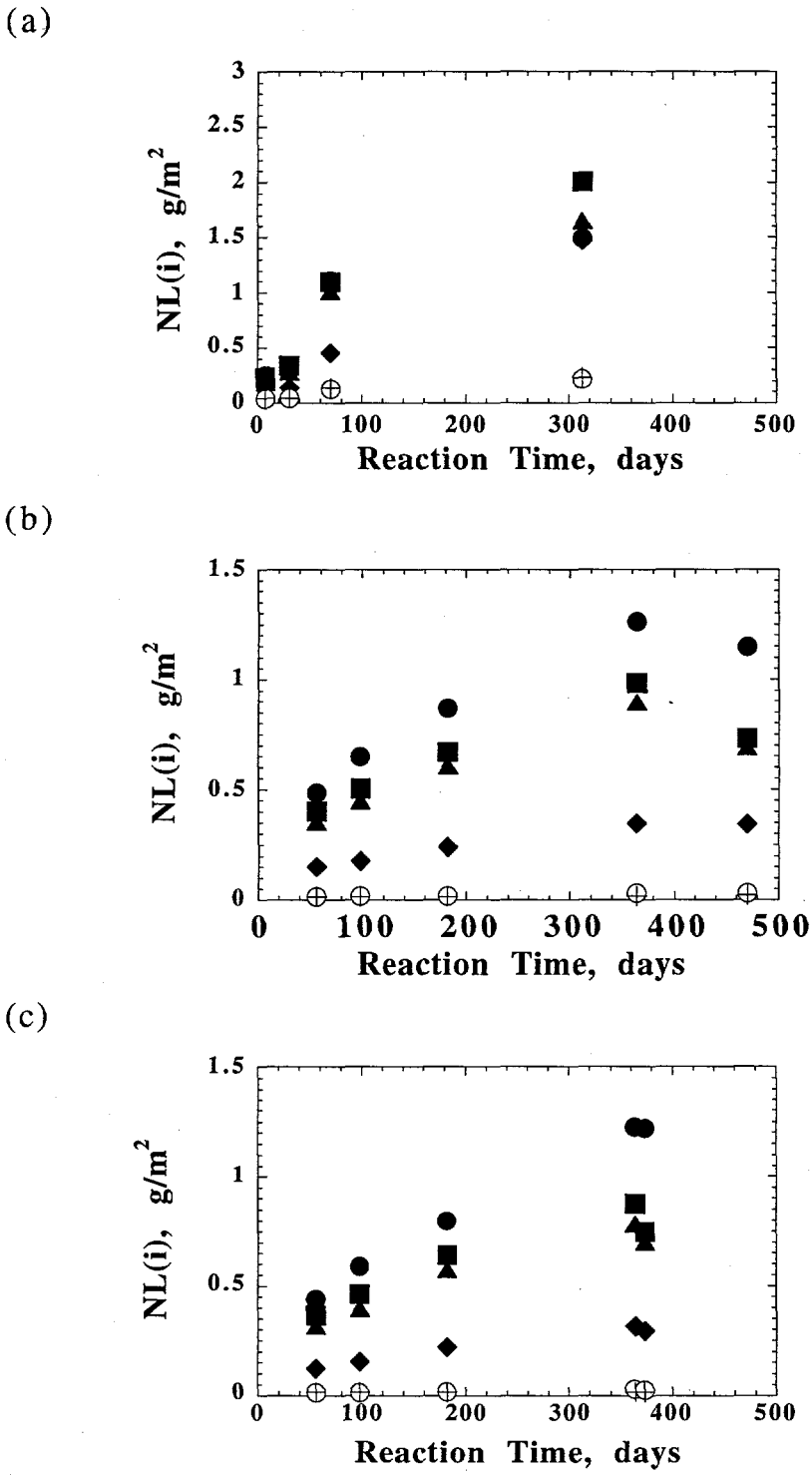

Fig. 17. Normalized Mass Loss from Static Tests with WV6 Glass at (a) 2000 m^{-1}, (b) 20,000 m^{-1} with -100+200 Mesh Glass, and (c) 20,000 m^{-1} with -200+325 Mesh Glass: B (●), Li (■), Na (▲), K (◆), Si (○), and U (+).

the solution slows the corrosion only slightly in tests at both S/V ratios. The dissolution rate based on the boron release is about 0.0026 g/(m^2•d) for tests at 20,000 m^{-1} with either size fraction through one year. The rate is slightly higher in tests at 2000 m^{-1}.

When glass dissolution is modeled, it is often assumed that the silicic acid concentration is the only glass component that affects the dissolution rate [56]. The maximum (or "saturation") concentration of orthosilicic acid (H_4SiO_4) is a glass-dependent parameter that is used to calculate the chemical affinity for glass dissolution. The saturation concentration of orthosilicic acid measured in these static dissolution tests can be used to calculate the saturation concentration of orthosilicic acid needed to model the long-term dissolution behavior of WV6 glass. The pH and the total amounts of silicon measured in these tests are plotted in Fig. 18 against the product of S/V and the reaction time. (We have used the parameter (S/V)t so the data can be plotted conveniently.) The pH values measured at room temperature have been plotted. They have not been adjusted for temperature or possible alkali interference. The silicon concentration of EJ-13 groundwater is indicated by the dashed line at 41 mg/L. Note that the silicon concentration (1) is nearly constant in tests at 10 m^{-1}, at a concentration slightly above that in the EJ-13 water; (2) increases with (S/V)t at values greater than about 1 x 10^4 d/m; and (3) is about the same in tests at 20,000 m^{-1} with crushed glass of the -100+200 and -200+325 mesh fractions. The increase in the silicon concentration with S/V is correlated with the increase in the solution pH. Dissociation of silicic acid at pH values greater than about 9.7 (at 90°C) results in an increase in the silicon concentration. Note that the high silicon concentration in the test conducted for 369 days at 2000 m^{-1} (the rightmost filled square in Fig. 18) corresponds with a high pH.

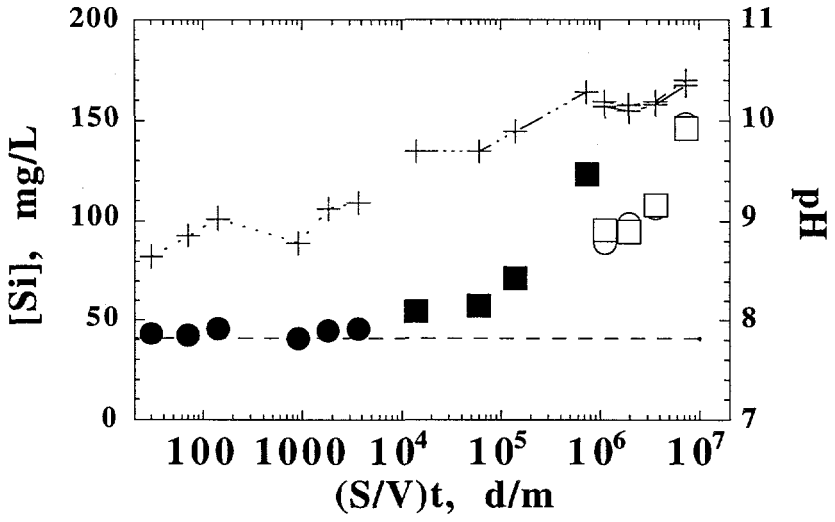

Fig. 18. Silica Concentration and pH for Static Tests of WV6 Glass at (●) 10 m^{-1}, (■) 2000 m^{-1}, (○) 20,000 m^{-1} with -100+200 Mesh, and (□) 20,000 m^{-1} with -200+325 Mesh Glass; (+) pH at each S/V. Dashed line shows [Si] in EJ-13 water.

The measured dissolution rate in the MCC-1 tests conducted at 10 m^{-1} is quite low at all times tested. These results indicate that the silicon concentration in the EJ-13 water is very near the saturation concentration for WV6 glass. The dissolution rate is higher in the PCT tests. The concentration of orthosilicic acid in the PCTs is probably less than the saturation concentration in all tests conducted through about one year, probably because of the increase in the solution pH and dissociation of silicic acid. Calculation of the orthosilicic acid concentration from the measured silicon concentration requires knowledge of the pH and pK_a values at the test temperature. While these calculations will be performed at a later date when more data are available, we can approximate the pH value at 90°C to be one unit lower than the value measured at room temperature. For example, a measured pH value of 10.4 at room temperature for the tests at the highest (S/V)t value in Fig. 18 corresponds to a pH of about 9.4 at 90°C. At pH 9.4, about 23% of the total silicon exists as orthosilicic acid (for pK_1 = 9.09, pK_2=-9.60). The rest exists as dissociated species. Therefore, of the measured total silicon concentration of about 150 mg/L, about 35 mg/L exists as H_4SiO_4. This amount is well below the saturation concentration that is predicted from the results of the tests conducted at 10 m^{-1}. Because of the high sensitivity of the silicic acid speciation to the pH at high pH values, small uncertainties in the measured pH will lead to large uncertainties in the calculated orthosilicic acid concentrations. Therefore, the results of several tests must be used to determine whether or not the solution concentration of orthosilicic acid is less than the saturation value. When the results of longer-term PCT tests become available, the orthosilicic acid concentrations will be calculated from the measured silicon concentrations and pH using geochemical equilibration codes to estimate how far the solutions in the PCT tests are from saturation, compared to the results of the MCC-1 tests.

4. Solids Analysis

Corrosion in PCT tests alters the glass surface. Examination of reacted glass particles with SEM showed the surface to attain a chain-mail appearance similar to that seen on other glasses during the formation of smectite clays. Analysis of cross-sectioned surfaces using AEM revealed the presence of thin strands of clay-like material that form the alteration layer. The composition and lattice spacings of this material are consistent with smectite clay.

Corrosion in vapor hydration tests at 200°C generated an alkali-depleted surface layer that transformed into smectite clay at longer test durations. Also, a variety of alteration mineral phases precipitated from the fluid and condensed on the sample during the test. Iron and ruthenium-containing inclusion phases are seen both in the unreacted glass and in the layer. The similarity of their distribution in the layer and the glass confirms that the clay layer is formed by *in situ* transformation of the alkali-depleted glass, while the observation that alteration minerals form on the outer surface indicates that they had precipitated from the fluid.

The key outcomes of the vapor hydration tests are (1) confirmation that alteration phases form and increase the dissolution rate, which indicates that corrosion of WV6 glass will eventually reach Stage III, and (2) identification of those alteration phases. The morphology and compositions of most phases are identical to those formed on other WVDP reference glasses [57]. These phases include analcime, an unidentified zeolite orthoclase (potassium feldspar), lithium phosphate, and weeksite. Since the ability of the phases to sequester radionuclides will depend on their composition, identification of the alteration phases that form is important for projecting the disposition of released radionuclides.

E. Future Studies

Results available to date indicate that WV6 glass is quite durable. Therefore, tests will be terminated infrequently until alteration phases that increase the glass dissolution rate form. At least one of the long-term PCT tests with reaction times greater than two years will be completed during FY 1996. The test results available in FY 1996 will be reported in a detailed topical report. The report will cover investigations into why WV6 corrodes slower than DWPF glasses and will discuss when the PCT tests are expected to reach Stage III.

VI. STATIC DISSOLUTION TESTING OF SRL EA GLASS

A. Introduction and Background

High-level radioactive wastes stored at DOE facilities at Savannah River, SC; West Valley, NY; and Hanford, WA will be vitrified to form high-level waste glasses that will eventually be sent to a federal repository for disposal. The DOE has established Waste Acceptance Preliminary Specifications (WAPS) for Vitrified High-Level Waste Forms to ensure that waste glasses produced at these facilities will be suitable for acceptance for disposal at a federal repository [58]. The current WAPS requires that high-level radioactive waste glasses are consistently more durable than a benchmark glass, which is the Environmental Assessment (EA) glass, when assessed using the PCT Method A [34]. A glass is deemed more durable if the amounts of boron, alkali metals, and silicon released from the glass are less than the amounts released from the EA glass.

The PCT was developed to provide confidence that waste glass products are consistently more durable than the EA glass. However, PCT Method A by itself does not provide insight into the long-term performance of a waste glass in a disposal environment. It remains to be demonstrated that requiring a waste glass to be more durable than EA glass under PCT Method A ensures that the glass will have acceptable long-term performance.

Tests with several DWPF glasses have shown that, while the dissolution rates of all glasses decrease as the contacting solution becomes more concentrated, the formation of some alteration phases increases the dissolution rates of some glasses. We have conducted several tests with the EA glass to assess its behavior at advanced stages of corrosion. These results can be compared to the long-term behaviors of other glasses to provide insight into the relationship between the behavior of a glass in a short-term test, such as a 7-day PCT, and its long-term behavior. Tests were conducted at two different S/V ratios to characterize the glass corrosion behavior under conditions in which the corrosion products build up in solution at different rates and promote the formation of alteration phases. In addition, tests were conducted at the same S/V ratio using two different size fractions of crushed glass to assess the effects of particle size on the long-term corrosion behavior.

B. Objectives

The purpose of this Task is to characterize the corrosion behavior of the SRL EA glass, including the behavior at advanced stages of corrosion relevant to long disposal times, i.e., under conditions in which the corrosion is controlled by alteration products. Tests are being conducted for long times and at high S/V ratios to promote the formation of alteration phases so they can be identified and the effect of their formation on the corrosion behavior can be measured. The results of these tests will form a basis for comparing the long-term behavior of other candidate waste glasses. These test results will also be used to determine if the fact that a glass performs better than the SRL EA glass in a 7-day PCT indicates that it will also perform better over long times.

C. Technical Approach

Crushed SRL EA glass was supplied by the SRTC from a large source fabricated for SRTC by Corning Glass Works. Glass from that source will be used for monitoring product consistency for all DWPF campaigns [59,60]. This glass has been characterized by both SRTC and Corning [8], and the composition is given in Table 1a. The glass received from SRTC was further crushed and sieved to isolate the -100+200 (74-140 μm) and -200+325 (43-74 μm) mesh size fractions. The crushed and sieved glass was washed to remove fines and allowed to dry. The glass was translucent and amber in color. There are three typical particle shapes in both size fractions: rods, plates, and chunks. The compositions of all three shapes were identical, as

measured with EDS (the B and Li concentrations were not measured). It is assumed that the relative amounts of particles of each shape are the same in each test and that the surface area is proportional to the mass of glass as 0.02 m^2/g for the -100+200 mesh fraction and as 0.04 m^2/g for the -200+325 mesh fraction.

Static dissolution tests were conducted using the -100+200 mesh fraction at glass:water mass ratios of 1:10 and 1:1 to achieve S/V ratios of about 2000 and 20,000 m^{-1}, respectively. The -200+325 mesh fraction was tested at a glass:water mass ratio of 1:2 to achieve an S/V ratio of about 20,000 m^{-1}. Tests at 20,000 m^{-1} were conducted using both the -100+200 and -200+325 mesh size fractions of crushed glass to determine whether the size fraction affects the long-term glass corrosion behavior.

We conducted tests at 90°C for reaction times between 7 and 600 days at an S/V ratio of 2000 m^{-1}, and between 56 and 527 days at an S/V ratio of 20,000 m^{-1}. All tests were conducted using EJ-13 water (Table 2). Seven-day tests at 2000 m^{-1} were also conducted using deionized water as a standard PCT Method A test.

All tests were conducted using 304L stainless steel reaction vessels that were sealed using Teflon gaskets and compression fittings. The glass and EJ-13 or deionized water were weighed into the reaction vessels, which were then gently agitated to assure that all the glass was wet. (This was especially important for tests at 20,000 m^{-1}, which were conducted with 7 g of glass and 7 g of water.) The vessels were sealed and placed in an oven set at 90°C. The oven temperature was verified using a National Institute of Standards and Technology traceable thermometer and was continuously monitored using a Type K thermocouple. The oven temperature remained at 90±1°C throughout the testing period.

After a predetermined test time, each vessel was removed from the oven, weighed, and opened immediately. Aliquots of the leachate solution were taken for carbon and pH analysis. (The pH was measured at room temperature.) The remaining leachate was passed through a preheated 450-nm cartridge filter to remove any suspended glass. The filtered solution was analyzed for anions and cations. Samples of the corroded glass were analyzed using optical microscopy, SEM/EDS, AEM with EDS and selected area electron diffraction (SAED). Secondary phases were isolated and analyzed using SEM/EDS, AEM, and X-ray diffraction (XRD).

D. Results and Discussion

Tests through 470 days have been completed and are discussed here; longer-term tests are in progress, and those results will be presented later. Both the solutions and reacted solids have been analyzed, and the results are presented below.

1. Solution Results

The extent of glass corrosion was calculated using the measured solution concentrations of key glass components and reported as the normalized mass loss, NL(i). Calculations of NL(i) were made using the initial surface area, although the surface area is known to decrease as the glass dissolves. The normalized dissolution rate can be adjusted to take the loss of surface area into account (see Sec. IV). The normalized mass loss represents the mass of glass that must dissolve to generate the measured solution concentration of species i. If the glass dissolves stoichiometrically, then the same value of NL(i) will be calculated based on the solution concentrations of all glass components. Differences in the values of NL(i) may indicate (1) that the glass is not dissolving stoichiometrically or (2) that some components are not released into solution as the glass corrodes, but are instead retained on the glass surface as insoluble residue or incorporated into secondary phases. Leachate solutions were filtered using a coarse filter (450 nm) to ensure the analyzed solutions did not contain suspended glass, although boron is not expected to

be removed by filtration. (Tests in which the glass has completely dissolved provide evidence that boron is not sorbed by the filter, although other glass components may be sorbed.) Filtration may have removed some colloidal material not associated with the glass. Colloids passing through the filter were included in the analysis to measure the total amount of reacted glass.

The solution pH values and the normalized mass loss values based on the release of B, Na, Li, and Si in tests at 2000 m^{-1} are plotted in Fig. 19. Duplicate tests were conducted for 7, 30, and 70 days, and single tests were conducted for 313, 470, 592, and 600 days. After an initial increase from the leachant pH of about 8.2 to a pH of about 11.6 after 7 days, the measured solution pH increases nearly linearly with the reaction time. The glass does not dissolve stoichiometrically; the NL(i) values based on boron and sodium are greater than those based on lithium and silicon. The nonstoichiometry is most obvious in tests conducted for 313 days and longer. Because boron is not incorporated into alteration phases to a significant degree, the amount of boron measured in solution indicates how much glass has dissolved. For example, the boron concentration measured in the leachate solution of a test run 592 days is 2520 mg/L. That test was conducted with 1.25 g of glass and 12.5 mL of EJ-13 water; at the end of the test, 31.5 mg B was measured in solution. The 1.25 g of glass added to the test contained 43.4 mg of B (EA glass contains 34.7 mg B per gram of glass). Therefore, 73% of the boron has been released from the glass into solution.

Figure 20a gives the solution pH values and the normalized mass loss values based on the release of B, Na, Li, and Si in tests at 20,000 m^{-1} with the -100+200 mesh size fraction (duplicate tests). The solution pH values are nearly constant through 182 days, but the pH values in tests conducted for 369 days and longer are significantly lower than in tests run for shorter times, probably as a result of sodium interference in measuring pH. The normalized mass losses based on B and Na are greater than those based on Li and Si, as they were in the tests conducted at 2000 m^{-1}. The difference between the fast release of B and Na and the slow release of Li and Si is greater in tests at 20,000 m^{-1} than in tests at 2000 m^{-1}.

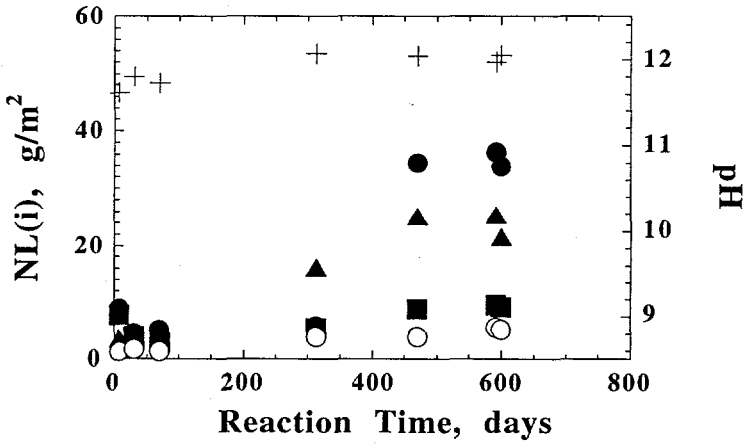

Fig. 19. Normalized Mass Loss from Tests of SRL EA Glass at 2000 m^{-1} with (a) -100+200 Mesh Glass: B (●), Li (■), Na (▲), Si (○), and pH (+)

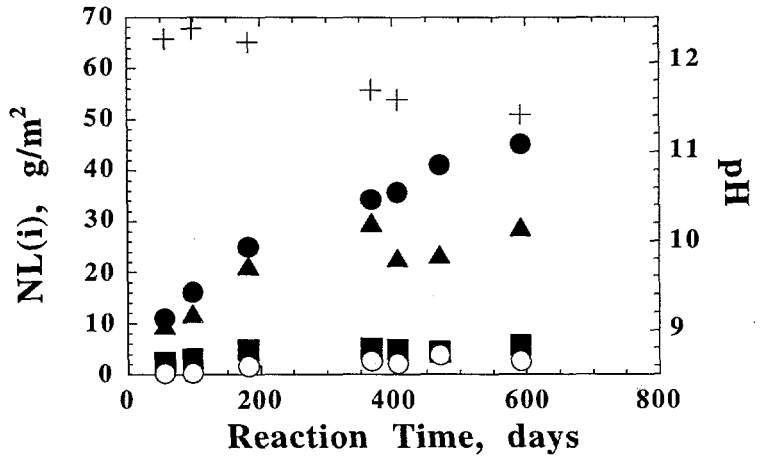

a.

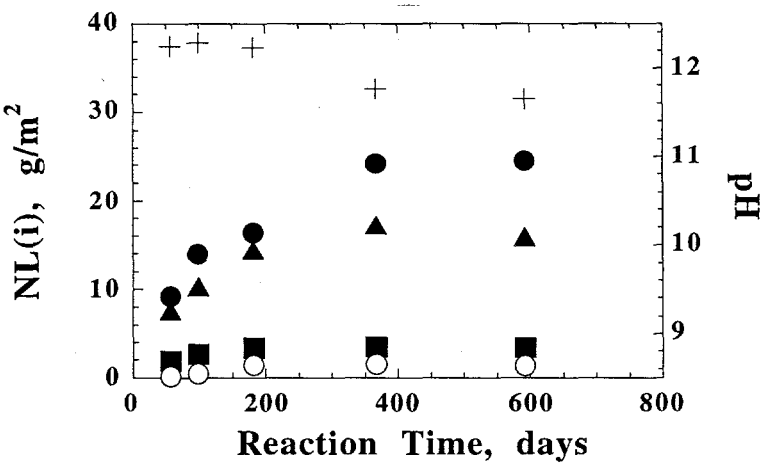

b.

Fig. 20. Normalized Mass Loss from Tests of SRL EA Glass at 20,000 m^{-1} with (a) -100+200 Mesh Glass and (b) -200+325 Mesh Glass: B (●), Li (■), Na (▲), Si (○), and pH (+)

The NL(B) values remain about constant at reaction times beyond about 1 year. The amount of boron measured in solution corresponds to about 91% of the boron that was initially present in the glass. This indicates that the glass has almost completely corroded after less than 2 years. The maximum possible normalized loss, as calculated based on the initial surface area, is about 50 g/m^2 for -100 +200 mesh glass.

The pH and NL(i) for tests at 20,000 m^{-1} with the -200+325 mesh size fraction shown in Fig. 20b follow the same trends as tests with the -100+200 mesh fraction, although the pH and NL(i) values are slightly less than those for corresponding tests with the -100+200 mesh size fractions. While part of the difference may be due to a systematic error in estimating the surface area of each size fraction, most of the difference is due to the greater proportional loss of surface area as the -200+325 mesh glass dissolves. Nearly identical solution concentrations of B, Li, Na, and Si occur in tests conducted for 378 and 600 days, which indicates that the glass has completely dissolved. The boron concentration measured in the leachate solutions of these tests indicates that about 99% of the glass has corroded. The measured NL(B) values are consistent with the maximum possible normalized loss, which is about 25 g/m^2 for -200+325 mesh glass.

2. Solids Results

Analysis of reacted glass using an optical microscope revealed the formation of a chalky white alteration layer on the glass grains and the formation of discrete secondary phases separate from the glass. Most of the glass had been transformed into altered material over the course of 1 year, although small cores of glass remained beneath the alteration layers. Altered glass grains were analyzed using an SEM. The altered surface has formed two layers: a thin outer surface, which has a beady appearance, and a thick inner layer that has partially spalled off the underlying glass.

In tests at 20,000 m^{-1} (both with the -100+200 and -200+325 mesh glass) for 98 days or more, about one half of the altered grains had a greenish tint. The other grains retained their initial amber color. The green and amber grains had identical compositions and morphologies. It is possible that the change in color is due to different oxidation states of a trace component, but it is not obvious why only some of the particles have changed color. Analyses are in progress to determine the cause of the color difference.

Particles of the reacted glass were also fixed in epoxy resin and cross-sectioned for examination with SEM/EDS. The layer material was analyzed using EDS, and the compositions of the unreacted glass and layer (the average of five analyses) are summarized in Table 11. The values given in the columns labeled "analyzed glass" and "analyzed layer" have been normalized to 100 wt % of the elements detected. The compositions have been adjusted by including the B_2O_3, Li_2O, and NiO contents measured by SRTC with wet chemical analyses in the glass composition. Based on the solution results, the layer is assumed to be totally depleted of B, while all the Li is assumed to be retained in the layer. The "recalculated glass" and "recalculated layer" values can be compared to determine the relative enrichment or depletion of glass components in the alteration layer. The layer is depleted in Na and B and enriched in Al, Mg, Si, and Fe relative to the unreacted glass.

Three morphologically distinct secondary phases formed in all tests at 20,000 m^{-1} with both size fractions: a translucent, spherical phase (referred to as phase 1), a transparent phase comprised of layered, hexagonal plates (referred to as phase 2), and a translucent, bulbous phase (referred to as phase 3). The size and abundance of these secondary phases increased with the reaction time. Representative phases were isolated and analyzed using SEM/EDS, AEM/SAED, and XRD. The formulae calculated from the compositions measured with EDS and the d-spacings measured using XRD are summarized in Table 12. The formulae have been normalized so that the

Table 11. Glass and Layer Compositions of SRL EA Glass Reacted in Static Tests at 20,000 m^{-1} for 98 Days or More, as Measured Using EDS, in Oxide wt %

Oxide	SRTC Composition Oxide wt %[a]	Analyzed Glass	Analyzed Layer	Adjusted Glass	Adjusted Layer
Al_2O_3	3.6	4.7	2.9	3.9	2.4
B_2O_3	11	NA[b]	NA	11[c]	0[c]
CaO	1.2	1.2	2.4	1.0	2.0
Fe_2O_3[d]	7.6	8.0	13	6.7	11
FeO[d]	1.6	NA	NA	—	—
K_2O	0.04	0.01	0.18	0.01	0.15
La_2O_3	0.28	NA	NA	0.28[c]	0.28[c]
Li_2O	4.2	NA	NA	4.2[c]	4.2[c]
MgO	1.8	1.2	4.2	1.0	3.4
MnO_2	1.4	1.5	2.0	1.2	1.7
Na_2O	17	25	4.6	20	3.8
NiO	0.53	NA	NA	0.53[c]	0.53[c]
SiO_2	49	58	69.9	48	58
TiO_2	0.65	1.5	0.92	1.2	0.77
ZnO	0.26	NA	NA	0.26[c]	0.26[c]
ZrO_2	0.48	NA	NA	0.48[c]	0.48[c]
Total	100	100	100	100	89

[a]Wet chemical analysis.

[b]NA = not analyzed.

[c]See text for discussion.

[d]All iron expressed as Fe_2O_3.

Table 12. X-Ray Diffraction and SAED Analyses of Isolated Secondary Phases

Phase 1 $Na_{5.7}Al_{4.4}Si_{10.3}O_{31}$ XRD		Sodium Aluminum Silicate Hydrate $Na_{5.7}Al_{5.7}Si_{10.3}O_{32}\cdot 12H_2O$ JDPS No. 34-0524		Phase 1 SAED
d-spacing, Å	I/I°	d-spacing, Å	I/I°	d-spacing, Å
7.12	80	7.132	85	7.23
		7.047	85	6.83
5.03	40	5.048	50	5.03
		4.914	25	4.90
4.11	80	4.108	95	
		4.049	20	3.92
		3.527	4	3.58
		3.328	18	
3.19	100	3.194	100	
3.14	70	3.117	65	
		3.036	10	3.03
2.69	50	2.694	45	
		2.679	30	
		2.653	20	2.64

Phase 2 $Na_{0.7}Al_{0.8}Si_2O_{5.5}$ XRD		Analcime $NaAlSi_2O_6\cdot 3H_2O$ JDPS No. 19-1180		Phase 2 SAED
d-spacing, Å	I/I°	d-spacing, Å	I/I°	d-spacing, Å
5.63	90	5.60	60	5.64
				5.51, 5.47
4.89	50	4.85	20	4.80
				4.28
		3.80	2	3.80
				3.82
3.69	10	3.67	8	3.64
3.45	100	3.43	100	
		3.24	2	3.28, 3.31
				3.10
2.93	100	2.927	50	2.91, 2.86
2.70	40	2.693	16	2.71
2.51	40	2.506	14	
		2.427	8	2.45, 2.46
				2.33
2.23	20	2.226	40	
		2.118	8	
1.90	20	1.904	14	
1.87	20	1.868	8	
		1.8353	2	1.81
1.74	50	1.743	20	
		1.7166	6	
		1.6902	6	1.69
1.36	10	1.3586	8	

Table 12 (contd)

Phase 3 $Na_{1.2}Al_{1.5}Si_4O_{11}$ XRD		Gmelinite $Na_2Al_2Si_4O_{12}•6H_2O$ JPDS No. 38-0435		Phase 3 SAED
d-spacing, Å	I/I°	d-spacing, Å	I/I°	d-spacing, Å
11.84	100	11.9	63	
7.72	20	7.68	29	
6.91	50	6.875	10	6.95, 6.86
5.96	10	5.95	9	
		5.121	23	
5.04	80	5.026	28	4.98
				4.91
				4.77
4.50	40	4.498	25	
4.14	90	4.106	100	
3.45	40	3.44	21	3.43, 3.41
3.25	30	3.227	41	3.23
2.98	80	2.978	55	3.10
2.87	50	2.922	18	
2.70	20	2.855	42	
2.61	20	2.69	44	2.67
		2.597	14	
		2.400	1	2.46
		2.355	1	2.39
2.09	20	2.086	12	
		1.9418	4	1.94
		1.9212	2	1.92
1.81	20	1.808	8	
1.72	20	1.719	9	
		1.6903	2	1.69
		1.6291	4	1.62

Phase 4 $Na_{3.0}K_{0.62}Al_{4.1}Si_{12.4}O_{33}$ XRD		Sodium Aluminum Silicate Hydrate $Na_{3.6}Al_{3.6}Si_{12.4}O_{32}•14H_2O$ JPDS No. 40-1464	
d-spacing, Å	I/I°	d-spacing, Å	I/I°
7.14	96	7.0924	91
5.04	26	4.9984	61
4.11	84	4.1014	53
		4.0846	16
		3.1818	33
3.18	100	3.1641	100
2.69	54	2.6774	97
2.52	1	2.5170	16
2.24	1	2.2366	21
1.97	3	1.9613	20
1.77	3	1.7737	52
1.72	4	1.7236	36
		1.7179	52
1.67	1	1.6665	49
1.48	1	1.4746	46
1.37	2	1.3619	41
1.27	2	1.2704	55

Table 12 (contd)

Clay Layer[a] XRD		Nontronite[b] JPDC No. 34-842		Montmorillonite[c] JPDS No. 29-1449		EA-43 SAED
d-spacing, Å	I/I°	d-spacing, Å	I/I°	d-spacing, Å	I/I°	d-spacing, Å
				21.5	100	
14.2	—[d]	14.6	100			
				10.6	18	
		7.56	10			
		4.98	10			
4.53	—[d]	4.53	100			4.53
				4.45	55	
		3.67	20			
				3.15	40	
		3.01	30			
2.58	—[d]	2.60	50	2.56	35	2.60
		2.27	10			
		1.72	20			1.73
				1.69	8	
1.51	—[d]	1.523	80	1.495	25	1.53
				1.325	8	
		1.310	30			1.33
		1.270	30			

[a]Clay layer: $Na_{0.50}Mg_{0.35}Ca_{0.15}Zn_{0.12}Fe_{0.55}Al_{0.18}Si_4O_{14}$.

[b]Nontronite: $(Mg,Ca)_{0.5}Fe_2(Si,Al)_4O_{10}(OH)_3 \cdot nH_2O$.

[c]Montmorillonite: $(Mg,Ca)_{0.5}(Al,Mg)_2(Si)_4O_{10}(OH)_3 \cdot nH_2O$.

[d]Intensity not determined due to high background.

silicon content is the same in the phase and in the mineral to which it is being compared. The morphologies, compositions, and d-spacings of these phases (referred to as Phases 1, 2, and 3 in the table) are consistent with those of sodium aluminum silicate hydrate [$Na_{5.7}Al_{5.7}Si_{10.3}O_{32}\cdot 12H_2O$], analcime [$NaAlSi_2O_6\cdot 3H_2O$], and gmelinite [$Na_2Al_2Si_4O_{12}\cdot 6H_2O$]. The d-spacings measured using AEM/SAED are included. Because the SAED analyses are performed on microtomed thin sections, not all crystalline angles are sampled. Thus, the number of observed peaks in an SAED diffraction pattern will be less than the number observed in an XRD spectrum.

Table 12 includes the results of XRD analysis of a clay layer that had formed on the corroded glass. The d-spacings and intensities of nontronite, the iron-rich end-member smectite clay, match well with the XRD results. Intensities are not reported because of the high background from the glass underlying the clay. However, the observed peaks are consistent with the strongest peaks from nontronite. The composition of the clay measured using SEM/EDS has less iron than does the reference nontronite. Compositions intermediate between nontronite and montmorillonite are common in nature [5]. The d-spacings and composition of montmorillonite are included for comparison.

Only one secondary phase formed in tests conducted at 2000 m^{-1} after about 1 year. The phase was opaque white and had a square bipyramid morphology. The composition of this phase measured using SEM/EDS and the d-spacings measured using XRD are included in Table 12 (this phase is referred to as phase 4). The composition and d-spacings are consistent with a sodium aluminum silicate hydrate phase that is different than that formed in tests conducted at 20,000 m^{-1}.

The tests conducted at 2000 and 20,000 m^{-1} access Stages II and III after different reaction times. Tests at 2000 m^{-1} through about 313 days react in Stage II, in which the high solution concentration of glass components (primarily silicic acid) slow the glass corrosion to a low rate. Tests at 2000 m^{-1} reach Stage III, in which the corrosion rate is strongly influenced by the formation of alteration phases, between 313 and 369 days. The transition from Stage II to Stage III is defined here by the increase in the boron concentration. The glass corrosion rate between 30 and 313 days is about 0.004 g/(m^2•d), based on the measured boron concentration, and the rate between 313 days and 1 year is about 0.2 g/(m^2•d), with no surface area correction.

Tests conducted at 20,000 m^{-1} have reached Stage III within the shortest time tested, which is 56 days. The rate calculated from the results of 56-day tests with -100+200 mesh glass is 0.2 g/(m^2•d). The glass corrosion rate is also about 0.2 g/(m^2•d) between 56 and 182 days. Note that the dissolution rates calculated for reaction in Stage III (after the formation of alteration phases that increase the dissolution rate) have not been adjusted for the loss of surface area as the glass dissolves. Instead, data from tests in which the loss of surface area is expected to be small were used to calculate the rates. In fact, slightly lower rates are measured in tests with -200+325 glass [0.16 g/(m^2•d) over the first 56 days and 0.11 g/(m^2•d) between 56 and 98 days] than in tests with -100+200 mesh glass over the same intervals, probably due to the greater loss of surface area as the small size fraction dissolves. A scheme to adjust the rates to account for the loss of surface area is being developed (see Sec. IV) and will be applied to these data to determine the dissolution rates.

The glass dissolution rate measured in a 7-day PCT in EJ-13 water is about 0.6 g/(m^2•d); this is about half the rate measured in PCT tests conducted with deionized water, which was about 1.2 g/(m^2•d) [58]. The difference is probably due to the effect on the corrosion rate of the approximately 40 mg/L silica present in the EJ-13 solution, which slows the dissolution. All dissolution rates given above are based on the measured boron concentrations. Rates based on silicon or alkali metal concentrations will be lower than those based on boron concentrations,

because these elements are incorporated into alteration phases and their solution concentrations do not provide an accurate measure of the amount of glass that has dissolved.

These tests suggest that the dissolution rate measured with a 7-day PCT provides a conservative upper bound of the long-term corrosion rate of the EA glass, even after increases in the pH and alteration phase formation. Accounting for the surface area in the long-term tests may result in a slight increase in the long-term rate, but it is not anticipated that the rate will exceed that measured in the 7-day PCT in deionized water. Tests with other DWPF glasses have also shown the long-term corrosion rate to be less than or equal to the rate measured in a 7-day PCT [34]. Table 10 summarizes the corrosion rates measured for the SRL EA glass and two other DWPF glasses, SRL 202 and SRL 131, in Stages II and III.

It has been suggested that the dissolution rate of a glass measured in the short-term PCT test provides a bound to its long-term dissolution rate. Specifically, "by bounding the short-term leach rate of production glasses, and requiring high confidence that this condition is met, the Product Consistency Specification provides high confidence that the long-term leach rate of production glass is bounded by that of the benchmark glass" [61]. The results in Table 10 indicate that a glass having a short-term dissolution rate less than that of the EA glass may have a long-term dissolution rate that is greater than that of the EA glass under the same test conditions: Based on the measured boron concentrations, the dissolution rate of SRL 131 glass at 2000 m^{-1} in Stage II, which is 0.006 $g/(m^2 \cdot d)$, is greater than that of SRL EA glass at 2000 m^{-1} in Stage II, which is 0.004 $g/(m^2 \cdot d)$. The corrosion behavior measured in Stage II is relevant to long disposal times prior to formation of alteration phases and will likely impact the performance of the disposal site. However, the dissolution rates in Stage II are much less than the rates measured in both 7-day PCT tests and the rates measured in Stage III.

E. Future Studies

Only a few tests remain in progress. It is likely that the glass in these tests has already been completely transformed into alteration phases. The tests will be allowed to continue into FY 1996 to determine if more stable phases replace the phases that form initially. Also, the measured rates will be adjusted to account for the loss of surface area as the glasses dissolve. A detailed description of the results of these tests will be provided in a topical report and journal article.

This page intentionally left blank.

VII. VAPOR HYDRATION TESTING OF SRL EA GLASS

A. Introduction and Background

The process of vapor phase hydration will be an important aging and alteration mechanism for vitrified waste forms in the proposed geologic repository at Yucca Mountain, Nevada [62]. The proposed repository at Yucca Mountain has been characterized as hydrologically unsaturated and large amounts of condensed water are not expected to be present in the repository at any time during its service life. The heat generated by the waste will also assure that localized unsaturated conditions will be maintained for several hundred to thousands of years after closure. The environment will result in the reaction of glass waste forms with water vapor at elevated temperatures for long periods of time. Although the scarcity of liquid water will prevent transport of radionuclides from failed containers during the containment period, exposure to water vapor may nevertheless result in alteration and aging of the waste [63]. Vapor hydration tests are being conducted to evaluate the corrosion of the EA glass in this environment. These tests will determine the tendency of the EA glass to reach Stage III reaction. Glass corrosion will be evaluated by examining the reaction products that form and estimating the rate of glass reaction as a function of temperature.

For this Task, the temperatures used to study glass reaction span the range between what might be expected in the repository (70°C) and temperatures that can be used to accelerate the reaction (120-200°C). The higher temperature tests were used to accelerate the hydration reactions. These tests are also used to determine whether the same phases are formed at different temperatures.

Under static PCT conditions with an S/V ratio of 20,000 m^{-1}, the SRL EA glass formed a number of crystalline silicate phases including smectite clay, a gmelinite, analcime, and other zeolites [48]. These PCT results will be compared with the present results. Also, vapor hydration testing of SRL 131 glass has been performed by Bates et al. [64], and results from the present study will be compared to that earlier study, in which SRL 131 glass was reacted at 120°C, 202°C, and 240°C. In Table 1a, the composition of SRL EA glass is listed, along with that of SRL 131 glass.

B. Objectives

The objectives of this study are to identify the alteration phases formed during corrosion of SRL EA glass and to measure the hydration rate of the EA glass as a function of temperature. These objectives will be accomplished by reacting glass under vapor hydration conditions and examining the samples with SEM and AEM.

C. Technical Approach

Tests were performed at 70°, 120°, 150°, and 200°C in controlled, constant-temperature ovens. These temperatures were selected to provide a range suitable for measuring the reaction kinetics of the glass. The EA glass was supplied by SRTC in the form of pulverized glass, which was remelted to form monoliths. These monoliths were cored and wafered to produce 1-cm-diameter disks 0.8-0.9 mm thick. The disks were polished to a uniform finish of 600 grit and ultrasonically cleaned. Two radially opposite notches were cut into the disks to allow the samples to be suspended by Teflon thread. Deionized water was used as the source of water in all tests.

Analytical characterization techniques included optical microscopy and SEM with EDS in which samples were analyzed in both surface normal and cross-section orientations. Optical microscopy was used to provide a general overview of the extent of corrosion, while SEM was

used to characterize the extent of reaction. Some samples were examined using AEM when the nature of the reacted layers could not be fully described by SEM.

D. Results and Discussion

Morphological and compositional information was provided by SEM for the thicker layers and by AEM for the thinner reacted layers. Layer thickness measurements were generally made using SEM and confirmed when possible with AEM. The results of these analyses are summarized in Table 13.

1. Tests at 70°C

After reaction at 70°C for 28 days, SRL EA glass showed minor coloration of the glass surface, indicative of the formation of a clay layer (Table 13). Examination using SEM revealed that the glass was partially covered with clay (Fig. 21), which suggests that pools of condensed water formed on the glass surface during reaction. Examination of AEM cross sections of the EA glass reacted for 28 days showed that the alteration layer was about 2 μm thick (see Fig. 21a), although the thickness of the outer clay region varied from sample to sample. After

Table 13. Summary of Results from Vapor Hydration Tests of SRL EA Glass

Temperature	Test No.	Time, days[a]	Comments
70°C	EAV-1	28	Evidence of clay formation. Analysis by AEM indicates that the layer consists of an outer fringe 100-200 nm thick and an alteration layer around 2 μm thick.
	EAV-2	91	Evidence of clay formation.
120°C	EAV-8	3	Discoloration of the glass surface indicates clay formation.
	EAV-9	7	Discoloration of the glass surface indicates clay formation.
	EAV-10	10	Discoloration of the glass surface indicates clay formation.
	EAV-12	20	Discoloration of the glass surface indicates clay formation.
150°C	EAV-16	7	Evidence of a small amount of reaction (SEM examination).
	EAV-22	14	Analcime and Ca, Na-tobermorite crystals. Some analcime is pitted.
	EAV-20	91	Extensive coverage of analcime and calcium silicate phases.
200°C	EAV-29	6	Analcime and Na, Ca-tobermorite formation.
	EAV-26	24	Rosette type sodium, calcium silicate particles. 100% surface coverage.
	EAV-27	48	Large number of analcime crystals and sodium, calcium silicates covering 100% of the surface.
	EAV-28	96	New type of calcium silicate appears. No glass remaining.

[a]Time in days except for tests at 200°C,which are in hours.

(a)

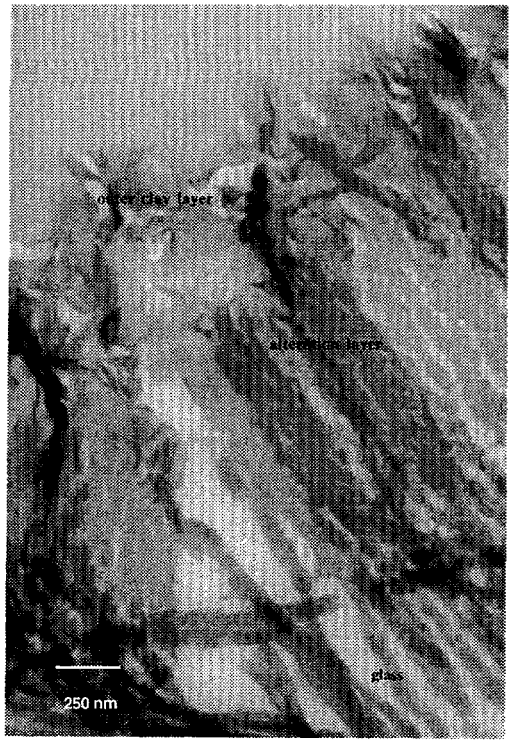

(b)

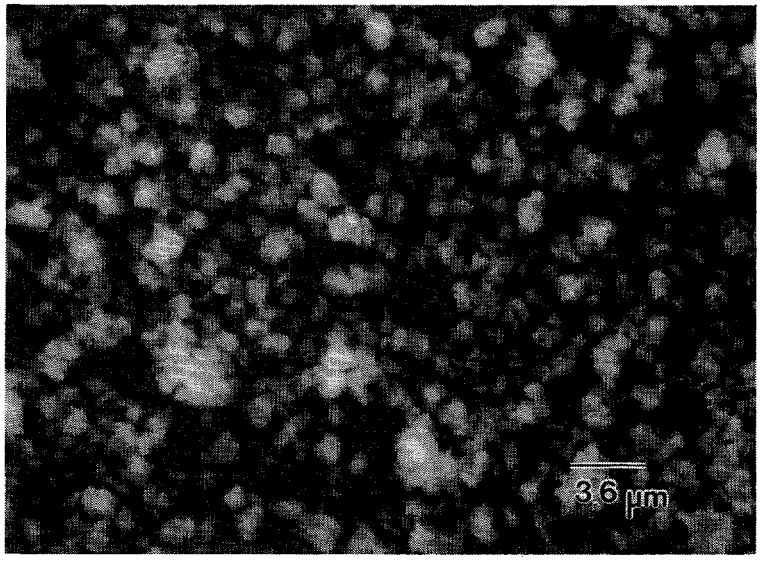

(c)

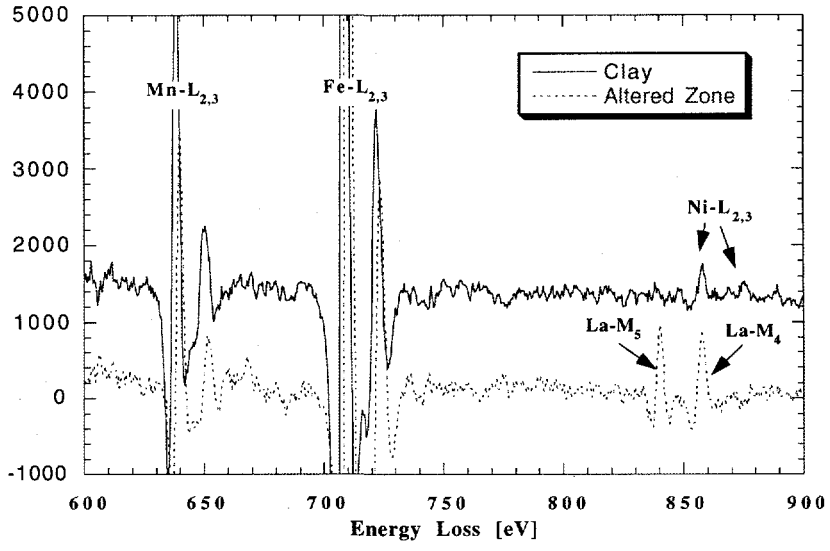

Fig. 21. (a) AEM Cross-Sectional View of Sample Reacted for 28 Days, (b) an SEM Image of Glass Reacted at 70°C in a Vapor Environment for 91 Days, and (c) Analysis of Iron, Manganese, and Lanthanum in the Clay Layer and Altered Zone Shown in (a) Using AEM/Electron Energy Loss Spectroscopy

91 days, there was little overall change in this pattern of corrosion; however, the clay appeared to be thicker (see Fig. 21b). In the 70°C tests, lanthanum was enriched in the alteration layer relative to the outer clay layer (Fig. 21c). In tests at higher temperatures in which calcium silicate alteration phases were found, lanthanum was often found to be incorporated into these phases. Analysis of the clay layer by SEM/EDS and AEM/EDS indicated that it was enriched in magnesium relative to the glass. Furthermore, detailed AEM examination suggested the presence of a magnesium aluminosilicate clay. This phase, ideally $[Mg_{2.88},Mn_{0.22},Fe_{0.02})Si_4O_{10}(OH_2)(Ca,Mg)_{0.07}]$, possibly stevensite, formed within this outer clay zone (Fig. 22). Similar magnesium-bearing clay phases were not identified in the PCT test. Based on the AEM results, further tests will be conducted at shorter times to examine the initial stages of clay formation.

2. Tests at 120°C

A number of tests were conducted at 120°C. Optical images indicated some reaction had occurred. The results are summarized in Table 13. The tests conducted at this temperature will allow direct comparison with the Bates et al. [64] study on SRL 131 glass. Tests will be performed for longer time periods such as 34, 41, and 92 days.

3. Tests at 150°C

At 7 days, the glass surface was covered with alteration phases. In Fig. 23, an optical image of the glass sample is presented that shows the onset of corrosion. After 14 days of reaction, analcime and a calcium silicate phase were observed on the surface of the glass (see Table 13). Uniformly sized analcime crystals precipitated almost equally spaced from each other. The analcime crystals were well crystallized, with only a few twins and defects (Fig. 24). The calcium silicate phases were typically needle shaped and contained sodium and a small amount of lanthanum. Cross-sectioned SEM examination is yet to be performed.

4. Tests at 200°C

At 200°C, alteration of the glass took place rapidly, and many phases precipitated on the reacted surface (Table 13, Fig. 25). After 6 h of reaction, a thin clay layer formed, and small analcime precipitates could be seen on the surface. The coverage of analcime crystals was about equal to that after 14 days of reaction at 150°C, although the individual crystals appeared to have more faulted than those formed at the lower temperature (Fig. 26). As the analcime crystals grew, their morphology changed and they no longer possessed the characteristic dome shape. The needle-like calcium silicate phases, which may be tobermorite, $[Ca_5(OH)_2Si_6O_{16}\cdot 4H_2O]$, or gyrolite, $[Ca_4(OH)_2Si_6O_{15}\cdot 3H_2O]$, formed within 6 h and, on occasion, nucleated on top of the analcime crystals. In comparison, SRL 131 glass reacted for 6 h under similar conditions (202°C in a vapor environment) formed analcime crystals but only a small amount of tobermorite [64]. After 36 h of reaction, the calcium silicate coverage for the SRL 131 glass was around 95%, which is similar to that for the SRL EA glass after 24 h at 200°C.

After 24 h, the calcium silicate phases consisted of rosette bundles about 100 μm in diameter (Fig. 27). The individual calcium silicate particles were rigid tubular crystals. In the center of the rosettes, extremely fine calcium silicates appeared; however, by 48 h, these rosette structures had disappeared, and many highly faulted analcime crystals appeared with calcium silicates precipitated on top of them. After 96 h of reaction, no glass was left and most of the reacted material had fallen off the Teflon wire. The remaining material was similar to that present at 48 h; the only new phase appeared to be another calcium silicate phase with a different morphology.

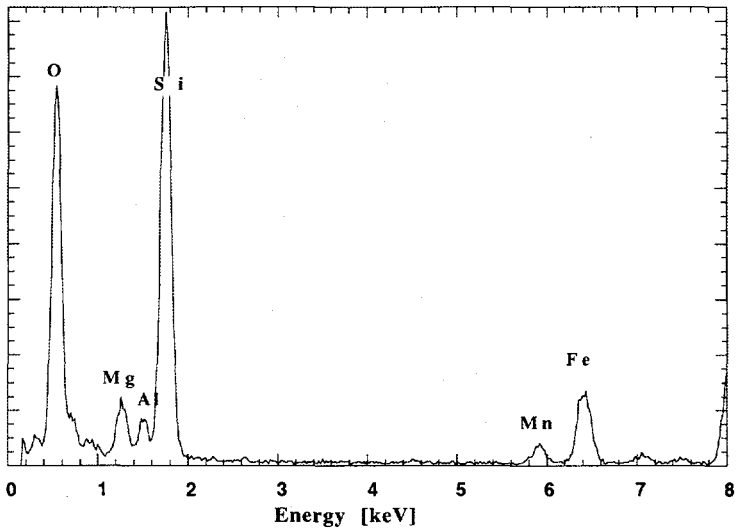

Fig. 22. Characterization of a Magnesium-Rich Clay in the 70°C, 28-Day Test; AEM/EDS Analysis

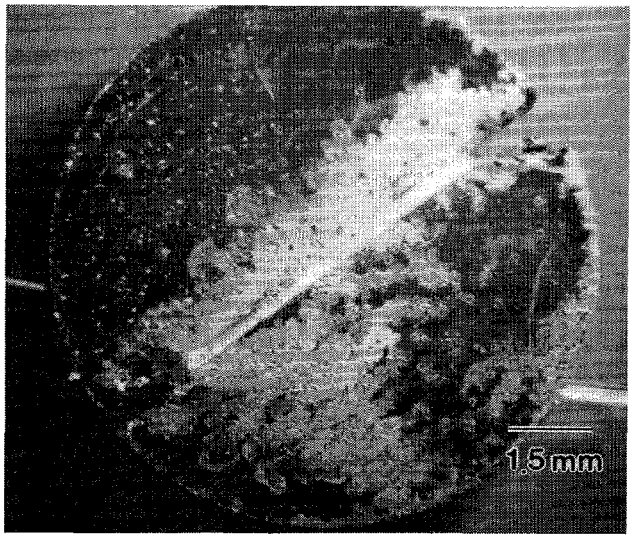

Fig. 23. Optical Image of SRL EA Glass Reacted for 7 Days at 150°C

(a)

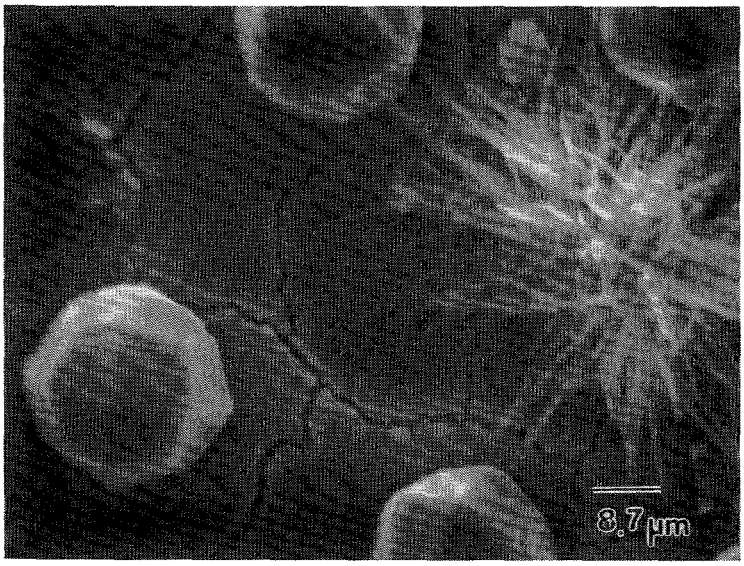

(b)

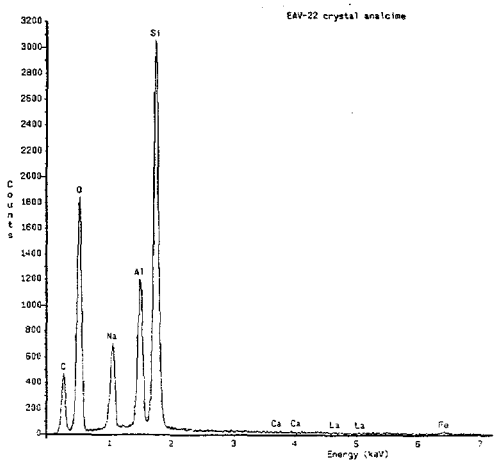

(c)

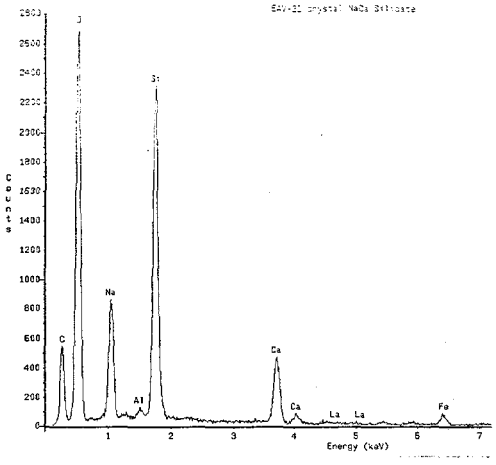

Fig. 24. (a) An SEM Image of Glass Reacted at 150°C in a Vapor Environment for 14 Days, Showing Analcime and a Calcium Silicate Phase, Possibly Tobermorite; (b) SEM/EDS Analysis of Analcime; and (c) SEM/EDS Analysis of Sodium Calcium Silicate Phase

(a)

(b)

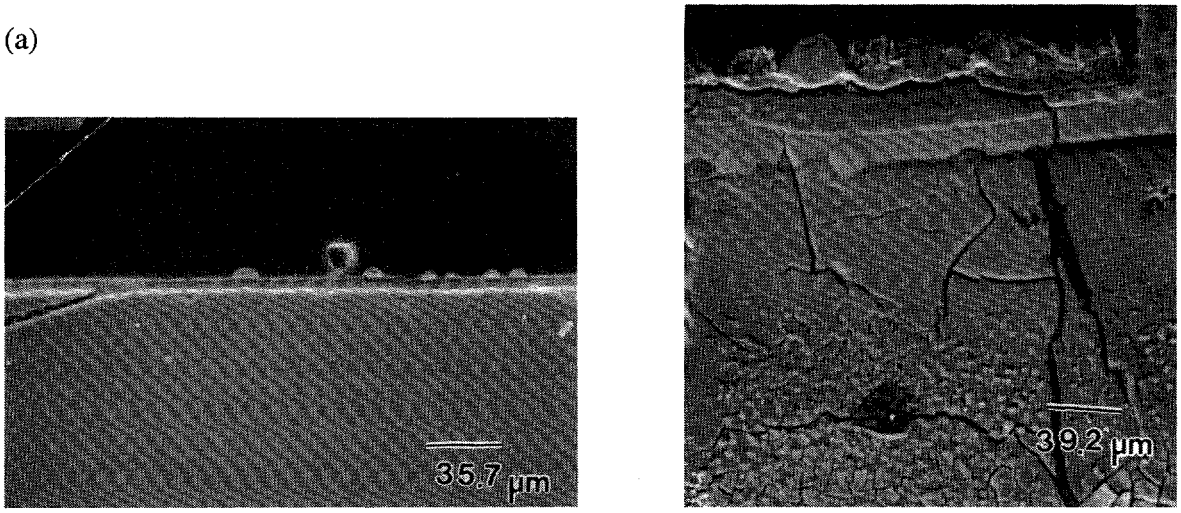

Fig. 25. SEM Cross-Sectional Images of Glass Reacted at 200°C in a Vapor Environment for (a) 6 h and (b) 24 h

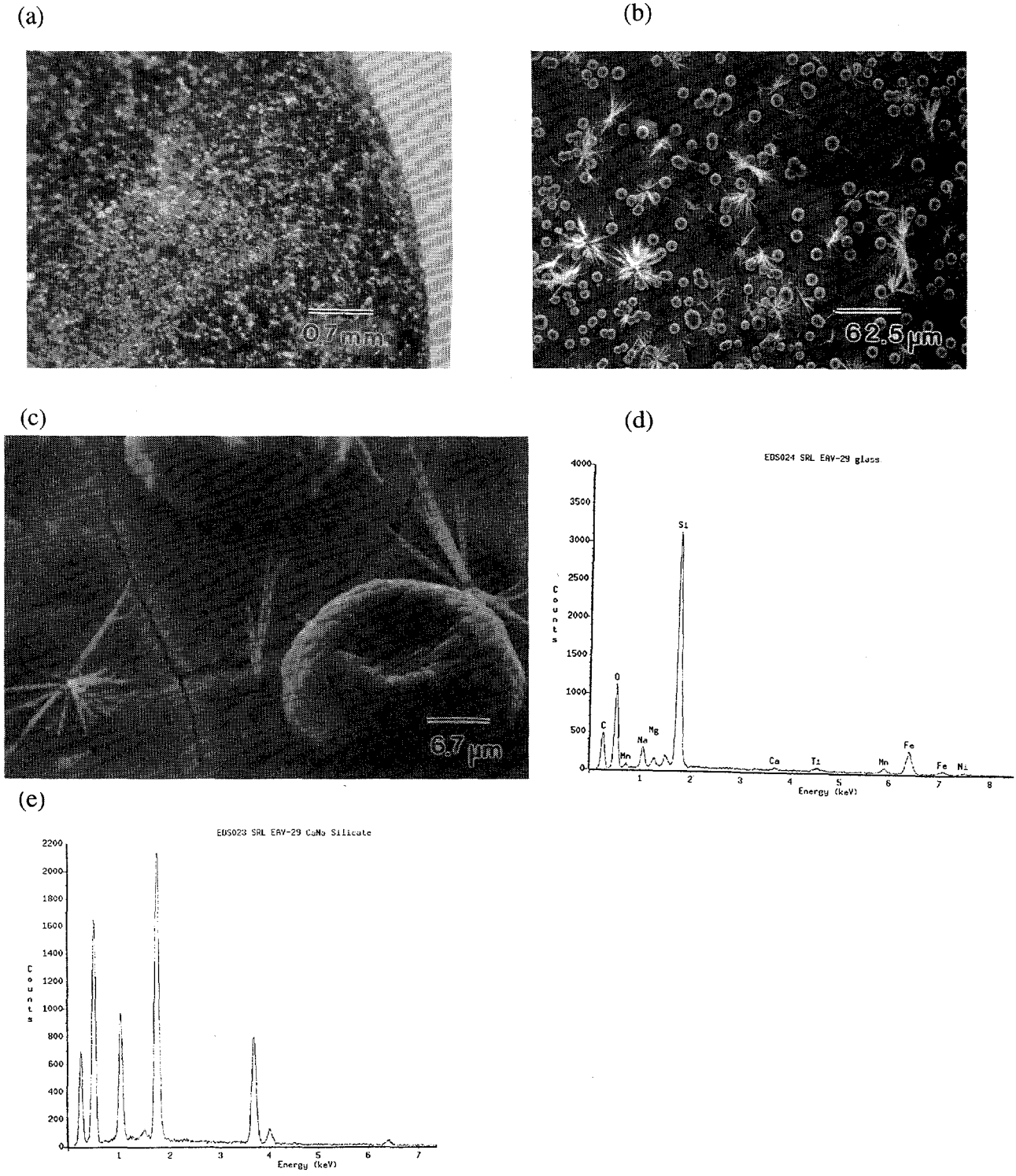

Fig. 26. (a) Optical Image of SRL EA Glass Reacted at 200°C in a Vapor Environment for 6 h; (b) Low-Magnification SEM Image Showing Presence of Analcime Crystals and Possibly Tobermorite; (c) Higher Magnification Image Showing the Pitting of Some Particles; (d) SEM/EDS Analysis of Glass Surface; and (e) SEM/EDS Analysis of the Calcium Silicate Phase

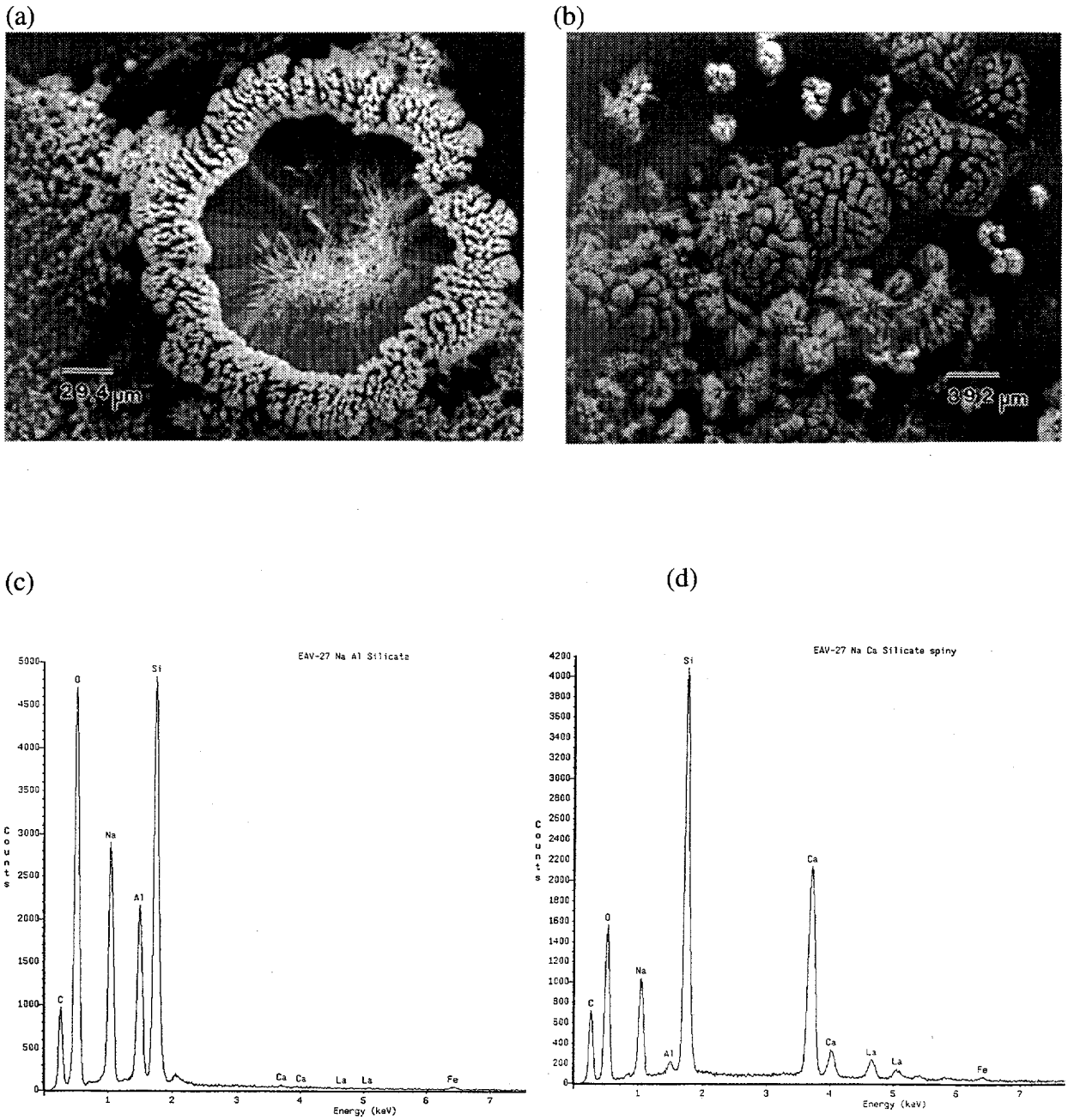

Fig. 27. Two SEM Images of Glass Reacted at 200°C in a Vapor Environment for (a) 24 h and (b) 48 h, Showing Extensive Coverage by Sodium Calcium Silicates, Also Containing Lanthanum, SEM/EDS Analyses of (c) Analcime and (d) Calcium Silicate in the 48 h Test.

While the analcime crystals always possessed the distinctive trapezoidal morphology, there was a difference in the morphology of the analcime crystals at different temperatures. At 200°C, the analcime was extensively twinned, whereas at 150°C, the analcime crystals were less faulted. This change, which has also been observed by others [48, 64], needs to be examined more closely in future tests. This pattern of crystal development is not unexpected and may be explained through the increased nucleation rate at high temperatures. Some of the analcime crystals found in the vapor hydration test appeared to depart from the ideal composition of [$NaAlSi_2O_6 \cdot H_2O$], possibly because of excessive evaporite precipitation on the crystal surface.

The distribution of alteration phases in the high-temperature (200°C) vapor tests appeared to be different than that in the PCT [5]. Calcium silicates, possibly tobermorite and gyrolite, and analcime were commonly found in the vapor hydration test; in the PCT tests, analcime, tobermorite, and a phillipsite-related zeolite were observed. The calcium silicates found in the vapor hydration test varied greatly in morphology between fibrous, tubular, and needle-like. Tobermorite and gyrolite are possible phases; others include nekoite [$Ca_3Si_6O_{12}(OH)_6 \cdot 5H_2O$] and afwillite [$Ca_3Si_2O_4(OH)_4$]. However, all the calcium phases observed contained significant quantities of sodium and lanthanum, which may change the structures from the ideal. A more detailed study using electron and X-ray diffraction will be required to identify these phases correctly .

E. Future Studies

Longer term tests are still in progress, and replicate tests at 175°C and 150°C will be performed to determine reaction kinetics. The alteration phases will be examined using AEM and XRD to provide positive characterizations of the phases. In particular, we need to know whether additional phases observed in PCT tests are present. Secondary ion mass spectrometry will also be performed on some samples to profile light elements through the reacted layer.

VIII. COMPONENTS FROM DRIP TESTS WITH ATM-10 GLASS

A. Introduction and Background

Samples of reacted ATM-10 waste glass and sensitized type 304L stainless steel, generated as part of the N3 series drip tests sponsored by YMP, have been maintained in storage since 1987 and 1988. The ATM-10 is an actinide-doped, former reference glass for the West Valley Demonstration Project (WVDP). These samples, together with the solution results from the tests, provide a valuable indication of the reaction of ATM-10 glass in the unsaturated environment that may exist at the proposed high-level waste repository site at Yucca Mountain, Nevada.

Tests using the Unsaturated Test Procedure [23,30,65] were initiated with the ATM-10 glass on July 6, 1987. The tests, designated "N3," followed the original matrix shown in the Task Plan, and during the first 52 weeks, eight tests were terminated. In addition to the test samples generated (glass and type 304L stainless steel), solutions were collected and analyzed. However, the test samples were never analyzed, and solution results were only recently made available [5,66].

B. Objectives

The objective of the N3 Components Task is to analyze the solid components from the N3 tests, using several techniques to evaluate (1) the process by which the glass reacts, (2) the interaction between the glass and the type 304L stainless steel that makes up part of the test assembly, and (3) the distribution of radionuclides between the glass and the steel. These results, when combined with published leachate solution data [5], provide important input for the glass source term in modeling of the repository.

Analyses performed have included optical microscopy, scanning electron microscopy (SEM), and analytical transmission electron microscopy (AEM). These microscopic techniques allow us to determine the size and distribution of reaction products and corrosion damage. Other studies performed were elemental analyses by energy dispersive X-ray fluorescence spectroscopy (EDS) and electron energy loss spectroscopy (EELS) and, in selected cases, crystal structure determination by electron diffraction (ED).

Other tests were performed on the type 304L stainless steel components to assess metal interaction with the glass waste form. High-resolution alpha spectroscopy of acid-wash from the stainless steel components was used to measure sorption of transuranic elements onto the steel. Inductively-coupled plasma/mass spectroscopy (ICP/MS) was also performed on the acid-wash solutions to validate the alpha spectroscopy measurements and also to measure B, Si, Th, and U deposition onto the metal. Oxalic acid treatment was used to determine the level of sensitization of the type 304L stainless steel used in the components.

C. Technical Approach

The Unsaturated Test (drip test) of the N3 batch samples has been completed according to standard procedure. The test matrix is shown in Table 14. Tests N3-9 through N3-12 remain ongoing under YMP guidance, with solution analyses being performed at each sampling period [5,66]. Test N3-11 is a blank (control) test, containing no waste form, and is used to monitor the performance of the groundwater injections into the test vessels.

Table 14. N3 Test Sample Identification

Test No.	Description	Date Started	Date Terminated	Cumulative Test Period (weeks)
N3-1	Batch	7/6/87	10/1/87	12.5
N3-2	Batch	7/6/87	10/1/87	12.5
N3-3	Batch	7/6/87	1/4/88	26
N3-4	Batch	7/6/87	1/4/88	26
N3-5	Batch	7/6/87	4/4/88	39
N3-6	Batch	7/6/87	4/4/88	39
N3-7	Batch	7/6/87	7/4/88	52
N3-8	Batch	7/6/87	7/4/88	52
N3-9[a]	Continuous	7/6/87	Ongoing	>400
N3-10[a]	Continuous	7/6/87	Ongoing	>400
N3-11[a,b]	Continuous-blank	7/6/87	Ongoing	>400
N3-12[a]	Continuous	10/6/87	Ongoing	>400

[a]N3-9 through N3-12 remain ongoing under YMP guidance as of this writing.
[b]N3-11 is a blank test; that is, it contains no waste glass or support.

1. Preparation and Selection of Initial Components

a. Preparation of ATM-10 Glass

The actinide- and technetium-doped West Valley ATM-10 reference glass was received in 1987 from the Materials Characterization Center (MCC) at Pacific Northwest Laboratory. The composition of the glass, from Maupin et al. [67], is given in Table 15. The glass was remelted to provide finished samples used in the tests. The samples consisted of eleven gently tapered cylinders, approximately 16.0 mm in diameter at the top, tapering to about 15.4 mm in diameter at the bottom, and approximately 20.2 mm in length. Each weighed about 10.5 g. Variation of each of these dimensional parameters among the samples was less than 5%.

b. Sensitization of the Type 304L Stainless Steel Support

The ATM-10 glass was held in place for the tests by a waste form support made of type 304L stainless steel that had been perforated with holes to allow free contact with the dripping water. This material was used because it is the same as that used in the construction of the glass pour canister. The type 304L components used in the N3 tests were sensitized by annealing for 24 hours in a 550°C oven. This sensitization of the type 304L test components was performed to simulate the heat treatment that may result when molten glass is poured into the canisters during production of actual waste. The final color of the metal was a deep blue. Metallurgical testing of the degree of sensitization was performed and is discussed in a later section.

2. Unsaturated Test Procedure

Detailed descriptions of the Unsaturated Test Procedure are given elsewhere [23,30,65,68]. Nonetheless, a brief description is appropriate here to set the context for the results to be presented.

Table 15. Composition of the ATM-10 Glass

Oxide	Mean wt%[a]	wt% Std. Dev.[a]
Al_2O_3	6.65	0.0209
AmO_2	0.0064	0.000073
B_2O_3	9.17	0.082
BaO	0.045	0.00131
CaO	0.60	0.0354
CeO_2	0.072	0.00127
Cr_2O_3	0.253	0.0107
CsO_2	0.062	0.0015
Fe_2O_3	11.5	0.2065
K_2O	3.34	0.125
La_2O_3	0.025	0.0020
Li_2O	2.88	0.0281
MgO	1.15	0.0296
MnO_2	1.29	0.0219
Na_2O	10.5	0.150
Nd_2O_3	0.168	0.0023
NiO	0.296	0.0135
NpO_2	0.021	0.00041
P_2O_5	2.34	0.258
PuO_2	0.0081	0.000527
RhO_2	0.012	0.0018
RuO_2	0.061	0.0108
SO_3	0.31	0.090
SiO_2	45.8	2.391
SrO	0.025	0.00096
Tc_2O_7	0.0031	0.000083
ThO_2	3.29	0.0336
TiO_2	0.858	0.0245
UO_2	0.527	0.0171
Y_2O_3	0.017	0.00082
ZrO_2	0.247	0.00513
Total	101.5	

[a]From Maupin et al. [67].

In the Unsaturated Tests, 0.075 mL (about 3 drops) of tuff-equilibrated groundwater from the J-13 well near Yucca Mountain (termed EJ-13 water) is dripped onto the waste package assembly (WPA) in a sealed stainless steel test vessel every 3.5 days. The WPA used in the tests consists of a cylindrical monolith of waste glass, plus a stainless steel support, as described above. Each glass monolith is contacted on the top and bottom by the two perforated support plates in each holder, which are held in place by two wire posts, also made from type 304L stainless steel. The entire test apparatus is held in a 90°C oven except when samples are taken and observations are made (for the batch tests discussed here, samples were taken only once, upon termination). Excess water dripped from the WPA to the bottom of the vessel; the samples were not immersed in liquid. A typical composition of EJ-13 groundwater is given in Table 2.

Upon termination, the WPA components were disassembled and weighed, then photographed and stored in labeled containers. The percent mass changes of the glass, steel, and the total WPA are plotted in Fig. 28. The total mass change is small, although it appears that initially mass is transferred from the glass to the stainless steel. At later times, cations in the EJ-13 water may have been adsorbed onto the reacted glass surface, reversing the initial mass loss of the glass.

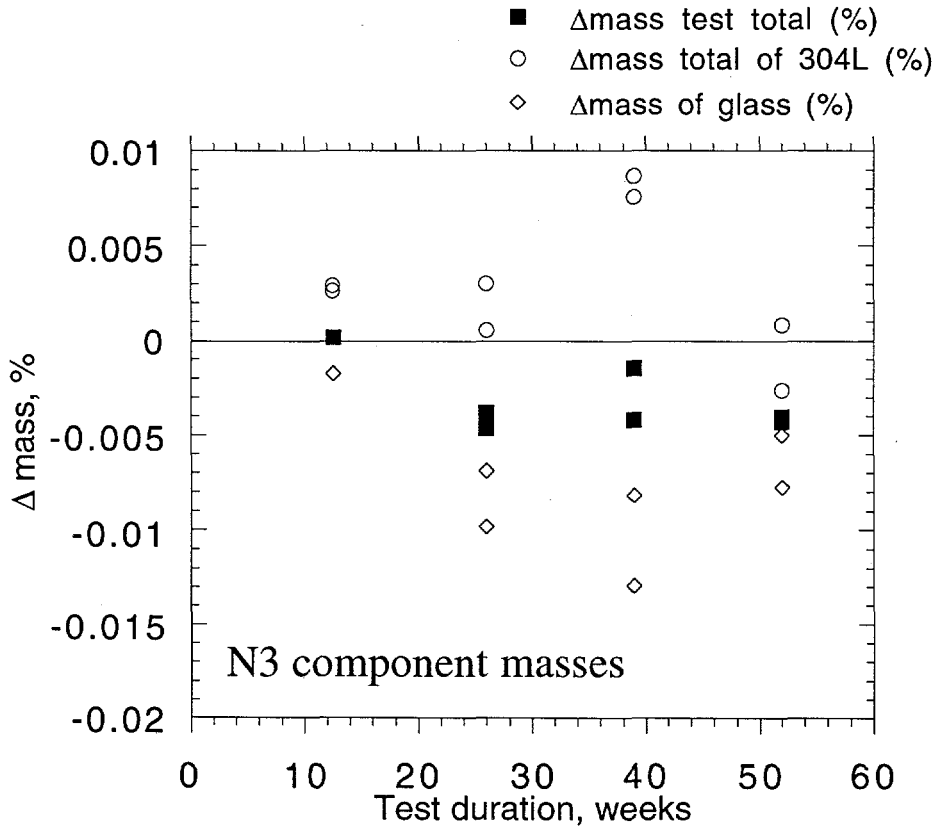

Fig. 28. Percent Mass Changes of the N3 Test Components. One outlier, the N3-2 glass, was inadvertently chipped between the initial weighing and the post-test weighing, and is not included in the figure. Two tests were terminated at 13, 26, 39, and 52 weeks.

D. Results and Discussion

1. Qualitative Description of Components

Qualitative optical examinations, including photographs taken in the optical microscope, have been completed for all relevant surfaces, both glass and type 304L stainless steel. Visually, increased quantities of clay and other secondary phases were observed on both the glass and stainless steel components with increasing test duration. The bottoms of the glass samples were much more likely to display substantial rust-colored markings, evidence of interaction with the stainless steel support, than did the tops; likewise, the bottom stainless steel supports displayed more evidence of corrosion than the top ones. The sides of the glass monoliths were water-marked but appeared much less corroded than either the tops or bottoms. For the tests of shorter duration (i.e., N3-1 and N3-2), the contact areas between the glass and stainless steel often had a light metallic blue appearance. This bluish coloration persisted in the longer duration tests, surrounding the rust-colored markings. Further details were given in the 1994 Annual Report [5].

Optical examination of the stainless steel supports revealed little material attached to the top components, and generally little rust. In sharp contrast, the bottom components were covered with increasing amounts (with test duration) of clay and secondary phases. In addition, heavy rust appeared in the area of the support posts, which had been welded to the bottom support. The concentration of the rust near the welds is consistent with increased sensitization of the type 304L stainless steel in this area. These areas of heavier rust also explained the diametrically opposed rust (or blue) markings on the bottom surfaces of the glass monoliths. These results allow us to examine how sensitization of the stainless steel affects its interaction with the waste glass, as different regions of the same glass surface have been exposed to differently sensitized stainless steel. Again, rust appearance, both near the posts welds and elsewhere on the bottom stainless steel components, increased with test duration.

Whole glass and stainless steel surfaces were examined in an ISI® Super II® SEM equipped with a PGT® EDS system for elemental identification. Images could be formed from either backscattered electrons or secondary electrons, the former provide atomic number (Z) contrast; the latter provide contour and electrical conductivity contrast. Most SEM micrographs were taken in backscatter mode. Usable magnifications of up to 5000X were achieved with this instrument.

The stainless steel components of the waste form support displayed increasing amounts of secondary phases on their surfaces with increased test duration. These secondary phases included clay, thorium-calcium-phosphate, iron oxide, iron silicates, and occasional uranium silicates, all of which were also found on the glass. The top portion of the stainless steel support generally had very little on it, while the bottom often was quite well covered with alteration phases.

Iron oxide and iron silicate particles were commonly seen in great quantity around the welds of the support posts of the support bottoms, regardless of test duration. These indicate rapid oxidation of the posts themselves, which contained more carbon within the type 304L stainless steel and were thus subject to greater sensitization than the perforated plates. As a test of this hypothesis, the sensitization of the type 304L stainless steel components was examined by the standard metallurgical procedure [69]. This procedure involved preparing a cross section of the metal support, imbedding the cross-sectioned sample in epoxy, polishing to 1 μm smoothness, then etching with oxalic acid in an electrolytic cell using the sample as the cathode. The etching reveals grain boundary precipitation of chromium carbide, typically caused by heat treatment. These etched grain boundaries are readily observed in the SEM. While the perforated plates comprising the bulk of the support assembly were found to be partly sensitized (Fig. 29a), the wire

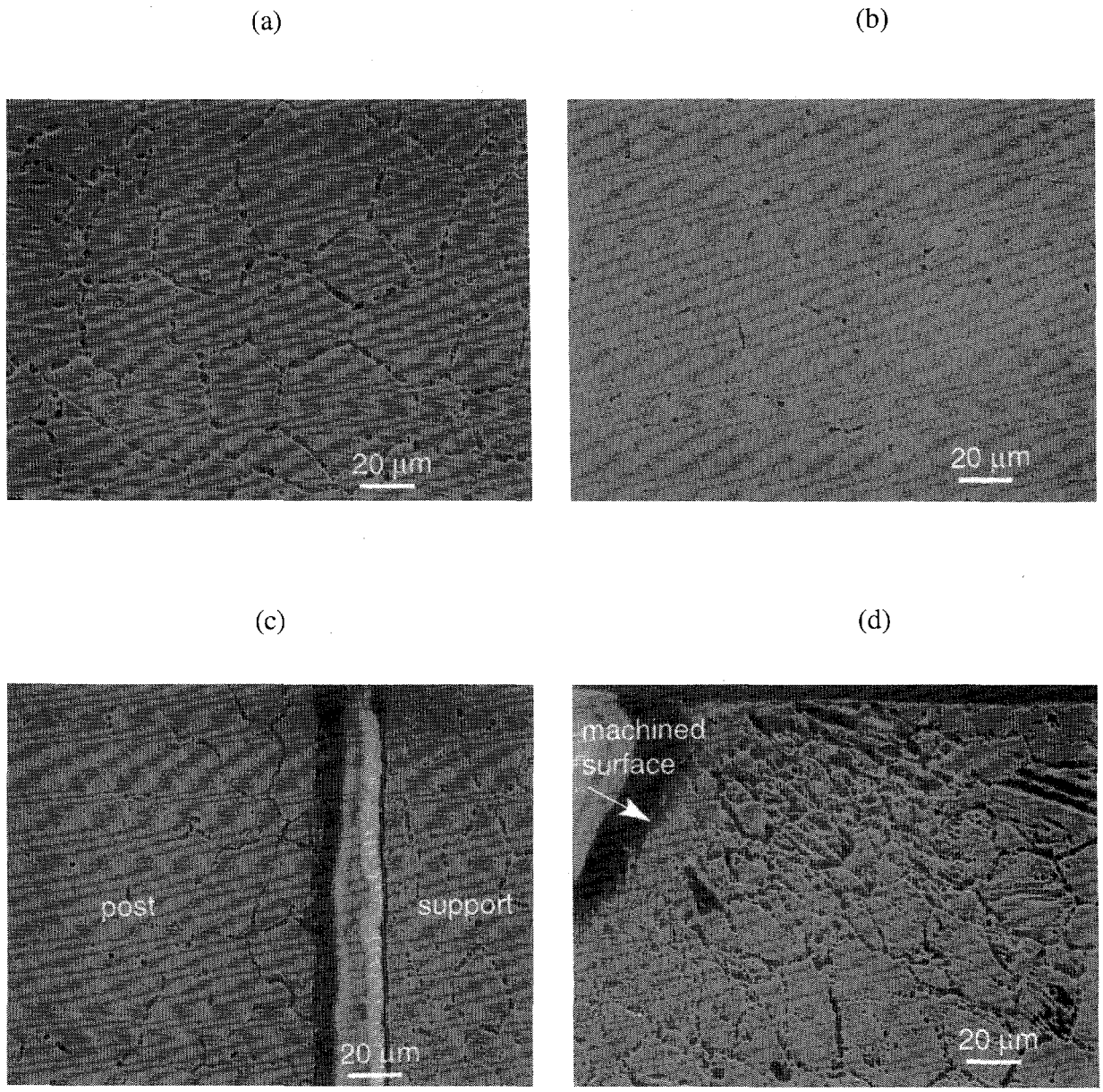

Fig. 29. Sensitization of the Type 304L Stainless Steel Support Components. The support plates were partially sensitized (a), as determined by the etching of the grain boundaries. The wire posts were not sensitized in their interior (b), but were heavily sensitized at the surface (c). Extensive sensitization also occurred near machined portions of the plates, as near a perforation (d).

support posts were not sensitized in the interior (Fig. 29b), but were highly sensitized within about 20 μm of the surface (Fig. 29c). Extensive sensitization was also noted in regions of the plates that had been machined (Fig. 29d). Overall, it appears that the desired partial sensitization of the stainless steel support components was achieved. The effects of these sensitized regions interacting with the glass were initially reported in the previous Annual Report [5,70], and are revisited in part later in this report.

2. Analytical Electron Microscopy Findings

Selected materials were removed from the glass surfaces of N3-1, N3-3, N3-5, and N3-8 for examination by AEM. Materials taken included chips of glass, often with an attached clay reaction layer, and secondary phases from the surface. These samples, measuring between 10 and 100 μm across, were imbedded in an epoxy resin and sectioned by ultramicrotomy with a glass knife to form ~500 to 1000 Å-thick sections. Typically, between five and eight samples were successfully prepared and analyzed from each glass surface.

The sample sections rested on a standard carbon-coated TEM grid and were analyzed in a JEOL 2000FXII transmission electron microscope operating at 200 keV. The microscope was equipped with a NORAN® ultrathin window EDS detector, a Gatan® parallel-EELS detection system, and a Gatan® slow-scan charge-coupled device camera. The microscope was operated in either an image mode, where usable magnifications from 1000X to more than 100,000X were recorded. The AEM could also be operated in a diffraction mode, which allowed positive identification of several crystalline secondary phases.

a. Formation of Smectite Clay Layers

The most common secondary reaction product to form on the surface of glass reacted with water is a smectite clay. Smectite clays form both within the dissolving gel layer, as remaining atoms rearrange, and in solution, where colloids form and eventually reprecipitate on the surface of the glass. Clays can also grow on the surface directly from dissolved ions in solution. These various mechanisms can lead to complex patterns in the structure of the clays. Clays have a layered network structure that is apparent in many of the AEM micrographs; however, they tend not to retain many of the elements present in the original glass. In particular, alkali metals, rare earths, thorium, and uranium are not retained in the clay structure; it is probable that boron and certain transuranic elements are not retained either.

After 39 weeks of testing, the N3-5 glass had developed a substantial clay layer that exceeded 500 nm in places and often have a well-defined backbone (Fig. 30). This backbone structure is believed to occur as the altered glass dissolves, with some of the cations reprecipitating as clay. The backbone forms in the vicinity of the original glass surface, while the clay grows outward in both directions from the original nucleation sites. The clay has a much simpler elemental composition than the glass, being depleted in alkalis, thorium, and uranium and somewhat enriched in iron, aluminum, and magnesium. Also note that an unusual thorium-titanium-iron-silicate secondary phase, distinct from the clay, makes an appearance between the glass and the clay in the micrograph. This thorium-titanium-iron-silicate phase appears to be completely amorphous, giving no crystalline diffraction pattern whenever it is observed, and is probably related to the metamict mineral thorutite. Note the extremely minute dimensions of these particles; they are generally only a few nanometers across and at best occur in clumps a few tens of nanometers across. These would surely escape detection in the SEM. This thorium-titanium-iron-silicate phase is discussed in greater detail later.

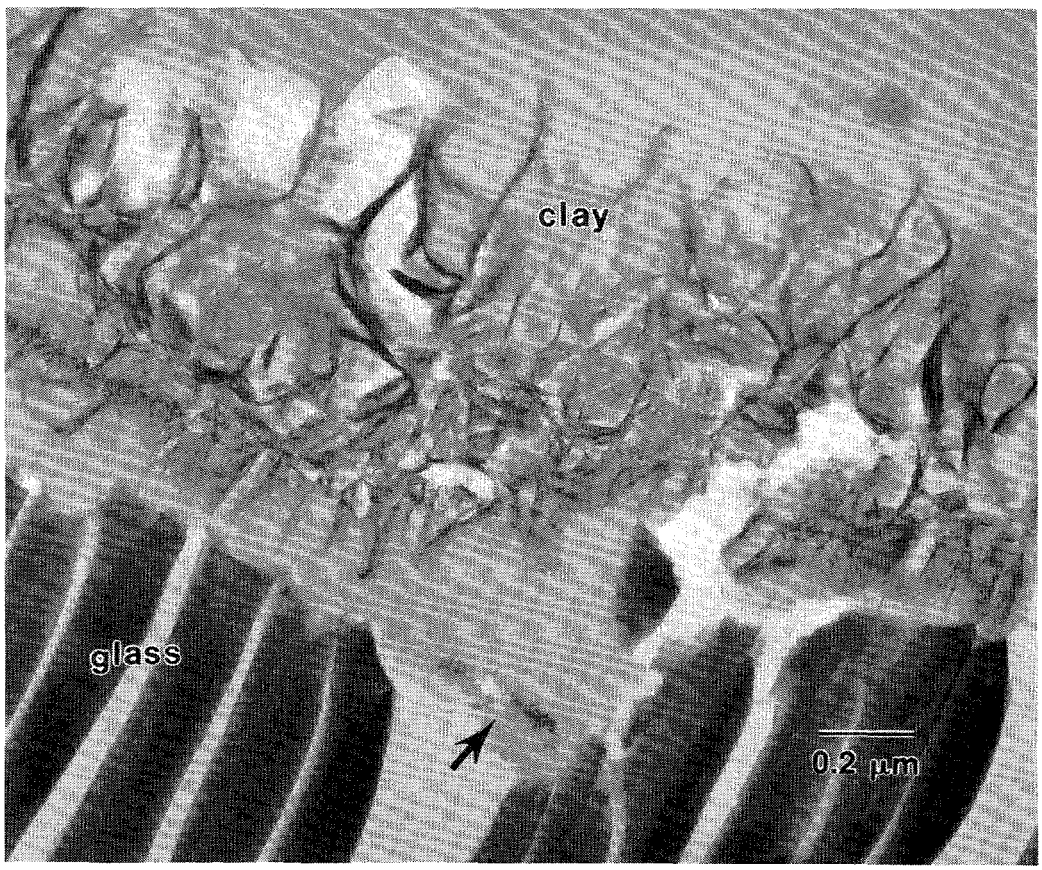

Fig. 30. AEM Micrograph of a Clay Layer on the Top Glass Surface from the N3-5 Test. A small amount of an amorphous thorium-iron-titanium phase is visible between the glass and the clay; an isolated clump of this material is indicated by the arrow. The chattering pattern observed in the glass is an artifact of the microtoming preparation.

b. Alteration Phases

A major finding on the bottom surfaces of the glass monoliths was a substantial iron-rich layer, as much as 150 nm thick on N3-8, that had formed on the glass under the clay layer where the glass had contacted the stainless steel support [5,70]. This finding suggests that sensitized stainless steel may accelerate the glass reaction. Crystalline iron silicates were also observed; one particle was identified by electron diffraction as fayalite (Fig. 31 and Table 16).

Particles having a composition of brockite (thorium-calcium-phosphate) were ubiquitous, sometimes exceeding 200 nm in length, and were generally imbedded in the surface clay layer [5,70]. Much larger particles having this composition were observed by SEM, the largest being over 3 µm across [5]. There appears to be a correlation between the size of the largest brockite particle observed on a surface and the duration of the test from which it came. Small brockite particles, often 50 nm or less, are found on all test surfaces examined to date, suggesting that there is continuous nucleation and growth of this phase. This contrasts with the observation of the smectite-type clay, which grows continuously with time, having nucleated on

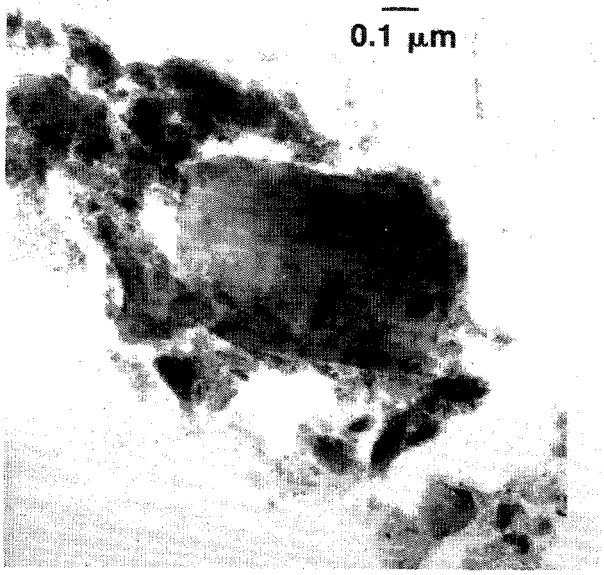

Fig. 31. AEM Micrograph of Iron-Silicate Crystals from the N3-3 Glass Sample. Electron diffraction (Table 16) identified one of the phases present as fayalite (Fe_2SiO_4).

Table 16. Electron Diffraction Results from an Iron-Silicate from the N3-3 Glass Surface. The pattern matches reasonably well, to within the ±5% experimental error, with the mineral *fayalite*.

Experimental d-Spacings[a] C15076 (Å)	Fayalite (Fe_2SiO_4) JCPDS 20-1139
	5.23, 4.38
4.0	3.98
	3.55
3.12	3.05
	2.828, 2.501
2.34	2.307, 2.348
	2.192
1.97	1.987
	1.838
1.682	1.680
1.536	1.536

[a]The JCPDS [71] values are from powder X-ray diffraction measurements. The electron diffraction measurements in the TEM are limited to available crystallographic orientation of the very small samples; thus, some d-spacings are not observed.

the original glass surface. Electron diffraction confirmed the brockite structure in at least two samples (Table 17). Figure 32 shows an AEM micrograph of a brockite particle, along with EELS spectra for the rare earth elements and actinides in this phase. The rare earth elements are partitioned into the brockite in rough proportion to their concentrations in the original glass. Furthermore, the Ce-$M_{4,5}$ edges appear to be shifted to lower energy by ~2 eV from the reference CeO_2; this finding is consistent with all rare earths being in the +3 oxidation state, rather than the +4 oxidation state of Th or Pu. The ATM-10 glass contains minute levels of Am and Pu (Table 15), and brockite is known to entrain transuranic elements [72]. The intensities of the Nd-$M_{4,5}$ and Ce-$M_{4,5}$ EELS edges from the brockite indicate that the Pu-$M_{4,5}$ edges would have been observable had this element partitioned in the same manner as the rare earths; despite the excellent signal-to-noise ratio, plutonium was not observed. The Pu and Am are presumed to have partitioned into the brockite in proportion to the Th, making it undetectable at three orders of magnitude lower concentration. This contrast between the behavior of the rare earth elements and the actinides suggests that the use of "surrogate" elements (in lieu of the actual actinides) in durability testing requires cautious interpretation.

The thorium-bearing phase containing substantial iron and titanium, mentioned earlier as existing at the interface between the glass and clay (Fig. 30), was also observed within voids or pits in the glass. In one unusual instance, it was observed as a double layer on the glass surface, separated by clay (Fig. 33). This material did not yield a crystalline diffraction pattern. It is probably related to the "amorphous" group minerals davidite, $(Fe,Ce,U)_2(Ti,Fe)_5O_{12}$ (JCPDS 13-505) [71], with thorium substituted for uranium, or thorutite, $(Th,U,Ca)Ti_2O_6$ (JCPDS 14-327) [71]. Both are described as amorphous and metamict, crystallizing after heating 1 h at temperatures near 1000°C. This material, however, had neither rare earth elements (such as Ce) as davidite has, nor Ca, as thorutite has. It would be arbitrary to identify this substance with a specific mineral, as amorphous materials are known to have a more

Table 17. Electron Diffraction from the Calcium-Thorium-Phosphate Phase. The diffraction pattern indicates a brockite structure.[a]

Experimental d-Spacings (Å) from N3-8	Experimental d-Spacings (Å) from N3-5	JCPDS 15-248 Brockite[b]
6.19		6.06
4.59	4.47	4.37
3.18	3.26	3.47
	3.02	3.03
2.93	2.81	2.83
2.48		2.37
2.226	2.10	2.15
1.926		1.92
		1.86
	1.74	1.75
	1.66	1.67

[a]See note in Table 16.

[b]Brockite: nominally, $(Ca,Th,Ln)(PO_4)\cdot H_2O$, rhabdophane group, hexagonal system, space group $P6_{222}$ [71].

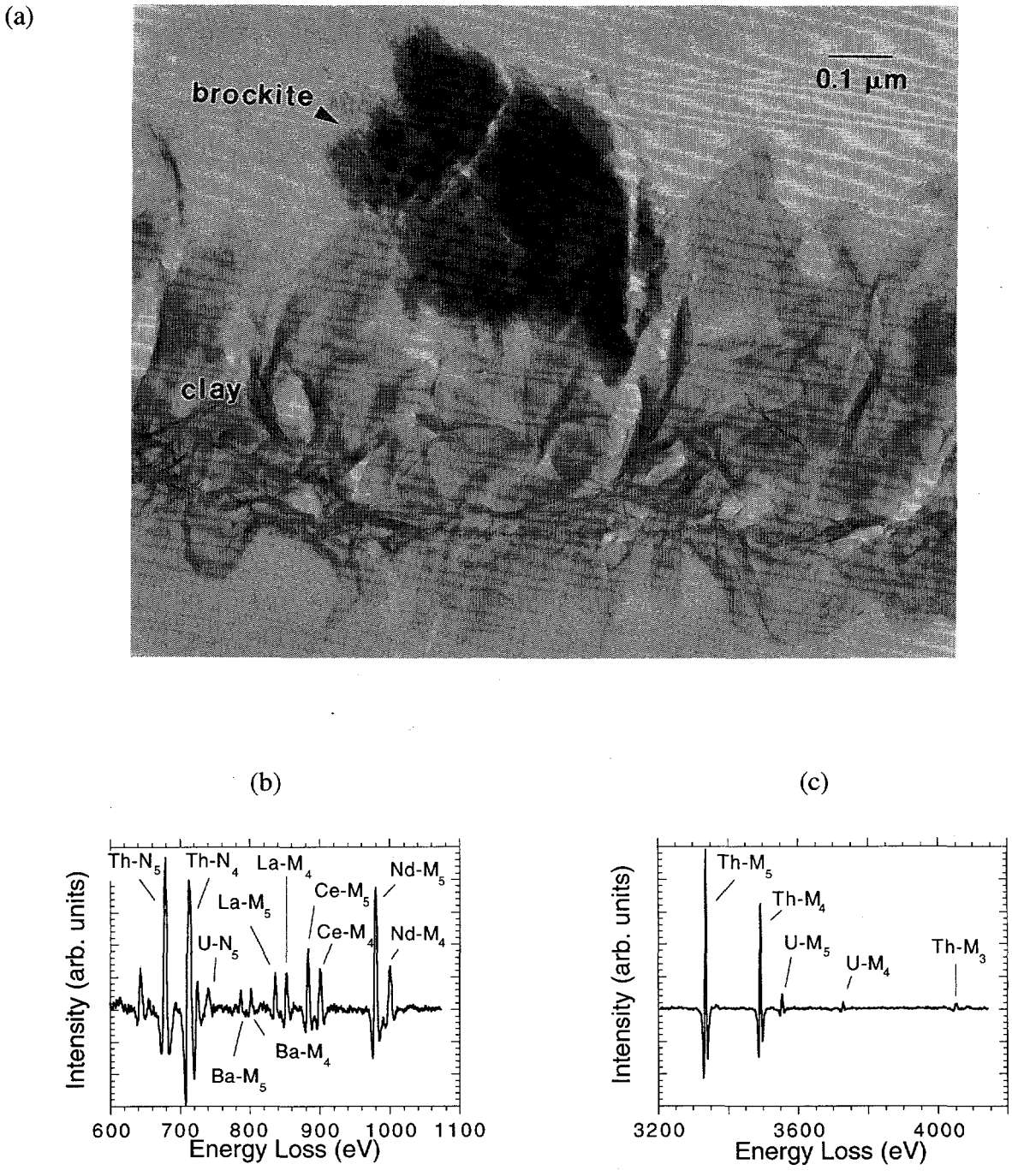

Fig. 32. (a) AEM Micrograph of a Brockite Particle Attached to Clay from the Top Surface of the N3-5 Glass. The clay has separated from the glass in this region, which is not visible in the micrograph; it was originally located on the side of the clay opposite the brockite. (b,c) EELS spectra of the rare earth and actinide elements in the brockite.

(a)

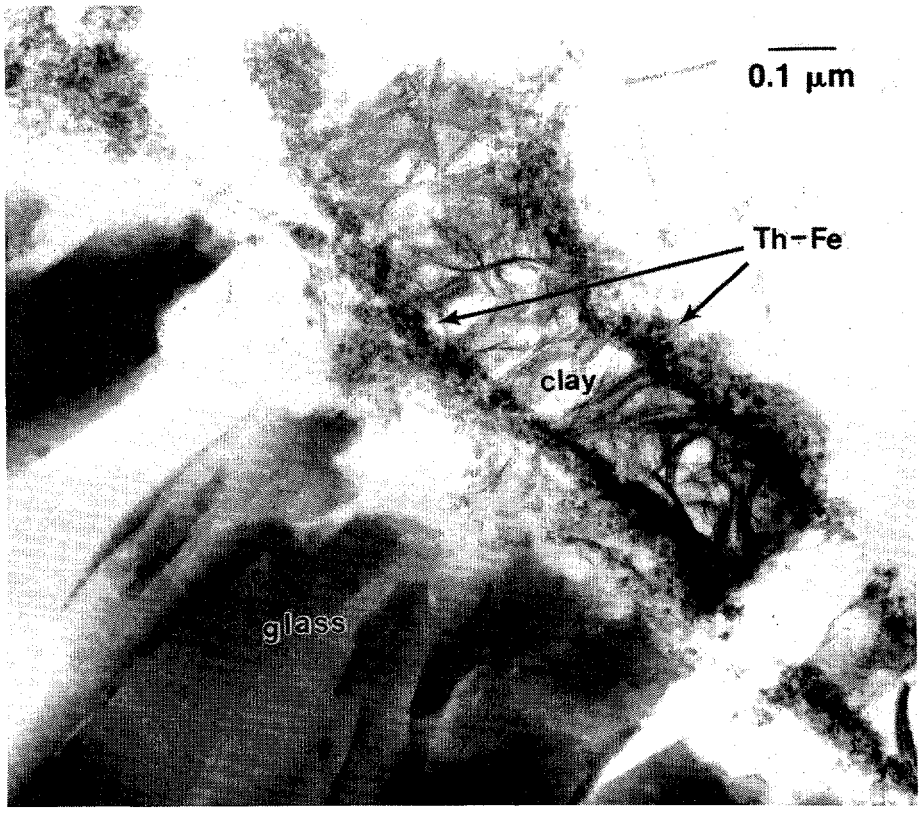

(b)

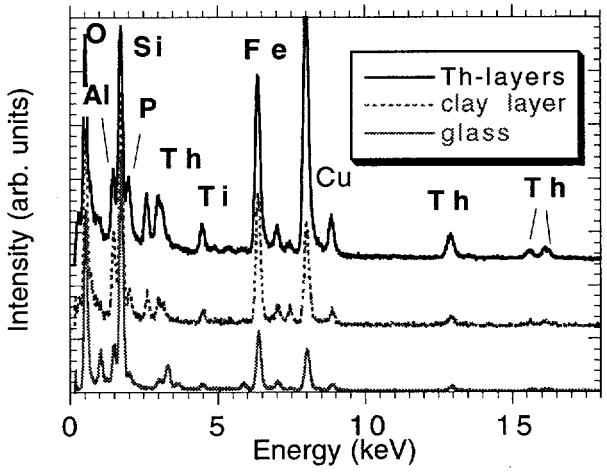

Fig. 33. (a) AEM Micrograph of Clay Layer on Glass from the Top Surface of N3-3, Showing Unusual Double-Layer of Thorium-Iron Precipitates. (b) EDS spectra, normalized to Si-Kα line, of the two thorium-rich layers (the inner and outer layers have similar compositions), the clay layer, and the ATM-10 glass.

variable composition than crystalline matter. The fact that this material is observed within cracks or near-surface voids in the glass suggests that it either forms as colloids, collecting where the flow of liquid is restricted, or that it forms *in situ*, where trapped liquid water concentrates dissolved cations. This phase did not contain any measurable rare earths, further distinguishing it from the brockite (Fig. 34). It is worth noting that both the brockite and the amorphous "thorutite" phases incorporated measurable uranium, and probably entrained transuranics. This hypothesis is partly supported by previous work [72] in which autoradiography and AEM were combined to identify a correlation between transuranic alpha activity (Pu or Am) and the presence of brockite in clay colloids. The notion of transuranic entrainment in the brockite is also supported by the fact that the brockite often appeared completely amorphous or at least highly disordered—consistent with substantial radiation damage—whereas natural brockite minerals are generally crystalline despite self-irradiation from the natural Th and U over geologic time periods.

3. Elements Retained on Stainless Steel Support

The release of elements to solution from a drip test effectively defines the source term at a point in time. To describe the observed solution behavior in terms of the corrosion of the WPA, it is necessary to determine how elements are released from the glass, including those that are temporarily retained by the stainless steel support. To this end, the stainless steel components of representative tests at each time interval, namely the N3-2 (12.5 weeks), N3-4 (26 weeks), N3-6 (39 weeks), and N3-7 (52 weeks) tests, were stripped with a mixture of hydrofluoric and nitric acids to remove all sorbed materials. The resultant solutions were submitted for spectroscopic analysis to determine actinide and lithium concentrations. Lithium release, it should be noted, is an important benchmark for glass corrosion because it is not present in the stainless steel, it is not a major component of the EJ-13 water, and it is not expected to be substantially incorporated into alteration phases.

In Fig. 35, the masses of transuranic elements released to solution (as determined by high-resolution alpha spectroscopy) and retained on the stainless steel support are compared (as determined by ICP-MS). Far less neptunium was deposited on the stainless steel than was released into solution, a reflection of the tendency of this element to remain dissolved in solution and not form alteration phases. The Pu and Am were generally retained on the stainless steel at all test times at levels comparable to or exceeding the release to solution. This most likely occurs because the Pu and Am become associated with suspended particles, which then become attached to the stainless steel retainer.

When comparing elements present in the glass in widely varying concentrations, it is useful to consider the normalized release, $N_i = M_i/(c_i\ A)$, where M_i is the mass of element i released from the sample, c_i is the atomic fraction of element i in the source glass, and A is the surface area of the glass monolith (1.36×10^{-3} m^2). While normalized releases are generally used to express release to solution rather than transfer to a nearby surface, the normalization facilitates comparisons with solution data [66]. The normalized release to the stainless steel support of the elements Li, Th, U, Np, Pu and Am appears in Fig. 36 (as determined by ICP-MS). Note that the behavior of Li and Np, both of which tend to remain in solution, are similar in all samples. Other elements, particularly uranium, are more apt to be retained by the stainless steel. The relatively low values for thorium probably reflect its retention on the surface of the glass (as brockite or davidite), and do not suggest that it remains in solution.

E. Future Studies

A final Topical Report will be issued, including all data and analyses to date. Further analysis will incorporate trends from solution results from published accounts of the ongoing tests.

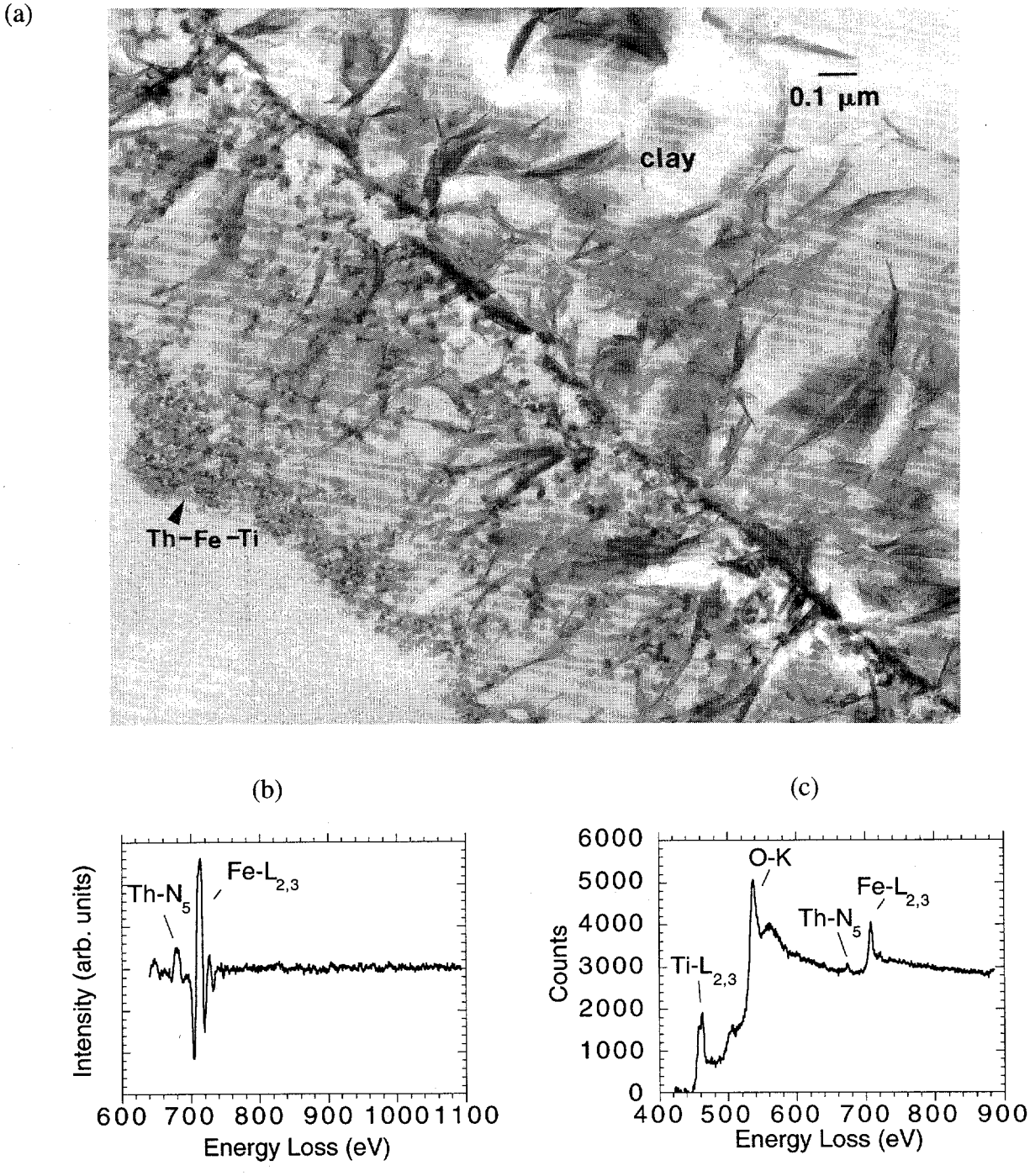

Fig. 34. (a) AEM Micrograph of Thorium-Iron-Titanium Precipitates under a Layer of Clay from the N3-5 Glass Monolith. The clay had pulled away from the glass in this region of the sample, but the glass was originally located on the side of the clay containing the precipitates. The EELS spectra (b, c) reveal that the precipitates do not contain rare earth elements (compare Fig. 32).

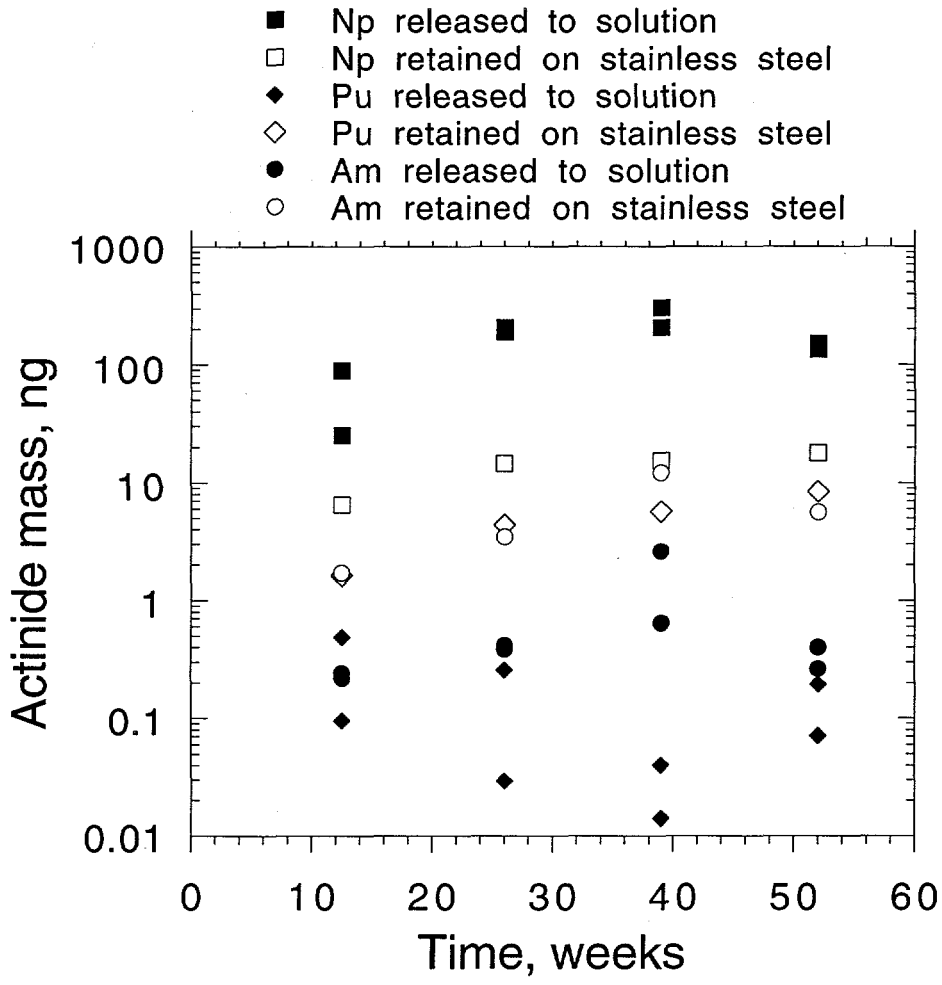

Fig. 35. Actinides from the Acid Strip of the Waste Form Supports (Open Symbols) Compared with the Actinides in Solution upon Test Termination (Closed Symbols)

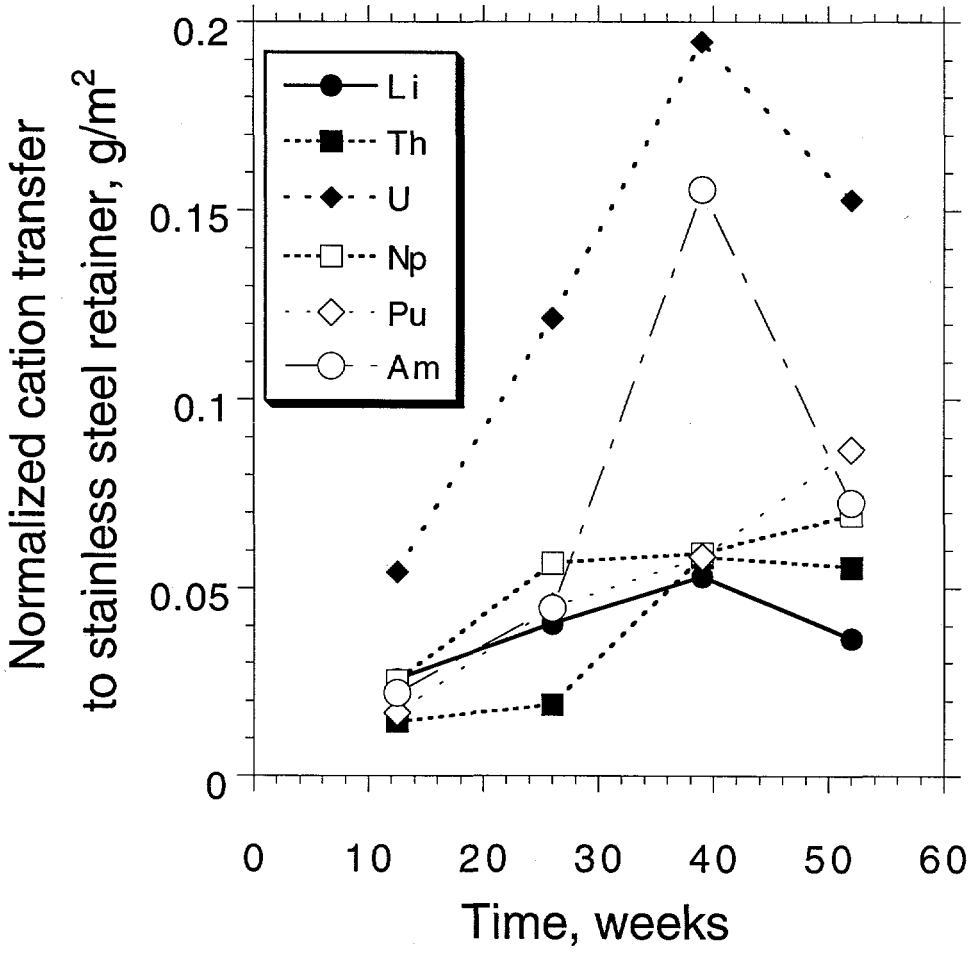

Fig. 36. Cations from the Acid Strip of the Waste Form Supports as Measured by ICP-MS. These values are normalized to the concentrations of each element present in the original ATM-10 glass and are divided by the surface area of the monolith.

IX. MECHANISTIC VALIDATION THROUGH NATURAL ANALOGUES

A. Introduction and Background

Natural glasses, some having survived for millions of years, are found in a variety of geologic environments [73]. The compositions of these glasses range from silica-rich obsidians (~70 wt % silica) to silica-poor basalt (~50 wt % silica). Because of the similarity in composition between nuclear waste glasses and natural glasses, it has been suggested that natural glasses may be useful analogues for projecting the long-term reaction of waste glass. Understanding the processes by which natural glasses corrode may assist in interpreting the reaction of nuclear waste glasses.

One method to investigate the processes that control the long-term corrosion of natural glasses is to reproduce in the laboratory reactions that have occurred in nature over thousands of years. This is done by exposing the natural glass to accelerated reaction conditions and comparing the corrosion of laboratory-reacted glass with that of natural glass. This method allows us to compare the alteration products, kinetics, and reaction mechanisms of the two glasses. If a clear relationship can be established between the corrosion of the analogue glass under laboratory and natural settings, then a means of accelerating the glass reaction can be established. This means of accelerated testing can then be applied to waste glasses.

Our studies have focused on three types of natural glasses: basaltic glass, tektite, and obsidian. Previous studies suggest that, in nature, basaltic glass reacts with water to form an amorphous, gel-like alteration phase called palagonite, in conjunction with a variety of secondary mineral phases [74,75]. The process by which basaltic glass reacts is disputed, although certainly a combination of molecular water diffusion, dealkalization, network hydrolysis, and network dissolution is involved. The rate-controlling reaction process appears to depend strongly on the environment in which a glass is altered.

B. Objectives

The objectives of this Task are to elucidate reaction mechanisms that control the reaction of natural glasses and to evaluate the effectiveness of laboratory test methods in reproducing the long-term reaction of glass. These goals will be achieved through (1) establishing the reaction kinetics both in nature and under the accelerating laboratory conditions (vapor hydration) for natural glasses, (2) identifying the alteration phases that form in nature over long periods of time and also in accelerated laboratory environments, and (3) determining the dominant reaction mechanisms that affect analogue glass reaction in natural environments and in accelerated laboratory experiments. A further correspondence will be made between reaction processes of natural glasses and waste glasses based on the reaction kinetics and the composition of the alteration phases.

C. Technical Approach

No new testing was initiated this fiscal year. Naturally altered glass samples that had been previously collected on Oahu, Hawaii (Table 18), were analyzed and characterized to determine the kinetics and the nature of glass alteration. The natural glasses were exposed to water in the form of precipitation, humid vapor, and surface runoff. Laboratory experiments have been performed on both natural glasses and waste glass. The glasses have been exposed to water vapor at 70-75°C in relative humidities (RH) ranging from 60% to 100%. Long-term laboratory tests were terminated as scheduled (Table 19). These samples are being analyzed and the results will be compared with those for the naturally reacted samples to evaluate the effectiveness of laboratory test methods in reproducing the long-term reaction of glass.

Table 18. Dated Volcanic Glass Samples from Oahu, Hawaii[a]

Bishop Sample No	ANL Sample No.	^{14}C Date	Appearance
50-OA-G5-101-TP7-1-769	NBG-1	Between 720 ± 80 and 750 ± 80 BP	Most of surface contains etching pits. A few palagonite particles are observed.
50-OA-G5-101-TP7-1-770	NBG-2	Between 720 ± 80 and 750 ± 80 BP	Most of surface covered by palagonite.
50-OA-G5-101-TP7-1-777	NBG-3	Between 720 ± 80 and 750 ± 80 BP	Most of surface covered by palagonite.
50-OA-G6-17-TP3-57	NBG-4	480 ± 80 BP	High density of etching pits in which palagonites formed and were preserved.
50-OA-G6-17-TP3-58	NBG-5	480 ±80 BP	Most of surface contains etching pits. A few palagonite particles are observed.
50-OA-G6-17-TP3-125	NBG-6	480 ± 80 BP	Dark green color; most areas are glass with etching pits. Yellow palagonite scatters on surface.
50-OA-G6-17-TP3-126	NBG-7	480 ±80 BP	Most areas are glass with etching pits. Yellow palagonite scatters on surface.
50-OA-G6-17-TP3-137	NBG-8	480 ± 80 BP	High density of etching pits on surface.
50-OA-G6-17-TP3-138	NBG-9	480 ±80 BP	Yellow palagonite layer covers entire surface.
50-OA-G6-17-TP3-139	NBG-10	480 ± 80 BP	Etching pits and palagonites are both observed on surface.

[a]Received from Bishop Museum, Hawaii.

Table 19. Terminated Long-Term Tests of Natural Glasses during FY 1995[a]

Sample ID	Test No. (Vessel Number)	Sample No.	Duration, Days	% RH	Date In	Date Out
			Nuclear Waste Glasses			
165-95RH	V-106	V111	3367	95	10/3/86	12/21/95
165-95RH	-	V153	2672	95	7/27/88	12/21/95
131-95RH	V-110	V119	3367	95	10/3/86	12/21/95
131-95RH	-	V163	2672	95	7/27/88	12/21/95
7668-95RH	V-114	V127	3367	95	10/3/86	12/21/95
7668-95RH	-	V127	2672	95	7/27/88	12/21/95
165-100RH	V-158	V158	2575	100	9/2/88	11/20/95
131-100RH	V-159	V165	2575	100	9/2/88	11/20/95
7668-100RH	V-161	V175	2575	100	9/2/88	11/20/95
			Obsidian Glasses			
OBS-95RH	V-118	V135	3367	95	10/3/86	12/21/95
OBS-95RH	-	V193	2672	95	7/27/88	2/21/95
OBS-100RH	V-165	V195	2575	100	9/2/88	11/20/95
			Basaltic Glasses			
BAS-95RH	V-122	V143	3367	95	10/3/86	12/21/95
BAS-95RH	-	V183	2672	95	7/27/88	12/21/95
BAS-100RH	V-163	V185	2575	100	9/2/88	11/20/95

[a]Selected natural glasses have been reacted with water vapor for a period of 7 to 9 years

We have completed a draft Critical Review of studies that use natural altered glasses as analogues to predict the long-term corrosion behavior of high-level nuclear waste glasses and to extrapolate short-term laboratory results to longer time frames. By comparing the alteration processes observed for both natural and waste glasses, we can assess the applicability of our current vapor test methods to accelerate glass reaction.

The reacted glasses were analyzed to characterize the corrosion of the glass and to identify alteration phases formed during reaction under different conditions. Scanning electron microscopy (SEM) with backscattered electron detection (BSE) was used for measuring the thickness of alteration layers and for locating various secondary phases formed during glass reaction. Our Robinson backscattered electron detector has a resolution of ±0.2 atomic number units and permits secondary phases to be differentiated in a relatively short time. Energy dispersive X-ray spectroscopy (EDS) and wavelength X-ray dispersive spectroscopy (WDS) are used in conjunction with SEM to detect elements present in various phases and semi-quantitatively analyze chemical compositions of each phase. X-ray mappings are performed on cross sections of reacted samples to provide information on the relationships among various phases. X-ray diffraction (XRD) is used to determine the crystal habits of selected alteration phases.

Analytical electron microscopy (AEM) is a combination of transmission electron microscopy (TEM), EDS, electron energy loss spectroscopy (EELS), selected area electron diffraction (SAED), and convergent beam electron diffraction (CBED). Analytical electron microscopy is an extremely powerful tool for investigating inhomogeneous, multiphased samples because it can handle small inclusions and crystallites at nanometer scale. Selected samples were studied using AEM to identify and characterize the various secondary phases, the general mineralogy of reacted sample, and interfaces between the unreacted glass and alteration phases and between various reaction layers that form on the glass. In particular, electron diffraction allows determination of crystal habits of various phases and, by combining with EDS and EELS information, semiquantitative compositions and oxidation state of elements can be deduced.

D. Results and Discussion

1. Natural Basaltic Glasses from Oahu, Hawaii

Ten samples of volcanic basaltic glass have been collected from two archaeological sites on the windward side of Oahu, Hawaii. These samples are from 5 to 85 cm below ground level in generally wet and cool windward environments of the Island. However, the exact humidity and temperature values are not known. The samples data from 480 to 720 ± 80 B.P. (Before Present) as reported using radiocarbon dating for the occupation layer of charcoal associated with the glass (Table 18). Quantitative EDS analysis indicates that these glasses have the composition range of typical basaltic glasses, with ~50 wt % SiO_2 (Table 20). The glasses have been altered by the meteoric water and humid atmosphere in their immediate environment.

Optical microscopy reveals similar surface features for all the samples regardless of age, suggesting that the same general reaction processes have occurred for these samples. These features include the formation of a brown palagonite layer on the glass (Fig. 37). Closer examination of surfaces using SEM indicates that the glass surface has a high density of etch pits (Fig. 38), indicating the dissolution of glass during the reaction with water. X-ray diffraction of the palagonite reveals it is an amorphous or poorly crystalline material as evidenced by the presence of broad peaks (Fig. 39). It has been noted that palagonite layers are often not continuous on surfaces (thus etching pits can be seen underneath), and its coverage of the glass surface differs substantially from sample to sample (Table 18). It is possible that the palagonite layer may have spalled off during cycles of rainfall and drying. This variation in coverage has serious implications in determining the reaction kinetics, because the reaction rates are calculated based on the measurement of the thickness of palagonite layers formed on the glass surface.

Table 20. Chemical Compositions of Major Elements Determined by SEM/EDS for NBG-9 Natural Glass and Its Hydrated Layer

Oxide	Glass (wt %)	Hydrated Layer (wt %)
Al_2O_3	14.2	19.1
CaO	6.8	2.5
Fe_2O_3	17.7	24.5
K_2O	0.6	0.2
MgO	5.5	0.9
Na_2O	3.6	0.4
SiO_2	46.9	45.3
TiO_2	1.6	4.7

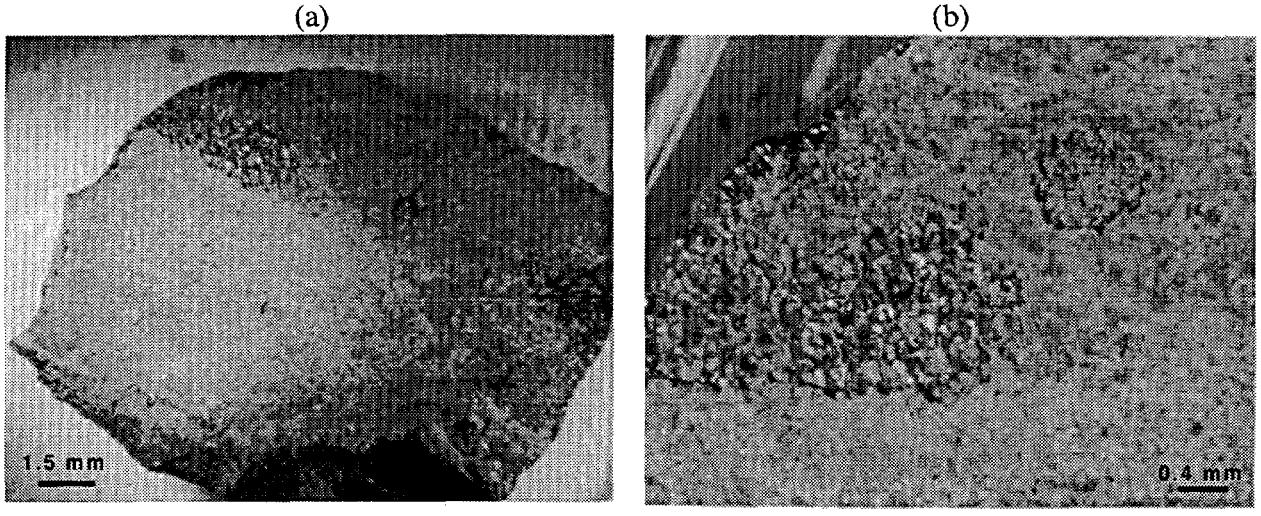

Fig. 37. (a) Hawaiian Basaltic Glass Enclosed by a Palagonite Shell and (b) Glass with Part of the Palagonite Layer Peeled Away, Revealing the Pitted Glass Surface

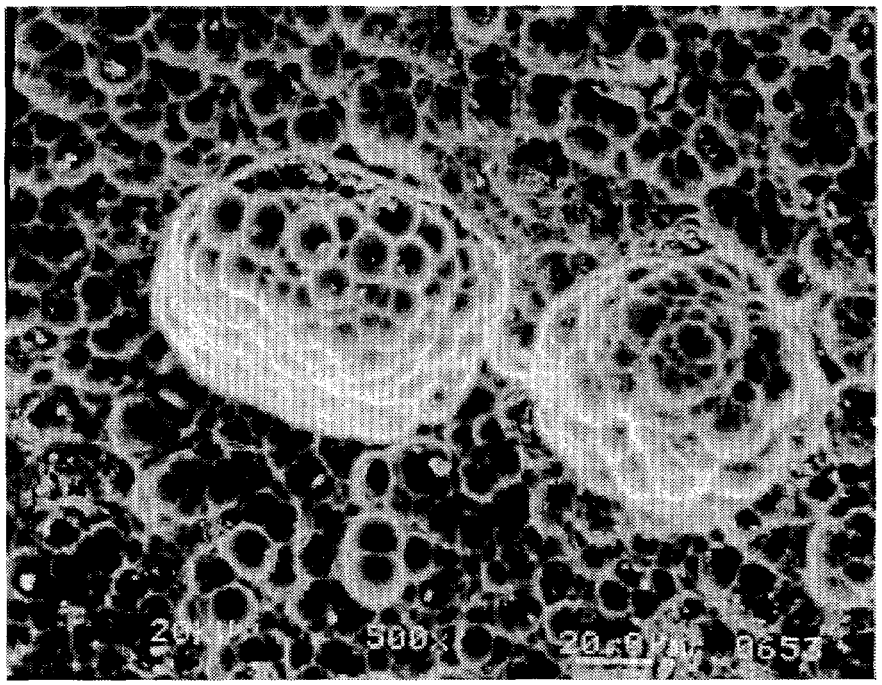

Fig. 38. Typical SEM Micrograph of Surface Pits Observed on the Naturally Altered Basaltic Glass NBG-6

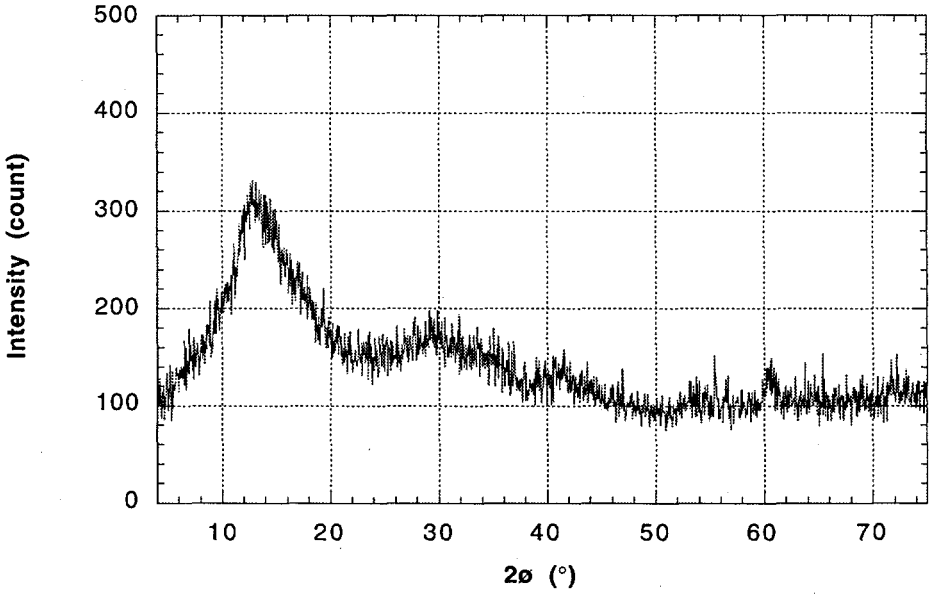

Fig. 39. Typical XRD Pattern for the Palagonite That Formed on the Surfaces of the Naturally Altered Basaltic Glass NBG-9

Cross sections perpendicular to surface have been examined using SEM on selected samples (NBG-2, NBG-6, and NBG-9) where an alteration layer had been at least partially preserved on the surface. On all the samples examined, the palagonite layers show a similar microstructure, which consists of primarily an amorphous matrix with various precipitates of (Fe,Ti)-oxides distributed inhomogeneously in the layer (Fig. 40). An EDS analysis of the palagonite layers showed depletion of Na, Mg, Ca and enrichment of Fe, Ti, compared to the unreacted glass core (Table 20).

Another interesting finding was that palagonite also forms along fractures in the glass. The palagonite formed at fractures shows microstructure features that are very different from those formed on the surface (Fig. 41). A typical altered zone formed along fractures shows a sandwich-like microstructure having two outer layers composed of an amorphous phase plus a central band with well-defined boundaries. The outer layers exhibiting a brighter contrast with backscattered electrons have a higher average atom number than the central band. Unlike in the alteration layers on the surface, no precipitation of (Ti,Fe)-oxides is observed in any of these zones, even though Fe and Ti are enriched in the layers adjacent to the unreacted glass. This can be clearly seen by X-ray mapping of the major elements in altered areas, as shown in Fig. 42: transition elements such as Fe are enriched (bright in contrast) in outer layers, whereas alkali metals are depleted (dark in contrast) in the entire altered area. The central band consists mainly of Al and Si, suggesting the formation of zeolites, which can be attributed to the particular environment setting along the fracture where the exchange rate is slow and the solution is rapidly saturated with dissolved species from the unaltered glass. The apparent reaction rate can be calculated by dividing the thickness of the altered layer by the glass age; for this sample the rate is ~12 μm/1000 yr at ambient temperature. This rate seems to be in good agreement with the rate that has been previously observed for subaerially altered basalt glasses [76] but higher than the rate for the basalt glasses altered under aqueous environments [77]. Unfortunately, the small number of samples in our study limit the number of fractures observed and, as a consequence, the statistics on the variation of the apparent reaction rate among samples are unknown.

An AEM examination of palagonite formed on the surface provides additional information at much finer scale (i.e., on the order of nanometers). At high magnification, it can be seen that palagonite is composed of aggregates of small, amorphous-like particles (~10 nm), together with some clay particles (Fig. 43). This microstructure seems to support a dissolution/ precipitation mechanism, in which glass is congruently dissolved into solution first, and then colloids (small amorphous particles) reprecipitate on the glass surface after their solubility in the solution is reached [78]. More samples are being examined by AEM to determine whether the palagonite formed along fractures has different microstructure features as that formed on the surface, since the two regions may have experienced very different conditions (e.g., different S/V).

2. Laboratory Vapor-Hydrated Glasses

Basaltic glass samples have been reacted previously in our laboratory under accelerating conditions to observe whether we can reproduce the natural alteration processes [62,79-85]. Most of experiments were short term (typically less than 1 year) and performed under both hydrothermal and vapor reaction conditions. Studies of naturally and experimentally altered basalt glasses seem to suggest that vapor hydration testing may be more appropriate than static leach testing as a means of accelerating glass reactions [80]. Additional experiments using natural and simulated waste glasses have been ongoing at ANL since 1986. In FY 1995, we terminated several long-term (7-9 years) laboratory tests (Table 19). These samples are being characterized using SEM/EDS and AEM/EDS.

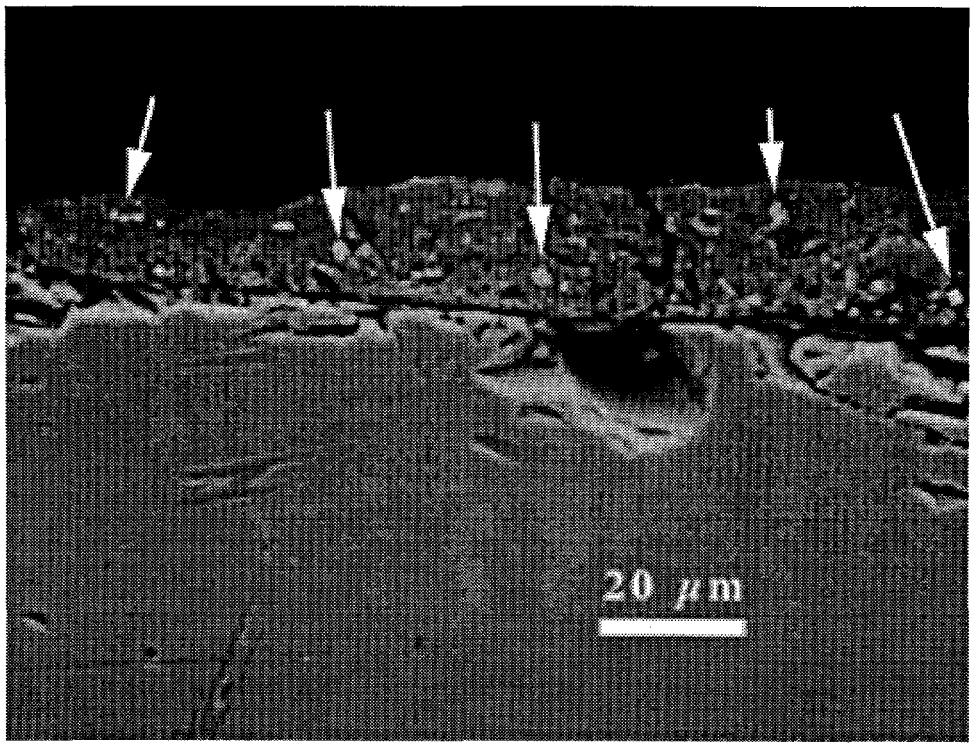

Fig. 40. SEM Cross-Sectional View of the Palagonite Layer Formed on NBG-9. Arrows indicate (Fe,Ti)-oxides.

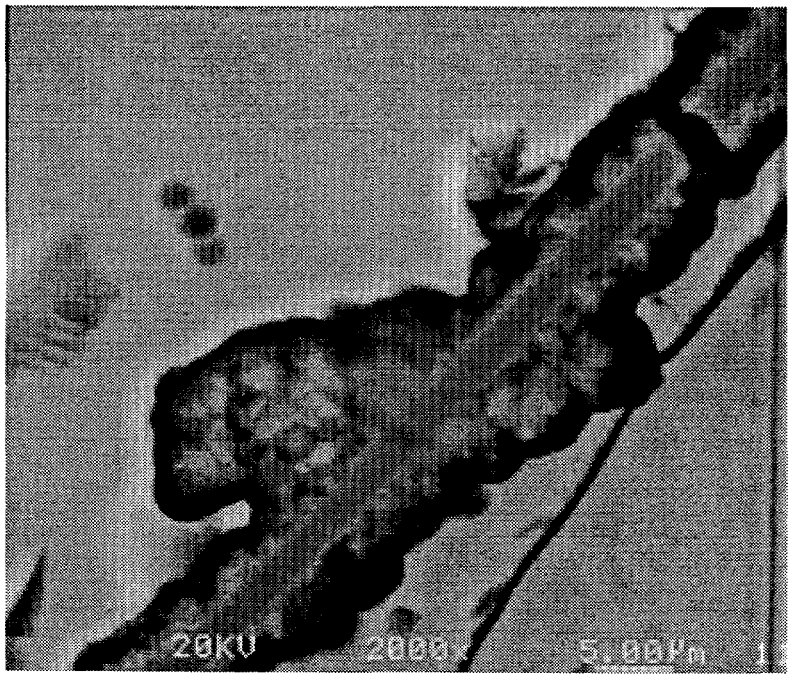

Fig. 41. Cross-Sectional Image of the Glass Altered along a Fracture Observed in Naturally Altered Basaltic Glass NBG-7

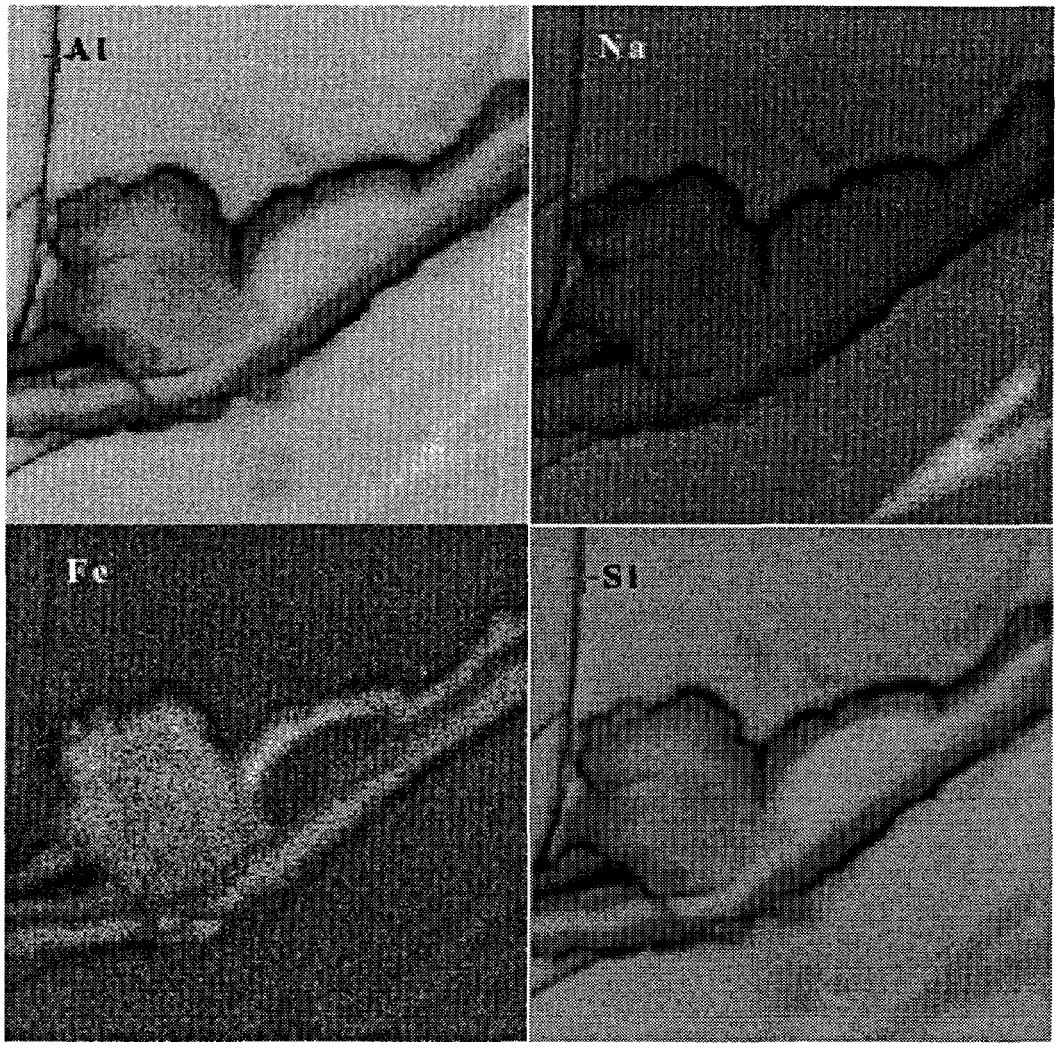

Fig. 42. X-Ray Mapping of the Major Elements (clockwise from top left: Al, Na, Fe, and Si) in the Area Shown in Fig. 41

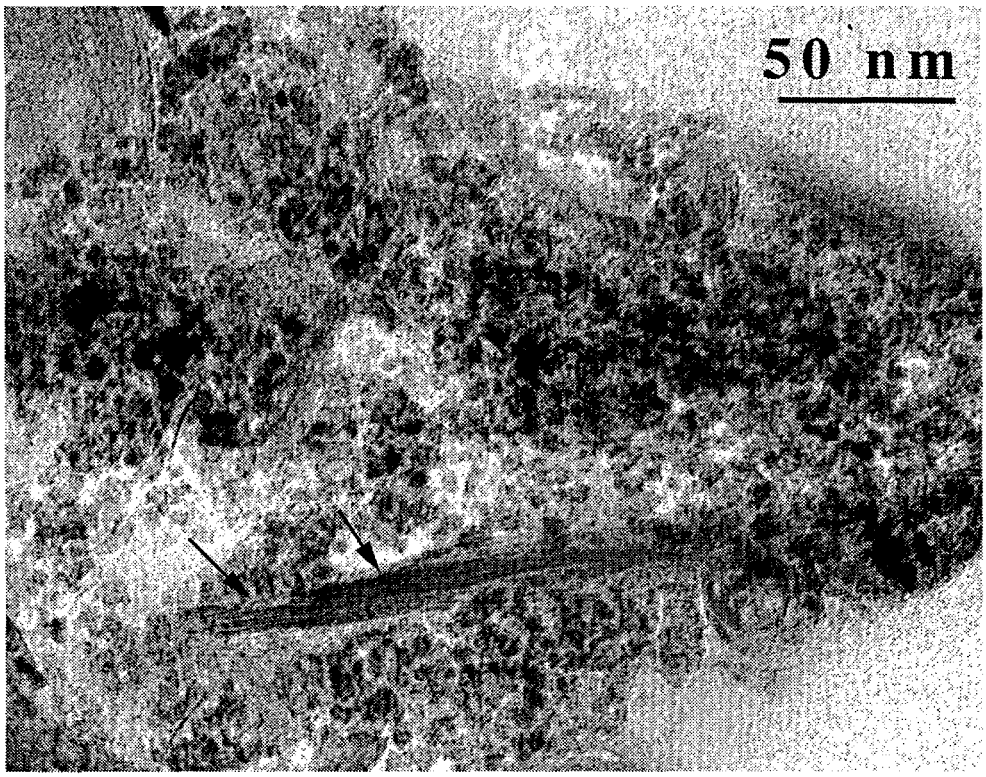

Fig. 43. An AEM Image of Palagonite Formed in Naturally Altered Basaltic Glass NBG-9 Showing Aggregates of Tiny Islands ~10 nm (Colloids) and Clay Particles (Arrows)

E. Future Studies

The long-term laboratory reacted samples (Table 19) will be fully characterized. Their microstructure will be compared to the naturally altered samples that have been studied during FY 1995. Similarly, the precipitated phases on surfaces will also be identified, analyzed, and compared to naturally reacted glasses. These studies will allow us to determine whether laboratory accelerating techniques alter the fundamental mechanisms of glass reaction and will provide insight into long-term corrosion processes of high-level nuclear waste glasses. Also, the Critical Review will be revised and published in FY 1996.

X. ANALYTICAL ELECTRON MICROSCOPY SUPPORT

A. Introduction and Background

Alteration phases, formed during the corrosion of waste glasses, are being examined with analytical transmission electron microscopy (AEM). This technique provides information regarding the composition and structure of the reacted layer in glasses. The nature of colloidal phases and the identity of crystalline and cryptocrystalline phases can be determined by using a combination of compositional and structural information. The AEM is used to probe the glass reaction process at a level that cannot be achieved by any other technique, providing unique insight about how glasses react. In AEM, compositions are determined by using transmission electron microscopy combined with the analytical capabilities of X-ray energy dispersive spectroscopy (EDS) and electron energy loss spectroscopy (EELS). The latter can also be used to obtain information about the oxidation state of metals in glasses. Structural information is obtained with electron diffraction.

B. Objectives

The objective of detailed electron microscope studies is to identify and characterize the submicrometer-sized alteration phases that form during glass reaction and to examine the nature of the corrosion process by examining transverse cross sections through the reacted layer [83]. These examinations are done in support of other Tasks.

C. Technical Approach

To study glass alteration phases by using AEM, it is necessary to produce transverse cross sections of the reacted glass layer. Electron-transparent thin sections are prepared by microtoming reacted particles of glass embedded in an epoxy resin [83]. In addition to analyzing reaction layers, we continue to examine colloidal particles present in the leachate, some of which may contain radionuclides. Colloidal and suspended particle samples have been collected by wicking the leachate through a "holey" carbon grid [86].

D. Results and Discussion

This section presents the results from both the solid, layered samples and the colloidal particles.

1. Analysis of Samples from the Long-Term Testing of Fully Radioactive Glass Task

The Long-Term Testing of Fully Radioactive Glass Task is being conducted to determine the long-term corrosion behavior of fully radioactive glass and compare it to the behavior of nonradioactive glasses. Samples of SRL 200S glass were examined with AEM. The results of sample analyses are described in Table 21. The reacted layer formed on SRL 200S glass in tests at 340 m^{-1} for 1456 days is shown in Fig. 44. The sample exhibited a well-ordered clay layer which was separated from the glass.

Uranium silicates phases formed as colloids during glass reaction at 340 m^{-1}, and there was a notable difference in the morphology, composition, and crystallinity of the phases for the nonradioactive and radioactive SRL 200 glasses (see Fig. 45). The uranium silicates that formed from the fully radioactive glass were better crystallized, whereas in the simulated glass

Table 21. Results of Sample Surfaces for Task "Long-Term Testing of Radioactive Glass"

Test Identification	Comments	Blocks Prepared
DP114/DP115 SRL 200S glass 340 m^{-1} 1456 days in EJ-13	Section was elongated. Sample had a clay layer ~1 μm thick that was separated from the glass in most regions (Fig. 44).	1414, 1415, 1416, 1417, 1418, 1419, 1420, 1421, 1422
DP98 SRL 200R glass 340 m^{-1} 1456 days in EJ-13	Three types of phases were observed on the grids: uranyl silicate, smectite clay, and a rare earth phase.	NA[a]
DP99 SRL 200R glass 340 m^{-1} 1456 days in EJ-13	Uranyl silicate particles and smectite clay were observed on the grids (Fig. 45). Because the same amounts of phases were found in both samples, the sample preparation methods were consistent.	NA
DP114 SRL 200S glass 340 m^{-1} 1456 days in EJ-13	Kaolinite-type particles. Very little on grid.	NA
DP115 SRL 200S glass 340 m^{-1} 1456 days in EJ-13	Uranium silicate particles observed; less crystalline than those uranium phases found in DP98/99. There were also higher levels of aluminum in the particle (Fig. 45).	NA

[a]NA = not applicable—colloidal samples.

(a) (b)

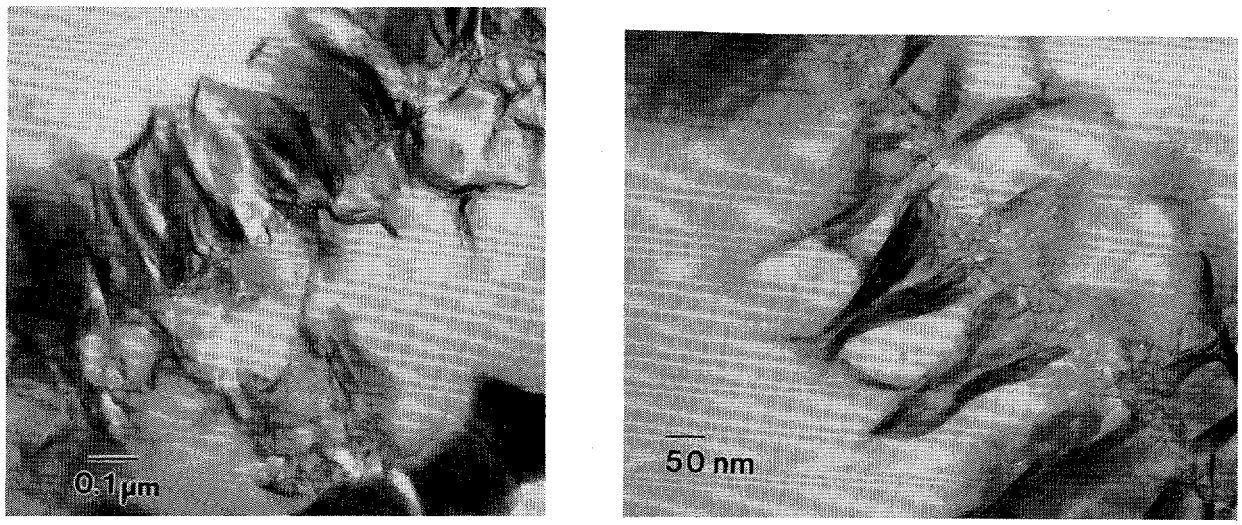

Fig. 44. TEM Image of Reacted Layer from an SRL 200S Glass Reacted at 340 m^{-1} in EJ-13 Water for 1456 Days (a) Showing Glass and Clay and (b) under Magnification of Clay Backbone Structure

(a) (b)

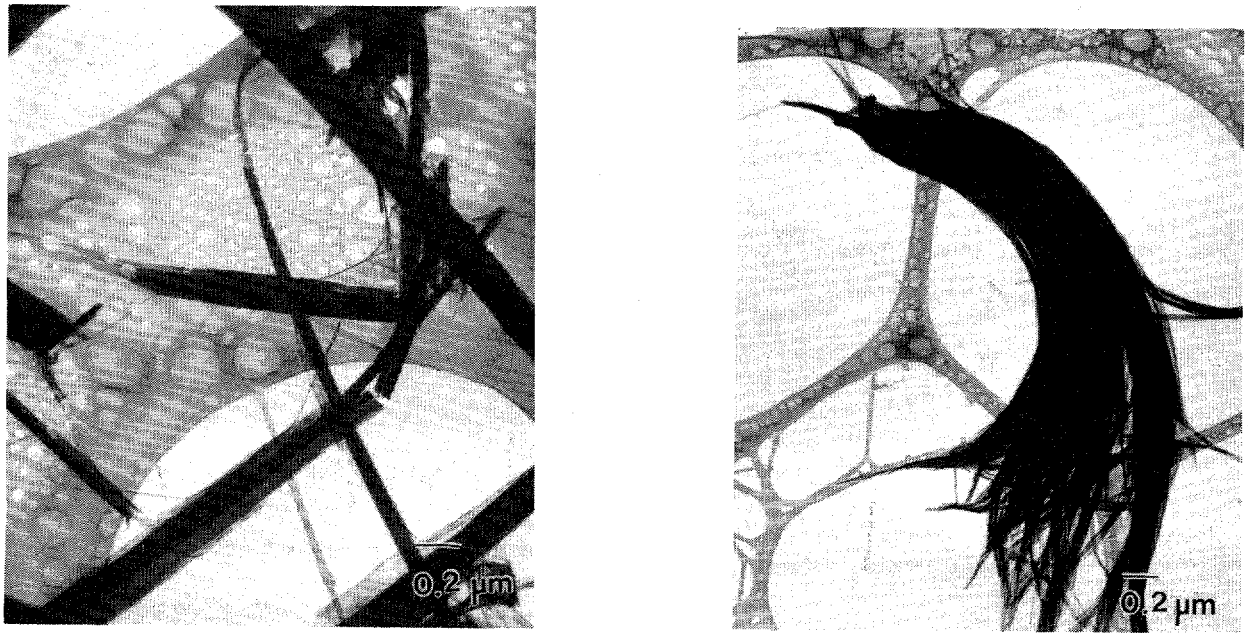

Fig. 45. TEM Images of Uranium Silicate Suspended Particles Found in (a) SRL 200R Test and (b) SRL 200S Test Reacted at 340 m^{-1} for 1456 Days

tests, the uranium silicate was curly and only two weak diffraction spots were obtained from the phase. The electron diffraction data from the uranium silicate from the SRL 200R glass are given in Table 22. The d-spacings of this phase matched closely with those of sodium boltwoodite. Data from other tests that will be discussed later are also shown.

A cryptocrystalline rare earth-bearing calcium phosphate phase also containing small amounts of Th and U was found in the leachate of a SRL 200R glass test reacted at 340 m^{-1} for 1456 days under static conditions. The same phase also was found in the leachate of the N4 drip test with the same type of glass (discussed below). Table 23 displays the electron diffraction data from this phase, which suggested that it was closely related to the apatite group. A large number of rare earth elements were detected in the phase with EELS. Figure 46 shows the spectrum of the rare earths in the phase; the M-edge intensities can be used to estimate the relative proportions of each element, as the intensities decrease only slightly across the series. In addition, the M_4:M_5 intensity ratios can be used to estimate the oxidation state of the individual rare earth elements [87,88]. Based on values obtained by Fortner et al. [88], the rare earths in the apatite-related phase were determined to be in the trivalent state. Although transuranic elements in these types of phases have been determined indirectly by using autoradiography [72], these elements have never been detected directly, as these concentrations are too low for detection by EDS. By using the high-energy M-absorption edges of the transuranics (>3500 eV), Pu and possibly Am were detected at around 50-100 ppm in this phase (see Fig. 47). This is the first direct evidence for these elements in a particular alteration phase. The Ca K-edge and the Th and U M-edges can also be seen. These high-energy M-edges were used for element identification because there was too much overlap with the M-edges of the rare earths and other elements at lower energy ranges. These rare earth-rich phosphate phases are most likely spalled phases, which initially formed within the reacted glass layer. The elements Pu and Am are known to be relatively insoluble compared to Np or U. Hence, spallation of such particles is a means by which the amount of Pu and Am in solution can be increased over the solubility limit.

2. Analysis of Samples from the Relationship between High S/V Experiments and MCC-1 Task

Glass samples of SRL 202U from the Relationship between High S/V Experiments and MCC-1 Task that had reacted for more than 1300 days have been examined with AEM (Table 24). The reacted clay layers formed on samples reacted at 2,000 m^{-1} and 340 m^{-1} have become more crystalline with time, but there has been little change in the thickness of the layer after 100 days. In Fig. 48, a SRL 202U glass reacted for 967 days at 2,000 m^{-1} shows etch pits, the formation of a clay layer separated from the glass, and uranium titanium precipitates trapped between the clay layer and the reacted glass, whereas at 340 m^{-1} the glass shows only a single layer.

Some uranium silicate particles found in the leachates from the high S/V experiments consisted of large (2-10 μm) bundles of elongated crystallites with particles of clay attached to them, suggesting that they had spalled from the reacted layer. In contrast, the uranium silicates in tests run at low S/V were much thinner, although they were still several micrometers in length.

The use of listings of electron diffraction d-spacings can yield results that are difficult to interpret in identifying a particular phase; however, in many instances, this is the only method available because of the cryptocrystalline nature and electron instability of many of the glass waste form alteration phases. In Fig. 49, a zone axis pattern and EDS spectrum of an uranyl silicate are shown. These patterns, when they are obtained, provide a less ambiguous method for identifying a crystal structure.

Table 22. Electron Diffraction Data from Uranium Silicate Phases in Selected Tests (d-spacing values in nanometers)

Colloids from Test DP98/99 (SRL 200R Glass Reacted at 340 m^{-1})	PZ20D (SRL 131A Glass Reacted at 20,000 m^{-1})	Weeksite[a] (JCPDS 12-462)	Uranophane Sodium Boltwoodite[b] (JCPDS 29-1044)
	0.931	0.898	
0.702	0.730	0.711	
0.689			0.692
0.683			
0.653	0.665		0.671
0.631			
0.610			
0.564	0.556, 0.554	0.577	
0.539			0.539
0.477, 0.465	0.457	0.458	0.470
0.438			
0.372			
0.358, 0.354, 0.346	0.363, 0.358	0.355	0.356
0.338, 0.326	0.335, 0.325		
0.313	0.315	0.315	
0.310, 0.308			0.310
0.295	0.295	0.91	
0.266			
0.258	0.242	0.241	0.243
0.230	0.234	0.237	
0.221	0.219	0.217	0.220
0.214	0.202	0.199	0.201
0.198	0.191	0.195	0.192
0.184	0.180		0.183
0.174	0.179	0.178	0.175
0.168	0.177		
0.166			
0.155			

[a]Weeksite, ideally $[K_2(UO_2)_2(Si_2O_5)_3 \cdot 4H_2O]$, orthorhombic phase.

[b]Boltwoodite, ideally $[K_2(H_3O)UO_2SiO_4 \cdot 0\text{-}1(H_2O)]$, monoclinic phase.

Table 23. Electron Diffraction from a Rare Earth-Bearing Phase Found in the Leachate from 200R Glass Static Immersion Test and Drip Test

Rare Earth-Bearing Phase in 200R Static Test	Rare Earth Bearing Phase in 200R Drip Test	Davidite[a]	Apatite[b]	Rhabdophane[c]
0.459	0.465 0.423	0.412	0.412	0.607 0.440
0.324	0.338	0.338	0.321	0.349, 0.302
0.266	0.298	0.298	0.266	0.283, 0.273, 0.236
0.248	0.257	0.259	0.227	0.228, 0.215
0.153			0.154	0.174

[a]From Pabst [89].

[b]From Liu and Comodi [90].

[c]From Fisher and Meyrowitz [91].

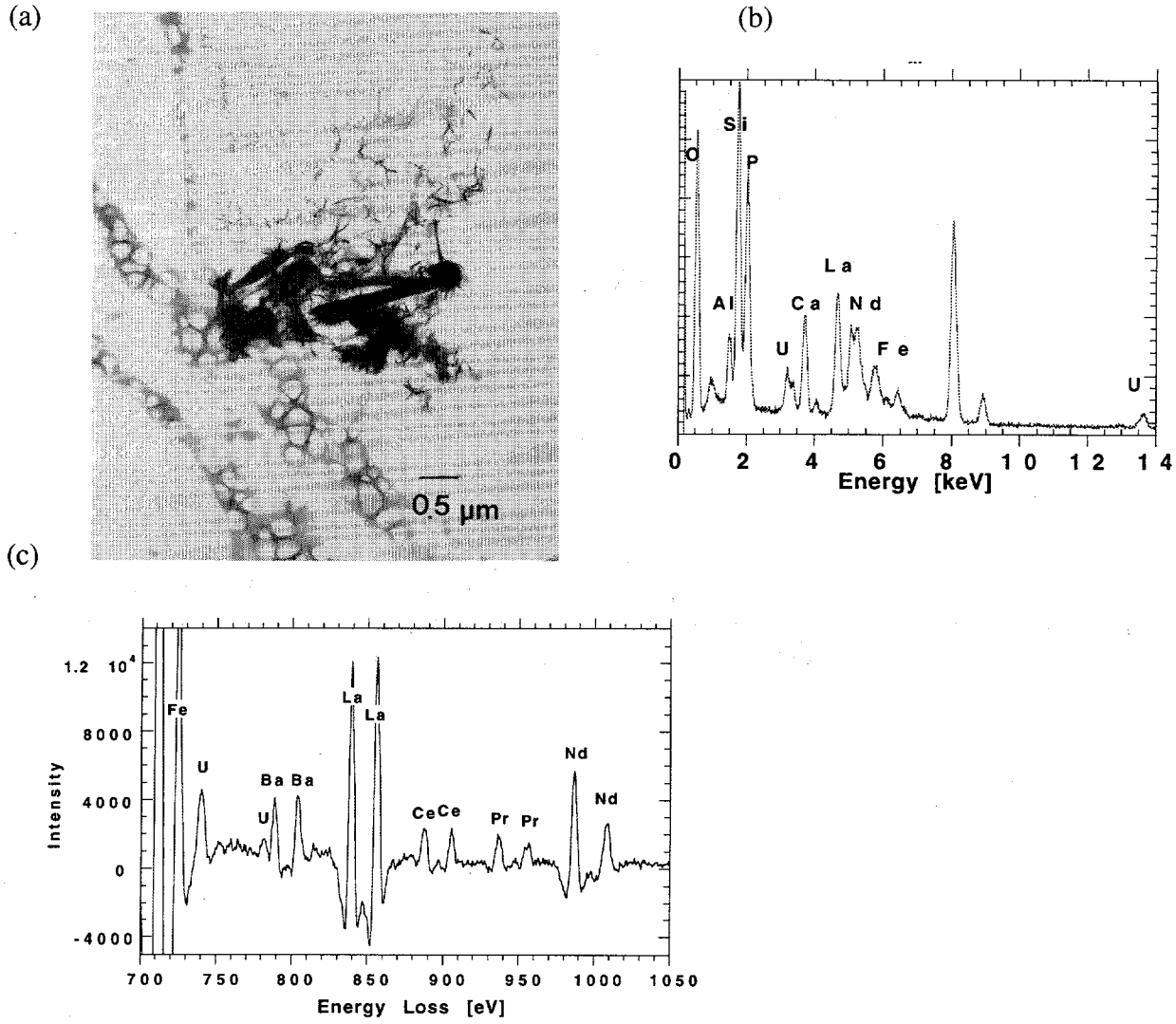

Fig. 46. (a) TEM Image of Rare Earth-Bearing Calcium Phosphate Colloidal Phase from a SRL 200R Glass Reacted at 340 m^{-1} for 1460 Days (Test DP99). (b) EDS analysis of phase. The phase contained the heavy elements La, Nd, Zr, Y, Th , and U. (c) EELS shows the distribution of rare earths in the phase.

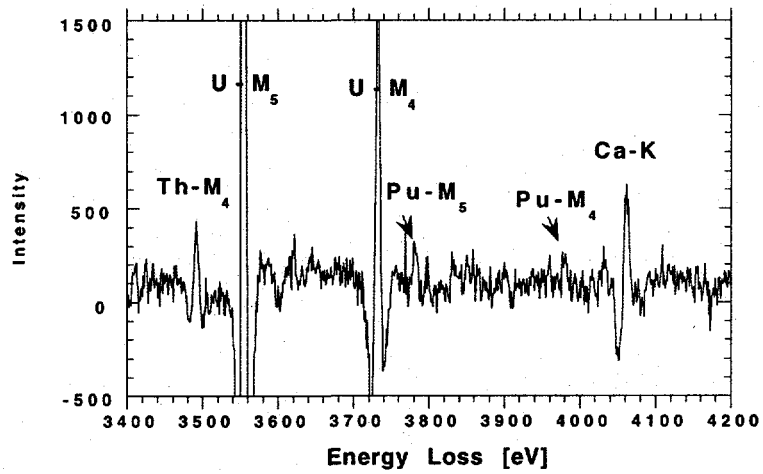

Fig. 47. EELS Data in the High Energy Range, Covering the Uranium M "White Lines," Indicating the Presence of Plutonium (M_5 = 3778 eV and M_4 = 3973 eV) in the Rare Earth-Rich Particle. The thorium M_4 and calcium K absorption edges can also be seen. This is the first time plutonium has been detected directly in alteration phases.

Table 24. Results of Sample Surveys for the Task "Relationship between High S/V Experiments and MCC-1"

Test Identification	Comments	Blocks Prepared
BX8 SRL 202A glass 10 m^{-1} 600 days in EJ-13	The section consisted of only one layer, although there was some evidence of altered glass/gel layer. Small uranium-titanium precipitates were visible in the alteration layer. These have been found in at all tested S/Vs except 20,000 m^{-1}.	1320, 1321, 1322, 1323
BY18 SRL 202A glass 2,000 m^{-1} 960 days in EJ-13	Thin clay layer ~100-200 nm thick.	1039
PZ20D SRL 131A glass 20,000 m^{-1} 980 days in EJ-13	One sample contained an extremely well crystallized uranium silicate phase (see Table 22 for electron diffraction data).	1325, 1326
TY19 SRL 202U glass 2,000 m^{-1} 967 days in DIW	Clay layer ~150 nm thick. Uranium titanium precipitates were visible underneath the backbone structure.	1410, 1411, 1412, 1413
TY21 SRL 202U glass 2,000 m^{-1} 967 days in DIW	A thin clay layer ~150-200 nm thick. Uranium titanium precipitates were observed in the voids with the altered zone of the glass (Fig. 48).	1380, 1381, 1382
TW47D SRL 202U glass 340 m^{-1} 967 days in EJ-13	A small region of clay material. A calcium titanium silicate phase—possibly pyroxene (a devitrification phase)—was observed in one sample (Fig. 48).	1376, 1377, 1378, 1379

(a)

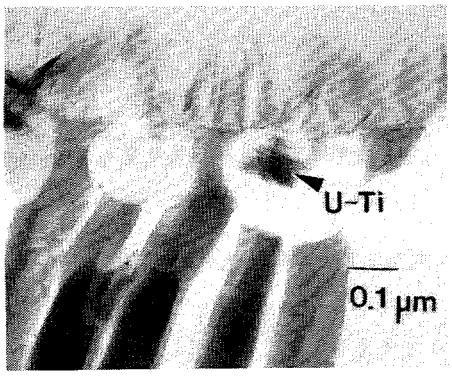

(b)

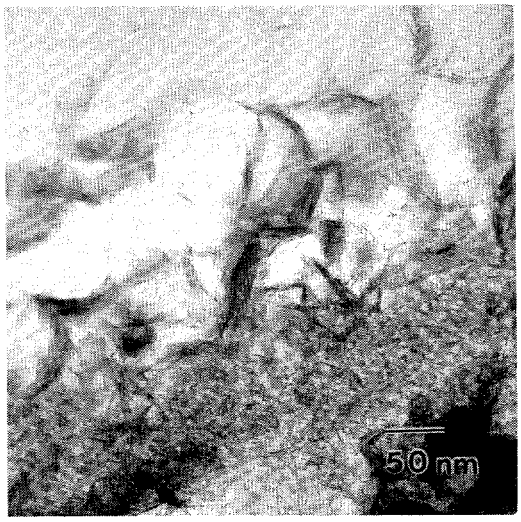

(c)

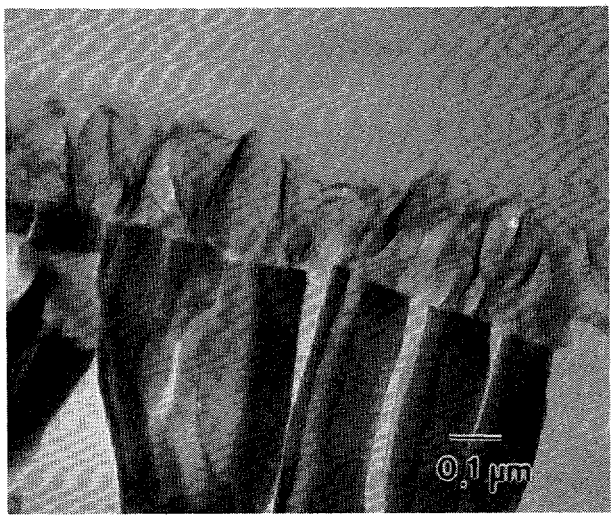

Fig. 48. TEM Images of Layers in SRL 202U Glass. (a) Glass reacted at 2000 m^{-1} for 967 days (Test TY21), with uranium titanium precipitates present in voids under the layer. The uranium titanium phases are cryptocrystalline and consist of extremely fine, elongated crystals. (b) A higher magnification image of the glass in (a) shows a clay layer. (c) Reacted layer of a SRL 202U glass reacted for 967 days at 340 m^{-1} (test TW47D).

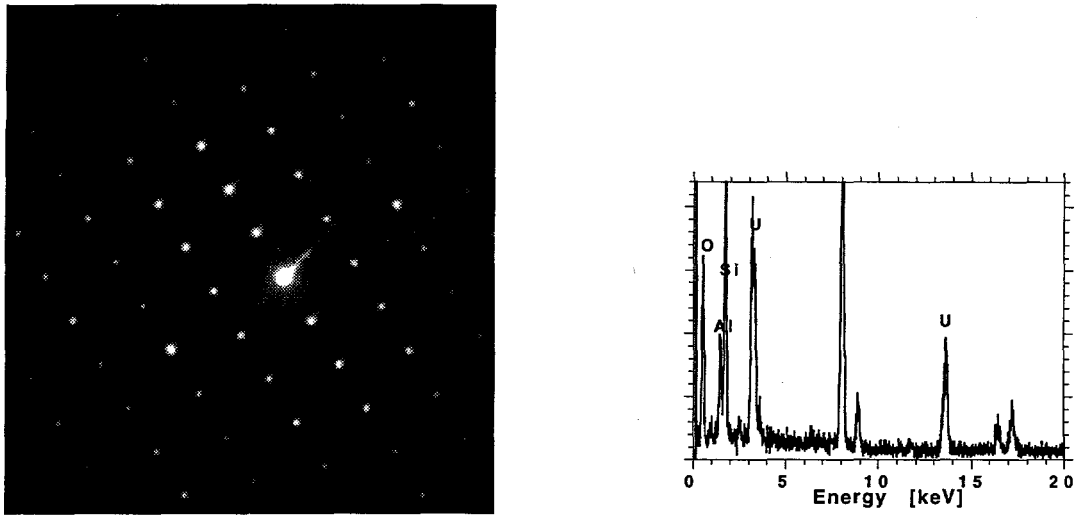

Fig. 49. (a) Electron Diffraction Pattern from Weeksite Found in SRL 131A Glass Reacted at 20,000 m^{-1} for 980 Days (Test PZ20D) and (b) EDS Analysis of Phase

Two types of uranyl silicates were observed; weeksite, ideally $[K_2(UO_2)_2(Si_2O_5)_3 \cdot 4H_2O]$ and uranophane group (sodium boltwoodite), ideally $[(Na,K)(H_3O)(UO_2)(SiO_4) \cdot H_2O]$. Both phases are composed of $[(UO_2)(SiO_4)]_n^{2n-}$ chains cross-linked by bridging oxygen atoms to form a uranyl silicate sheet. The sheets are cross-bonded by charge balancing cations [92]. Table 22 shows the electron diffraction from these phases.

The disposition of transuranics in the S/V tests with 202A glass has been determined by Ebert et al. using ultrafiltration and wet chemical analysis. Results indicate that neptunium was retained in the reacted glass layer in some tests [39]. Using AEM, we located an alteration phase containing neptunium. The difficulty in detecting this element is that many of its lines overlap with other elements, such as rare earths, which are often present at trace levels in the uranium-bearing phases. By using EELS, trace levels of neptunium were detected in the uranyl silicate alteration phases (see Fig. 50a). On the basis of the levels of neptunium in the glass samples, we estimated that around 70-100 ppm of neptunium was in the alteration phase. The neptunyl ion $[Np(V)O_2^+]$ may behave similarly to the uranyl ion $[U(VI)O_2^{2+}]$ and become incorporated into the sheet structure of the uranyl silicate phase. We have found that use of the high-energy M-edges to detect neptunium is the only method available to positively identify this element; the lower energy N-edges overlap with the M-edges of trace levels of lanthanum in the phase. X-ray fluorescence methods are unable to detect such low levels of a transuranic element because of high background from the many other X-ray lines in any waste glass sample. The presence of neptunium in the uranyl silicate phase suggests that this element may follow uranium under certain solution conditions. In a test of SRL 200R glass, we were also able to detect neptunium within an uranyl silicate alteration phase (see Fig. 50b).

Uranium is known to sorb onto smectite clays [93]. The large amounts of clay observed in the waste glass test leachates suggests that there will be many sites available for sorption of both uranium and transuranics. Although traces of uranium were detected in the clay colloids during waste glass corrosion, uranium is more often associated with discrete phases, e.g., weeksite and uranophane.

(a)

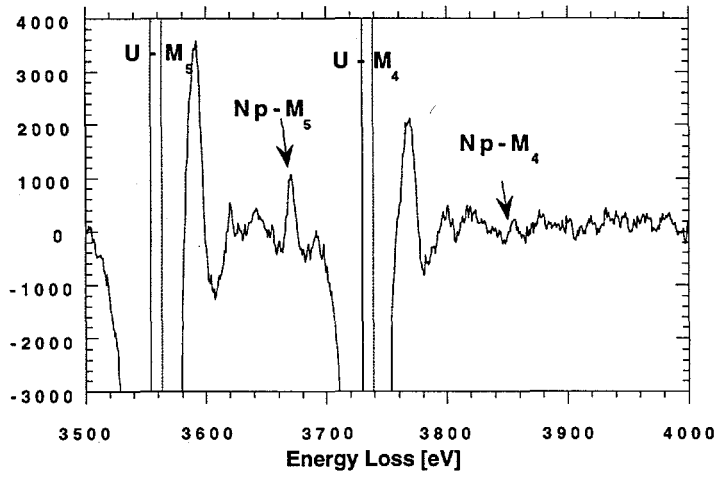

(b)

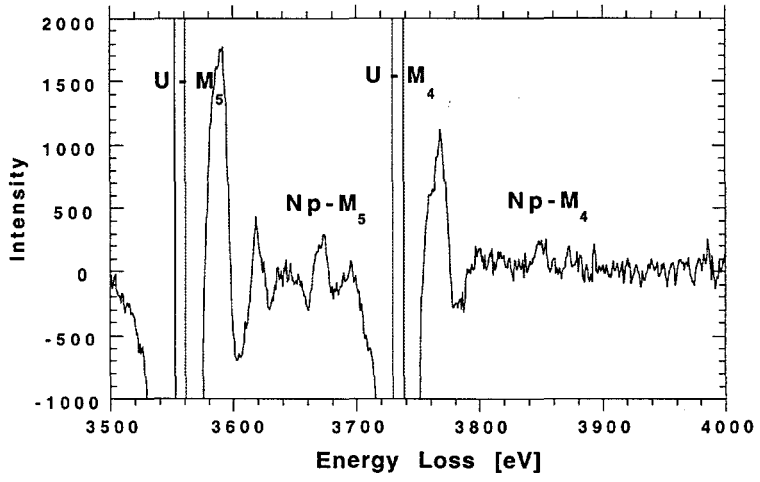

Fig. 50. EELS Data for Uranium Silicate Colloid Showing Trace Levels of Neptunium from Tests with (a) SRL 131A Glass and (b) 200R Glass (for Comparison)

In addition, in tests conducted at 340 m^{-1} and 2000 m^{-1}, small uranium-titanium particles, typically 50-150 nm in diameter, have been found in the reacted layer, usually underneath the backbone structure. A TEM image of such a particle, from a SRL 202A glass test, is shown in Fig. 51. These particles are cryptocrystalline, but we have yet to determine the structure of this phase.

3. Analysis of Samples from SRL EA and WV6 Glass Testing

The West Valley 6 reference glass and the SRL EA glass are being tested to determine the glass corrosion rate, assess the long-term stability of the glass, and identify the alteration phases that form when the glass corrodes (see Tables 25 and 26). The WV6 glass forms only a thin clay layer about 50-150 nm thick under high S/V conditions (see Fig. 52). Several alteration phases have been found during testing of SRL EA glass. These include a thick clay layer, zeolites, and calcium silicates (see Sec. VI).

The identification of calcium silicate phases with AEM or any other diffraction technique is difficult, because there is very little difference in the d-spacings of the various calcium silicate hydroxide hydrates. The large spacing at around 1.11 nm is common to several of these phases. Therefore, simply using a list of electron diffraction d-spacings is insufficient to identify these phases. We also use the Ca/Si ratio measured with EDS to assist in the identification of the silicate phase. For example, the high Ca/Si ratio of the phase formed in test EA-77 (Table 27) suggests that phase may be gyrolite.

4. N4 Series Colloids

Particles having dimensions within the range 1 nm to 1 μm are considered to be colloidal [94]. The potential role of colloids in the transport of radionuclides from a permanent nuclear waste geological repository is significant [95,96]. Colloids have the potential to increase the transport of the less soluble radionuclides, such as Am and Pu, if these radionuclides are associated with the colloids. Under dynamic test conditions [23], alteration phases that have formed on the surface of the glass (as a result of glass-water reaction) may spall off into the leachate, resulting in the formation of radionuclide-bearing colloids, termed "primary colloids" [72,97]. The presence of colloids formed during waste glass corrosion has been demonstrated in static immersion waste glass tests by electrophoretic light scattering [86].

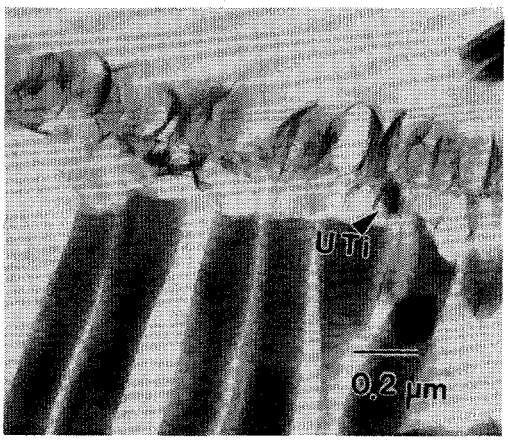

Fig. 51. TEM Image of an SRL 202A Glass Reacted at 2000 m^{-1} for 960 Days (Test BY18), Showing the Presence of a Uranium-Titanium Precipitate

Table 25. Results of Sample Surveys for Task "WV6 Glass Testing"

Tests Identification	Comments	Blocks Prepared
WV6-8 10 m^{-1} 182 days in DIW	Evidence of reaction observed along fractures in the glass. There was a thin, 20-nm gel-like layer.	1268, 1269
WV6-27 2,000 m^{-1} 30 days in EJ-13	Slight degree of reaction. Iron-rich oxides observed, which were identified as a maghemite (γ-Fe_2O_3) with some Cr in solid solution with Fe. A few samples exhibited a thin clay layer ~50 nm thick.	1088, 1089, 1090, 1118, 1119, 1120, 1121
WV6-41 20,000 m^{-1} (-100 +200 mesh), 98 days in EJ-13	A 100-nm-thick clay layer observed on the glass surface. The reacted region was lower in Na and K than the glass.	1244, 1245, 1246
WV6-43 20,000 m^{-1} (-100 +200 mesh), 98 days in EJ-13	Devitrification crystals visible in the samples. Less than 10 nm of alteration was visible in samples.	1247, 1248, 1249, 1250
WV6-45 20,000 m^{-1} (-100 +200 mesh), 182 days in EJ-13	A thin clay layer ~50-100 nm thick observed in the samples.	1229, 1230, 1231, 1232, 1233, 1234
WV6-47 20,000 m^{-1} (-100 +200 mesh), 364 days in EJ-13	A smectite clay layer ~100-150 nm thick. There was an indication of increased levels of Th in the gel region of the glass (Fig. 52) and higher levels of K in the clay layer.	1372, 1373, 1374, 1375
WV6-71 20,000 m^{-1} (-200 +325 mesh) 56 days in EJ-13	Clay layer was ~20 nm thick; bunches of clays visible. The altered zone appeared to be enriched in Th. Mg and Mn were enriched in the clay layer.	1251, 1252, 1253
WV6-73 20,000 m^{-1} (-200 +325 mesh) 98 days in EJ-13	Some evidence of etching underneath the clay layer.	1254, 1255, 1256
WV6-76 20,000 m^{-1} 182 days in EJ-13	An outer reaction zone consisting of orientated crystallites ~100-150 nm thick. EDS analysis of the reacted zone indicated higher Mn but lower Na and Ca contents.	1257, 1258, 1259

Table 26. Results of Sample Surveys for Task "EA Glass Dissolution Testing"

Test Identification	Comments	Blocks Prepared
EA-27 2000 m^{-1} 70 days in EJ-13	Formation of an outer structured layer 50-100 nm thick and an alteration layer 200-500 nm thick. A crystalline (Fe, Cr)-oxide was found in the alteration layer.	1083, 1084, 1085, 1086, 1087, 1106, 1107, 1108
EA-73 20,000 m^{-1} 98 days in EJ-13	Two well-defined reacted smectite clay zones: an outer clay zone (0.2-0.5 μm thick) consisting of textured crystallites and an altered zone consisting of randomly ordered nanocrystalline particles. In some blocks, analcime was identified using electron diffraction.	1136, 1137, 1138, 1139, 1140, 1141
EA-77 20,000 m^{-1} (-200 +325 mesh) 367 days in EJ-13	Large amount of an iron silicate clay. Calcium silicate alteration phase observed.	1435, 1436, 1437, 1438, 1439

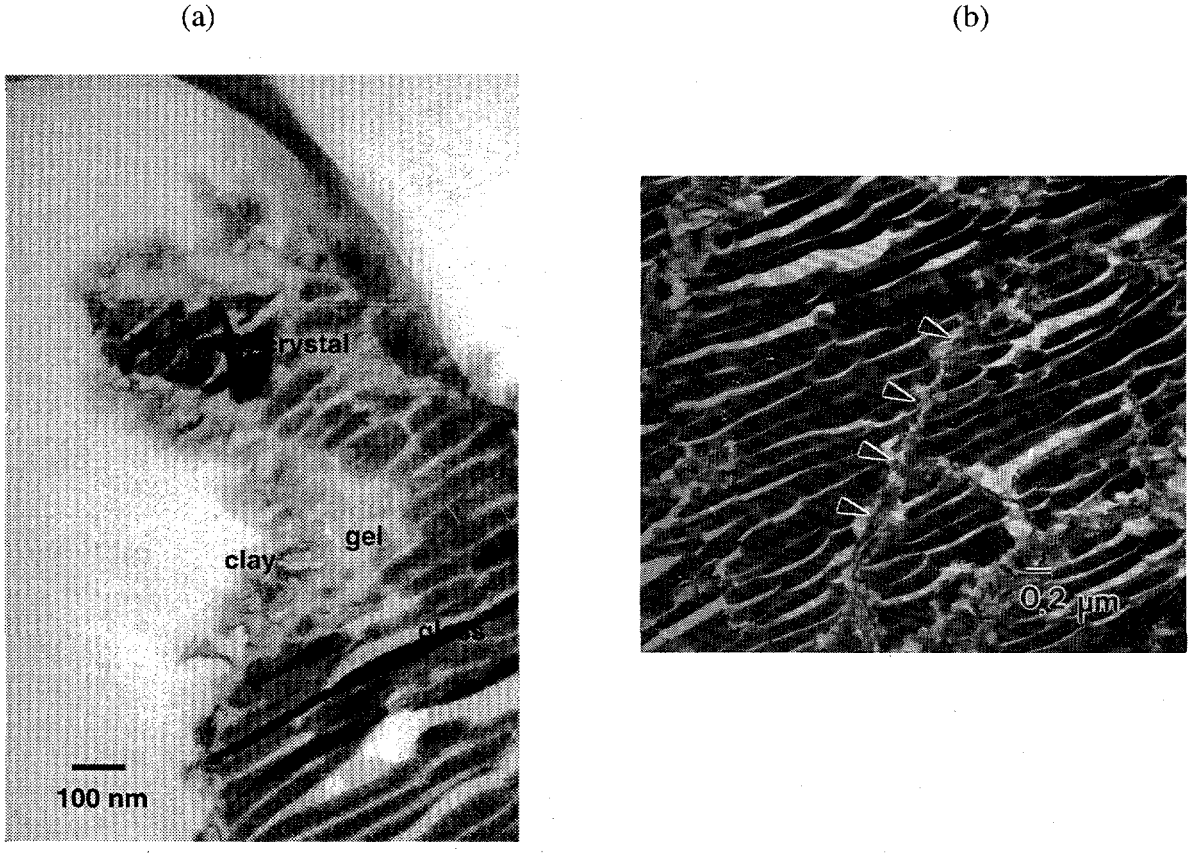

Fig. 52 (a) An Iron Chromium Oxide Crystalline Particle in the Reacted Glass, Now Surrounded by a Gel Layer and Clay, and (b) Reacted Cracked Glass

Table 27. Measured Electron Diffraction Parameters from a Calcium Silicate Alteration Phase in a Reacted SRL EA Glass (values in nanometers)

Experimental d-spacings	Literature Values	
SRL EA Glass Phase	Tobermorite JCPDS 19-1364	Gyrolite JCPDS 12-217
1.12	1.13	1.11
0.530	0.548	0.549
0.349	0.353	0.355, 0.347
0.324	0.331	0.316
	0.308	0.310
0.302	0.298	0.300
0.293	0.282	0.283
0.264	0.274	0.264
0.258	0.253, 0.215	0.256
0.194	0.200	0.213, 0.201
	0.184	0.192
		0.183
	0.154	0.157
	0.144	0.134

Colloidal samples from sampled dynamic drip tests of 200R glass (see Sec. III.4) were examined in the AEM. In some samples, large pieces of the reacted clay layer had spalled off into the leachate. As well as clay, AEM showed calcium phosphate phases, a rare earth-bearing phase, and iron oxide particles. The rare earth phase was compositionally very similar to the one found in static tests with the same 200R glass. In Figs. 53 and 54, TEM images and EDS analyses of the clay and rare earth-bearing phase are shown. The TEM image shows the small size of the rare earth phase, around 75 nm in diameter. This type of phase may be actinide-bearing, although this was not established during AEM examination. The nature of reaction under dynamic conditions results appears to result in clay particles and other phases being released into the leachate. The AEM provides some characterization information for these colloids, but other techniques, such as autoradiography and measurement of electric potential and size distribution, are required to fully understand the role of colloids in radionuclide transport.

E. Future Studies

We will continue to examine the alteration phases and reacted layers from the WV6 and SRL EA vapor and static tests and the drip tests of SRL 200 glasses. As these tasks near completion, new tests of fully radioactive SRL Tank 51 sludge and West Valley sludge glasses will be started, and the corroded glasses from these tests will be studied using AEM. Efforts to obtain chemical state information using EELS will continue. A number of journal publications are currently under review concerning the TEM and EELS analysis of glass dissolution and colloid formation. These papers will be submitted to the appropriate journals in the near future.

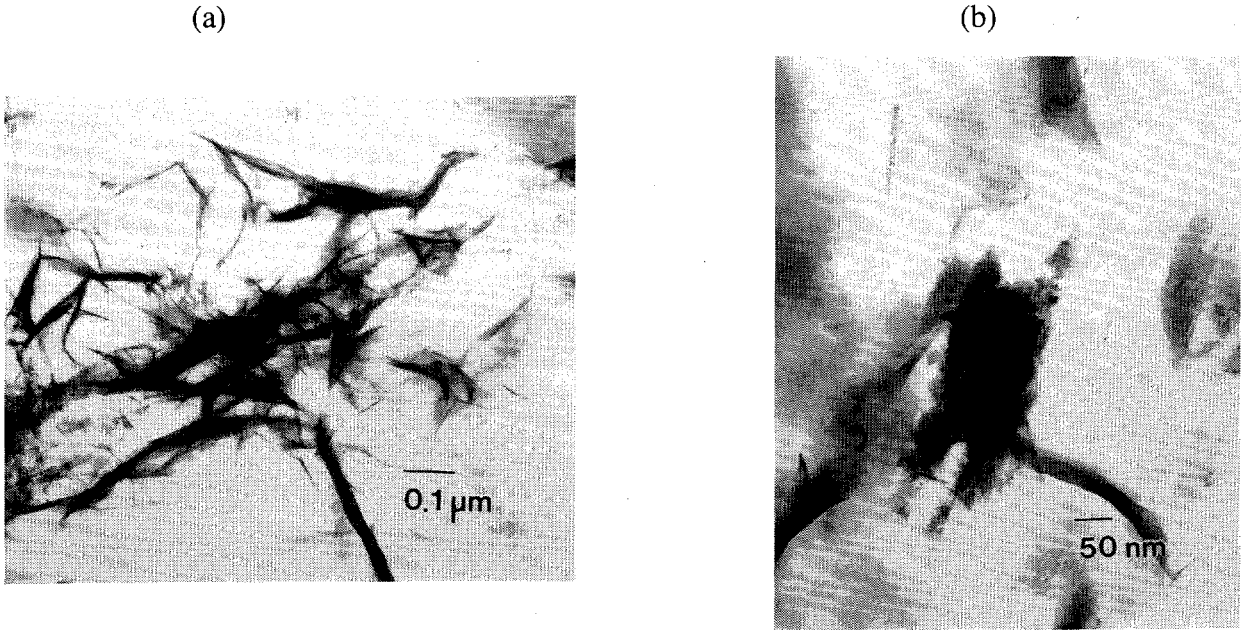

Fig. 53. (a) Clay Colloids Found in 200R Glass Drip Test and (b) Rare Earth-Bearing Phase from Same Test

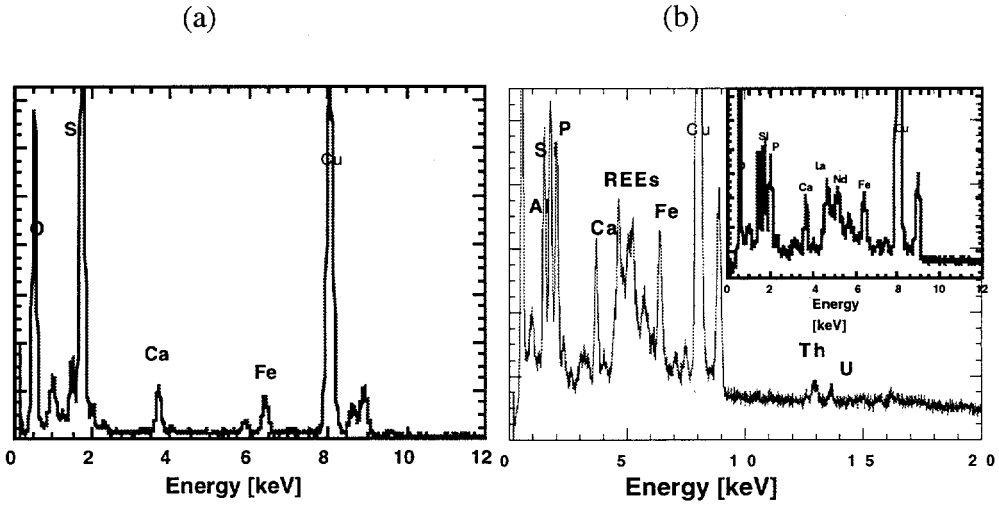

Fig. 54. (a) EDS Analysis of Clay Material from 200R Drip Test and (b) EDS Analysis of Rare Earth-Bearing Phase, Which Also Contains Trace Thorium and Uranium

This page intentionally left blank.

XI. CRITICAL REVIEW OF PARAMETERS AFFECTING GLASS REACTION IN AN UNSATURATED ENVIRONMENT

A. Introduction and Background

The repository environment at Yucca Mountain has been predicted by the YMP as being hydrologically unsaturated and having possible air exchange with the neighboring biosphere. Emplacement scenarios for the waste include both thermally "hot" and "cold" modes, which will affect the length of time the container remains dry, but which should not affect the ultimate waste/water contact modes. We have identified several environmental conditions that can affect the durability of waste emplaced in such an environment over repository-relevant time periods. To date, much of what is known about these conditions and their potential effect on glass corrosion has not been compiled for use by waste glass researchers, and we identified the need for such a critical review. That task is now underway.

During the projected repository lifetime, large amounts of liquid water are not expected to come into contact with the waste; however, water vapor or small volumes of transient water may contact the waste at any time during the emplacement. We have identified the amount of water contacting the glass waste to be a primary parameter affecting waste glass durability. Other identified primary parameters include the waste temperature, radiation fields, glass composition, and weathering of the glass to form alteration phases. Detailed critical reviews of how each of these parameters affects waste glass corrosion are part of this task, as is a review of models for evaluating waste performance.

B. Objectives

The purpose of the Critical Review Task is to review the existing literature to evaluate the state of knowledge regarding the influence of each of the identified critical parameters on glass reaction. Each review will be issued as a stand-alone document; they already have been integrated into a summary document, *High-Level Waste Borosilicate Glass: A Compendium of Corrosion Characteristics* [53], that was published in FY 1994. The results from this Task will be used to support start-up of the DWPF and WVDP and will provide input to the development of high-level waste forms for Hanford and for wastes at the Idaho National Engineering Laboratory (INEL).

C. Technical Approach

The technical approach for this task has been to assemble all known and pertinent sources of scientific literature on how each critical parameter affects nuclear waste glass reaction and to objectively and critically consider the current state of knowledge. We have included reviews and discussions regarding materials other than nuclear waste glasses when we considered it useful to relate waste glass reaction to the parameter being reviewed.

D. Results and Discussion

A preliminary critical review has already been performed to provide a foundation for subsequent detailed reviews of each parameter [98]. Reports have been issued on effects of temperature on waste glass performance [99], glass performance modeling [100], effects of radiation [101], and effects of waste glass composition [102].

The parameter reviewed during FY 1995 was the effects of S/V, as reported in *The Effects of the Glass Surface Area/Solution Volume Ratio on Glass Corrosion: A Critical Review* [28].

E. Future Studies

Reports are also being written to evaluate the effect of unsaturated conditions on glass reaction and the role of natural analogues in understanding long-term glass corrosion. These reports are undergoing review and revision and will be published in FY 1996.

In addition to critically reviewing the literature on selected parameters, we compiled Data Reports to present all of the data generated from the testing tasks of this program. These Data Reports may be included with the Critical Review reports, as was done for the S/V report, or may be issued as stand-alone documents. Data reports are being written on the testing of radioactive glasses and on radiation effects on glass reaction. These reports will be published in FY 1996.

ACKNOWLEDGMENTS

The authors gratefully acknowledge the contributions of Roberta Riel and Sy Vogler in providing quality assurance coordination and oversight to the program. Roberta Riel's contribution in preparing this report is also greatly appreciated. This report was improved by the careful and thorough technical editing of Jane Andrew.

This work is supported by the U.S. Department of Energy, Office of Environmental Management, under Contract W-31-109-ENG-38.

This page intentionally left blank.

REFERENCES

1. J. K. Bates, C. R. Bradley, J. P. Bradley, N. L. Dietz, W. L. Ebert, J. W. Emery, T. J. Gerding, J. C. Hoh, J. J. Mazer, and J. E. Young, *Unsaturated Glass Testing for DOE Program in Environmental Restoration and Waste Management, Annual Report, October 1989-September 1990*, Argonne National Laboratory Report ANL-90/40 (1991).

2. J. K. Bates, C. R. Bradley, W. L. Bourcier, E. C. Buck, J. C. Cunnane, N. L. Dietz, W. L. Ebert, J. W. Emery, R. C. Ewing, X. Feng, T. J. Gerding, M. Gong, W.-T. Han, J. C. Hoh, J. J. Mazer, L. E. Morgan, J. K. Nielsen, S. A. Steward, M. Tomozawa, L. M. Wang, and D. J. Wronkiewicz, *ANL Technical Support Program for DOE Environmental Restoration and Waste Management, Annual Report, October 1990-September 1991*, Argonne National Laboratory Report ANL-92/9 (1992).

3. J. K. Bates, W. L. Bourcier, C. R. Bradley, E. C. Buck, J. C. Cunnane, N. L. Dietz, W. L. Ebert, J. W. Emery, R. C. Ewing, X. Feng, T. J. Gerding, M. Gong, J. C. Hoh, H. Li, J. J. Mazer, L. E. Morgan, L. Newton, J. K. Nielsen, B. L. Phillips, M. Tomozawa, L. Wang, and D. J. Wronkiewicz, *ANL Technical Support Program for DOE Environmental Restoration and Waste Management, Annual Report, October 1991-September 1992*, Argonne National Laboratory Report ANL-93/13 (1993).

4. J. K. Bates, W. L. Bourcier, C. R. Bradley, N. R. Brown, E. C. Buck, S. A. Carroll, J. C. Cunnane, N. L. Dietz, T. DiSanto, W. L. Ebert, J. W. Emery, X. Feng, T. J. Gerding, M. Gong, L. D. Hafenrichter, J. C. Hoh, J. J. Mazer, L. Newton, B. L. Phillips, R. Pletcher, and D. J. Wronkiewicz, *ANL Technical Support Program for DOE Environmental Restoration and Waste Management, Annual Report, October 1992-September 1993*, Argonne National Laboratory Report ANL-94/19 (1994).

5. J. K. Bates, N. R. Brown, E. C. Buck, N. L. Dietz, T. DiSanto, W. L. Ebert, A. J. G. Ellison, J. W. Emery, J. A. Fortner, L. D. Hafenrichter, J. C. Hoh, J. J. Mazer, M. T. Surchik, S. F. Wolf, and D. J. Wronkiewicz, *ANL Technical Support Program for DOE Environmental Restoration and Waste Management, Annual Report, October 1993-September 1994*, Argonne National Laboratory Report ANL-95/20 (1995).

6. C. M. Jantzen, *Glass Compositions and Frit Formulations Developed for DWPF*, memo to M. J. Plodinec, Savannah River Laboratory Report DPST-88-952 (1988).

7. *Defense Waste Processing Facility Waste Form Compliance Plan*, Westinghouse Savannah River Company Report WSRC-SW4-6, Rev. 1A (1992).

8. C. M. Jantzen, N. E. Bibler, D. C. Beam, C. L. Crawford, and M. A. Pickett, *Characterization of the Defense Waste Processing Facility (DWPF) Environmental Assessment (EA) Glass Standard Reference Material*, Westinghouse Savannah River Company Report WSRC-TR-92-346, Rev. 1 (1993).

9. N. E. Bibler, Westinghouse Savannah River Company Report WSRC-TR-94-0505 (1994).

10. D. M. Strachan, W. L. Bourcier, and B. P. McGrail, "Towards a Consistent Model for Glass Dissolution," Radioactive Waste Mgmt. and Environ. Restoration 12, 129-145 (1994).

11. A. R. Hall, A. Hough, and J. A. C. Marples, *Leach Testing of Fully Active MW Glass*, Harwell Laboratory, United Kingdom Atomic Energy Authority Report AERE-R-13071 (1988).

12. L. Werme, I. K. Bjorner, G. Bart, H. U. Zwicky, B. Grambow, W. Lutze, R. C. Ewing, and C. Magrabi, "Chemical Corrosion of Highly Radioactive Borosilicate Nuclear Waste Glass under Simulated Repository Conditions," J. Mater. Res. 5, 1130 (1990).

13. *JSS-Project Phase II: Final Report of Work Performed at Studsvik Energiteknic AB and at Swiss Federal Institute for Reactor Research*, Japanese, Swiss, and Swedish Project Report JSS-85-01 (1985).

14. J. A. C. Marples, N. Godon, F. Lanza, and P. Van Iseghem, "Radionuclide Release from High-Level Waste Form under Repository Conditions in Clay or Granite," in *Radioactive Waste Management and Disposal*, L. Cecille, Ed., Elsevier, Amsterdam, pp. 287-301 (1991).

15. J. K. Bates, "Disposal of Vitrified Waste in an Unsaturated Environment," High-Level Radioactive Waste Management, Proc. 2nd Ann. Inter. Conf., 1, 700-707 (1991).

16. X. Feng and J. K. Bates, "Initial Comparison of Leach Behavior between Fully Radioactive and Simulated Waste Glass through Long-Term Testing, Part 1. Solution Analysis," Proc. Third Internat. Conf. on High-Level Radioactive Waste Manage., 925-933 (1992).

17. X. Feng, J. K. Bates, E. C. Buck, C. R. Bradley, and M. Gong, "Long-Term Comparison of Dissolution Behavior between Fully Radioactive and Simulated Waste Glasses," Nucl. Technol. 104, 193-206 (1993).

18. N. E. Bibler, "Leaching of Fully Radioactive SRP Nuclear Waste Glass in Tuff Ground Water in Stainless Steel Vessels," Adv. Ceram. 20, 619 (1986).

19. N. E. Bibler, G. G. Wicks, and V. M. Oversby, "Leaching Savannah River Plant Nuclear Waste Glass in a Saturated Tuff Environment," Mater. Res. Soc. Symp. Proc. 44, 247-256 (1985).

20. N. E. Bibler and J. K. Bates, "Product Consistency Leach Tests of Savannah River Site Radioactive Waste Glasses," Mater. Res. Soc. Symp. Proc. 176, 327-338 (1990).

21. N. E. Bibler and G. G. Wicks, *Leaching Savannah River Plant Nuclear Waste Glass in a Saturated Tuff Environment,* Lawrence Livermore National Laboratory Report UCRL-91258 (1984).

22. N. E. Bibler, "Characterization of Borosilicate Glass-Containing Savannah River Plant Radioactive Waste," Am. Chem. Soc. Symp. Ser. 246, 359-372 (1983).

23. J. K. Bates and T. J. Gerding, *One-Year Results of the NNWSI Unsaturated Test Procedure: SRL 165 Glass Application*, Argonne National Laboratory Report ANL-85-41 (1986).

24. J. K. Bates, T. A. Abrajano, Jr., D. J. Wronkiewicz, T. J. Gerding, and C. A. Seils, *Strategy for Experimental Validation of Waste Package Performance Assessment*, Argonne National Laboratory Report ANL-90/21 (1990).

25. G. W. Brindley, in *Crystal Structure of Clay Minerals and Their X-Ray Identification*, G. W. Brindley and G. Brown, Eds., Mineralogical Society, London, p. 170 (1980).

26. N. E. Bibler, W. F. Kinard, R. A. Dewberry, and C. J. Coleman, *A Method for the Determination of Waste Acceptance Radionuclides in DWPF Glass and Demonstration of that Method Using SRS Tank 51 Radioactive Sludge and Glass*, Westinghouse Savannah River Compnay Report WSRC-TR-94-0505 (1994).

27. M. K. Andrews and N. E. Bibler, "Radioactive Demonstration of DWPF Product Control Strategy," Ceram. Trans. 39, 205-221 (1993).

28. W. L. Ebert, *The Effects of the Glass Surface Area/Solution Volume Ratio on Glass Corrosion: A Critical Review*, Argonne National Laboratory Report ANL-94/34 (1994).

29. J. K. Bates, T. A. Abrajano, Jr., D. J. Wronkiewicz, T. J. Gerding, and C. A. Seils, *Strategy for Experimental Validation of Waste Package Performance Assessment*, Argonne National Laboratory Report ANL-90/21 (1990).

30. J. K. Bates and T. J. Gerding, *Application of the NNWSI Unsaturated Test Method to Actinide Doped SRL 165 Type Glass*, Argonne National Laboratory Report ANL-89/24 (1990).

31. J. I. Kim, W. Treiber, Ch. Lierse, and P. Offerman, "Solubility and Colloid Generation of Plutonium from Leaching of HLW Glass in Salt Solutions," Mater. Res. Soc. Symp. Proc. 44, 359-368 (1985).

32. J. K. Bates et al., *Annual Report to the Repository Technology Program*, submitted to the Repository Technology Program (1990).

33. "Test Method for Static Leaching of Monolithic Waste Forms for Disposal of Radioactive Waste," American Society for Testing and Material Standard C1220-92, Philadelphia, PA (1992).

34. "Standard Test Methods for Determining Chemical Durability of Nuclear Waste Glasses: The Product Consistency Test (PCT)," American Society for Testing and Materials Standard C1285-94, Philadelphia, PA (1994).

35. J. R. Fowler and M. J. Plodinec, "Projected Compositions and Radiogenic Properties of DWPF Glasses," Proc. of Third International High-Level Radioactive Waste Management (IHLRWM) Conference, Las Vegas, NV, Apr. 12-16, 1992, pp. 904-910 (1992).

36. J. K. Bates, W. L. Ebert, X. Feng, and W. L. Bourcier, "Issues Affecting the Prediction of Glass Reactivity in an Unsaturated Environment," J. Nucl. Mater. 190, 198-227 (1992).

37. W. L. Bourcier, W. L. Ebert, and X. Feng, "Modeling Surface Area to Volume Effects on Borosilicate Glass Dissolution," Mater. Res. Soc. Symp. Proc. 294, 577-582 (1993).

38. E. C. Buck, J. K. Bates, J. C. Cunnane, W. L. Ebert, X. Feng, and D. J. Wronkiewicz, "Analytical Electron Microscopy Study of Colloids from Nuclear Waste Glass Reaction," Mater. Res. Soc. Symp. Proc. 294, 199-206 (1993).

39. W. L. Ebert, J. K. Bates, E. C. Buck, M. Gong, and S. F. Wolf, "Disposition of Actinides Released From High-Level Waste Glass," Ceram. Trans. 45, 231-241 (1994).

40. W. L. Ebert, J. K. Bates, E. C. Buck, and C. R. Bradley, "Accelerated Glass Reaction Under PCT Conditions," Mater. Res. Soc. Symp. Proc. 294, 569-576 (1993).

41. W. L. Ebert, J. K. Bates, and E. C. Buck, "The Reaction of SRL 202 Glass in J-13 and DIW," Mater. Res. Soc. Symp. Proc. 294, 137-144 (1993).

42. W. L. Ebert, "The Effects of the Leachate pH and the Ratio of Glass Surface Area to Leachant Volume on Glass Reactions," Phys. Chem. Glasses 34(2), 58-65 (1993).

43. W. L. Ebert and J. K. Bates, "A Comparison of Glass Reaction at High and Low Surface Area to Volume," Nucl. Technol. 104(3), 372-384 (1993).

44. W. L. Ebert, J. K. Bates, C. R. Bradley, E. C. Buck, N. L. Dietz, and N. R. Brown, "The Long-Term Alteration of Borosilicate Waste Glasses," Ceram. Trans. 39, 333-340 (1993).

45. W. L. Ebert, *The Effects of the Glass Surface Area/Solution Volume Ratio on Glass Corrosion: A Critical Review*, Argonne National Laboratory Report ANL-94/34 (1994).

46. W. L. Ebert, J. K. Bates, E. C. Buck, M. Gong, and S. F. Wolf, "Disposition of Actinides Released from High-Level Waste Glass," Ceram. Trans. 45, 231-241 (1994).

47. W. L. Ebert, S. F. Wolf, and J. K. Bates, "The Release of Technetium from DWPF Glasses," presented at the 1995 Fall Meeting of the Materials Research Society, Boston, MA, November 27-December 1, 1995.

48. W. L. Ebert and J. K. Bates, "The Corrosion Behavior of DWPF Glasses," Ceram. Trans. 61, 479-488 (1995).

49. W. L. Ebert and D. M. Strachan, letter report to US DOE Richland Operations Office (1995).

50. K. G. Knauss, W. L. Bourcier, K. D. McKeegan, C. I. Merzbacher, S. N. Nguyen, F. J. Ryerson, D. K. Smith, and H. C. Weed, "Dissolution Kinetics of a Simple Analogue Nuclear Waste Glass as a Function of pH, Time, and Temperature," Mater. Res. Soc. Symp. Proc. 176, 371-381 (1990).

51. T. Advocat, J. L. Crovisier, E. Vernaz, G. Ehret, and H. Charpentier, "Hydrolysis of R7T7 Nuclear Waste Glass in Dilute Media: Mechanisms and Rate as a Function of pH," Mater. Res. Soc. Symp. Proc. 212, 57-64 (1991).

52. B. P. McGrail and D. K. Peeler, *Evaluation of the Single-Pass Flow-Through Test to Support a Low-Activity Waste Specification*, Pacific Northwest Laboratory Report PNL-10746 (1995).

53. J. C. Cunnane, Ed., *High-Level Waste Borosilicate Glass: A Compendium of Corrosion Characteristics*, U.S. Department of Energy Report DOE-EM-0177 (1994).

54. T. J. Wolery, *Calculation of Chemical Equilibrium between Aqueous Solutions and Minerals: The EQ3/6 Software Package*, Lawrence Livermore National Laboratory Report UCRL-52658 (1979).

55. L. R. Eisenstatt, *Description of the West Valley Demonstration Project Reference High-Level Waste Form and Canister*, U.S. Department of Energy Report DOE/NE/44139-26 (1986).

56. S. O. Bates, G. F. Piepel, and J. W. Johnston, *Leach Testing of Simulated Hanford Waste Vitrification Plant Reference Glass HW-39*, Pacific Northwest Laboratory Report PNL-6884 (1989).

57. B. Grambow, "A General Rate Equation for Nuclear Waste Glass Corrosion," Mater. Res. Soc. Symp. Proc. 44, 15-24 (1985).

58. Office of Environmental Restoration and Waste Management, *Waste Acceptance Product Specifications for Vitrified High-Level Waste Forms, Rev. 0*, U.S. DOE Document EM-WAPS, U.S. Department of Energy, Germantown, MD (1993).

59. S. L. Marra and M. J. Plodinec, *DWPF Waste Form Compliance Plan*, Westinghouse Savannah River Company Report WSRC-IM-91-116-0, Rev. 2 (1993).

60. S. L. Marra and M. J. Plodinec, *DWPF Glass Product Control Program*, Westinghouse Savannah River Company Report WSRC-IM-91-116-6, Rev. 0 (1992).

61. M. J. Plodinec and W. G. Ramsey, *Glass Consistency and Glass Performance*, Westinghouse Savannah River Company Report WSRC-MS-94-00311, p. 2 (1994).

62. T. A. Abrajano, J. K. Bates, and J. J. Mazer, "Aqueous Corrosion of Natural and Nuclear Waste Glasses. II. Mechanism of Vapor Hydration of Nuclear Waste Glasses," J. Non-Cryst. Sol. 108, 269-288 (1989).

63. J. K. Bates, M. G. Seitz, and M. J. Steindler, "The Relevance of Vapor Phase Hydration Aging to Nuclear Waste Isolation," Nucl. Waste Chem. Mgmt. 5, 63-73 (1984).

64. J. K. Bates, L. J. Jardine, and M. J. Steindler, *The Hydration Process of Nuclear Waste Glass: An Interim Report,* Argonne National Laboratory Report ANL-82/11 (1982).

65. J. K. Bates and T. J. Gerding, *NNWSI Phase II Materials Interaction Test Procedure and Preliminary Results*, Argonne National Laboratory Report ANL-84-81 (1984).

66. J. A. Fortner and J. K. Bates, "Long Term Test Results from Unsaturated Testing of Actinide-Doped DWPF and WVDP Waste Glasses," Mater. Res. Soc. Symp. Proc. 412, 205-211 (1996).

67. G. D. Maupin, W. M. Bowen, and J. L. Daniel, *Fabrication and Characterization of MCC Approved Testing Material– ATM-10 Glass*, Pacific Northwest Laboratory PNL-5577-10 (1988).

68. A. B. Woodland, J. K. Bates, and T. J. Gerding, *Parametric Effects on Glass Reaction in the Unsaturated Test Method*, Argonne National Laboratory Report ANL-91/36 (1991).

69. G. L. Kehl, *The Principles of Metallographic Laboratory Practice*, McGraw-Hill, NY, pp. 61-79 (1949).

70. J. A. Fortner, T. J. Gerding, and J. K. Bates, "Long-Term Test Results from a West Valley Actinide-Doped Reference Glass," Ceram. Trans. 61, 455-462 (1995).

71. *Mineral Powder Diffraction File, Group Data Book*, P. Bayliss, L. G. Berry, M. E. Mrose, A. P. Sabina, and D. K. Smith, eds., JCPDS, Swarthmore, PA and references therein (1983).

72. J. K. Bates, J. P. Bradley, A. Teetsov, C. R. Bradley, and M. Buchholtz ten Brink, "Colloid Formation during Waste Form Reaction: Implications for Nuclear Waste Disposal," Science 256, 649-651 (1992).

73. I. Friedman and W. Long, "Volcanic Glasses: Their Origins and Alteration Processes," J. Non-Cryst. Sol. 67, 127-133 (1984).

74. W. Lutze, G. Malow, R. C. Ewing, M. J. Jercinovic, and K. Keil, "Alteration of Basalt Glasses: Implications for Modelling the Long-Term Stability of Nuclear Waste Glasses," Nature 314(21), 252-255 (1985).

75. P. B. Adams, "Glass Corrosion. A Record of the Past? A Predictor of the Future?," J. Non-Cryst. Sol. 67, 193-206 (1984).

76. M. Morgenstein and P. Rosendahl, "Basaltic Glass Hydration Dating in Hawaiian Archaeology," in *Advances in Obsidian Glass Studies: Archaeological and Geochemical Perspectives,* R. E. Taylor, ed., Noyes Press, Park Ridge, NJ, pp. 141-164 (1976).

77. B. Grambow, M. J. Jercinovic, R. C. Ewing, and C. D. Byers, "Weathered Basalt Glass: A Natural Analogue for the Effects of Reaction Progress on Nuclear Waste Glass Alteration," Mater. Res. Soc. Symp. Proc. 50, 263-272 (1985).

78. J. L. Crovisier, J. Honnorez, B. Fritz, and J.-C. Petit, "Dissolution of Subglacial Volcanic Flasses from Iceland: Laboratory Study and Modeling," Appl. Geochem. 1992, Suppl. Issue No. 1, pp. 57-64 (1992).

79. T. A. Abrajano, J. K. Bates, and C. D. Byers, "Aqueous Corrosion of Natural and Nuclear Waste Glasses. I. Comparative Rates of Hydration in Liquid and Vapor Environments at Elevated Temperatures," J. Non-Cryst. Sol. 84, 251-257 (1986).

80. C. D. Byers, M. J. Jercinovic, and R. C. Ewing, *A Study of Natural Glass Analogues as Applied to Alteration of Nuclear Waste Glass*, Argonne National Laboratory Report ANL-84-46 (1984).

81. J. J. Mazer, "The Role of Natural Glasses as Analogues in Projecting the Long-Term Alteration of High-Level Nuclear Waste Glasses: Part 1," Mater. Res. Soc. Symp. Proc. 333, 159-165 (1994).

82. J. J. Mazer, J. K. Bates, C. M. Stevenson, and C. R. Bradley, "Obsidians and Tektites: Natural Analogues for Water Diffusion in Nuclear Waste Glasses," Mater. Res. Soc. Symp. Proc. 257, 513-520 (1992).

83. T. A. Abrajano, J. K. Bates, A. B. Woodland, J. P. Bradley, and W. L. Bourcier, "Secondary Phase Formation during Nuclear Waste-Glass Dissolution," Clays and Clay Miner. 38(5), 537-548 (1990).

84. C. D. Byers, M. J. Jercinovic, R. C. Ewing, and K. Keil, "Basalt Glass: An Analogue for the Evaluation of the Long-Term Stability of Nuclear Waste Form Borosilicate Glasses," Mater. Res. Soc. Symp. Proc. 44, 583-590 (1985).

85. C. D. Byers, R. C. Ewing, and M. J. Jercinovic, "Experimental Alteration of Basalt Glass Applied to the Alteration of Nuclear Waste Glass," Adv. Ceram. 20, 733-744 (1986).

86. X. Feng, E. C. Buck, J. K. Bates, C. Mertz, J. C. Cunnane, and D. Chaiko, "Colloid Formation during Nuclear Waste Glass Dissolution," Radiochim. Acta 66/67, 197-205 (1994).

87. B. T. Thole, G. van der Laan, J. C. Fuggle, G. A. Swatzky, R. C. Karnatak, and J.-M. Esteva, Physical Review B32, 5107-5118 (1985).

88. J. A. Fortner, Argonne National Laboratory, private communication (1996).

89. A. Pabst, "X-Ray Crystallography of Davidite," Am. Miner. 46, 700-718 (1961).

90. Y. Liu and P. Comodi, "Some Aspects of the Crystal-Chemistry of Apatites," Miner. Mag. 57, 709-719 (1993).

91. F. G. Fisher and R. Meyrowitz, "Brockite, A New Calcium Thorium Phosphate from the Wet Mountains, CO," Amer. Miner. 47, 1346-1355 (1992).

92. F. V. Stohl and D. K. Smith, "The Crystal Chemistry of the Uranyl Silicate Minerals," Am. Miner. 66, 610-624 (1981).

93. C. J. Chisholm-Brause, S. D. Conradson, P. G. Eller, and D. E. Morris, "Changes in U(VI) Speciation Upon Sorption onto Montmorillonite from Aqueous and Organic Solutions," Mater. Res. Soc. Symp. Proc. 257, 315-322 (1992).

94. H. van Olphen, *Clay Colloid Chemistry,* John Wiley & Sons, New York, pp. 92-108 (1977).

95. J. F. McCarthy and J. M. Zachara, "Subsurface Transport of Contaminants," Environ. Sci. Technol. 23, 496-502 (1989).

96. I. R. Triay, A. Simmons, S. Levy, S. Nelson, H. Nuttall, B. Robinson, W. Steinkampf, and B. Viani, *Colloid-Facilitated Radionuclide Transport at Yucca Mountain*, Los Alamos National Laboratory Report LA-12779-MS (1995).

97. J. K. Bates and E. C. Buck, "Waste Glass Weathering," Mater. Res. Soc. Symp. Proc. 333, 41-47 (1994).

98. J. K. Bates, T. A. Abrajano, Jr., B. M. Biwer, C. R. Bradley, W. L. Ebert, J. J. Mazer, D. J. Wronkiewicz, and J. E. Young, *Critical Review of Parameters Affecting Glass Reaction in an Unsaturated Environment*, internal review to DOE-CH (1991).

99. J. J. Mazer, *Temperature Effects on Waste Glass Performance*, Argonne National Laboratory Report ANL-91/17 (1991).

100. W. L. Bourcier, *Critical Review of Glass Performance Modeling*, Argonne National Laboratory Report ANL-94/17 (1994).

101. D. J. Wronkiewicz, *Effects of Radionuclide Decay on Waste Glass Behavior - A Critical Review*, Argonne National Laboratory Report ANL-93/45 (1994).

102. A. J. G. Ellison, J. J. Mazer, and W. L. Ebert, *Effect of Glass Composition on Waste Form Durability: A Critical Review*, Argonne National Laboratory Report ANL-94/28 (1994).

APPENDIX A. ESTIMATED LOSS OF SURFACE AREA BASED ON BORON RELEASE

An expression for the loss of surface area during glass dissolution is derived assuming the glass grains are spherical particles having an initial diameter equal to the average mesh opening.

In this expression, d_i is the initial diameter of the spherical particle, and ρ is the glass density.

The initial surface area of each particle is

$$S_i = \pi d_i^2 \tag{A-1}$$

For N particles in a test, the total initial surface area is

$$S_i = \pi N d_i^2 \tag{A-2}$$

The initial volume of N particles is

$$V_i = \left(\frac{N \pi d_i^3}{6} \right) \tag{A-3}$$

The initial mass of N particles in a test is

$$m_o = V\rho = \left(\frac{N \rho \pi d_i^3}{6} \right) \tag{A-4}$$

The mass of N particles in a test at a time t is

$$m_t = \left(\frac{N \rho \pi d_t^3}{6} \right) \tag{A-5}$$

The total surface area in a test at a time t is

$$S_t = \pi N d_t^2 \tag{A-6}$$

Solving Eq. A-4 for N and solving Eq. A-5 for d_t^2 then substituting into Eq. A-6 gives an expression for the total surface area at time t based on mass and the initial particle radius.

Solving Eq. A-4 for N:

$$N = \frac{6 m_o}{\rho \pi d_i^3} \tag{A-7}$$

Solving Eq. A-5 for d_t^2:

$$d_t^2 = \left\{ \frac{6 m_t}{\pi \rho N} \right\}^{2/3} \tag{A-8}$$

Substituting Eq. A-7 and Eq. A-8 into Eq. A-6:

$$S_t = \frac{\left(6\, m_o^{1/3}\, m_t^{2/3}\right)}{\left(\rho d_i\right)} \tag{A-9}$$

The values of ρ, m_o, and d_i are known and m_t can be calculated from test results as

$$m_t = m_o - \frac{m_B}{f_B} \tag{A-10}$$

where m_B is the mass of B released to solution and f_B is the mass fraction of B in the glass. (The solution concentration of B usually provides the best measure of the extent of glass dissolution, since B is usually not incorporated into alteration phases.) Equation A-9 can be rewritten as

$$S_t = \frac{\left(6 m_o^{1/3} \left(m_o - \frac{m_B}{f_B} \right)^{2/3} \right)}{\left(\rho d_i\right)} \tag{A-11}$$

This is the surface area of the remaining glass. The loss of surface area can be calculated as S_i-S_t.

Distribution for ANL-96/11

Internal:

A. J. Bakel
J. K. Bates (20)
E. C. Buck
J. C. Cunnane
N. L. Dietz
T. DiSanto
W. L. Ebert
J. W. Emery
P. A. Finn
J. Fortner
L. D. Hafenrichter
J. E. Harmon
J. C. Hoh
T. R. Johnson
J. J. Laidler
J. S. Luo
C. J. Mertz
L. Nuñez
R. T. Riel
M. J. Steindler
D. M. Strachan
M. T. Surchik
C. E. Till
S. Vogler
S. F. Wolf
D. J. Wronkiewicz
TIS Files

External:

DOE-OSTI (2)
ANL-E Library
ANL-W Library
Manager, Chicago Operations Office, DOE
A. Bindokas, DOE-CH
J. Haugen, DOE-CH
Chemical Technology Division Review Committee Members:
- H. U. Anderson, University of Missouri-Rolla, Rolla, MO
- E. R. Beaver, Monsanto Company, St. Louis, MO
- D. L. Douglas, Consultant, Bloomington, MN
- R. K. Genung, Oak Ridge National Laboratory, Oak Ridge, TN
- J. G. Kay, Drexel University, Philadelphia, PA
- R. A. Osteryoung, North Carolina State University, Raleigh, NC
- G. R. St. Pierre, Ohio State University, Columbus, OH

J. Allison, Westinghouse Savannah River Company, Aiken, SC
N. E. Bibler, Westinghouse Savannah River Company, Aiken, SC
W. Bourcier, Lawrence Livermore National Laboratory, Livermore, CA
K. A. Chacey, USDOE, Office of Environmental Management, Germantown, MD
M. O. Cloninger, Mac Technical Services, Inc., Richland, WA
S. P. Cowan, USDOE, Office of Waste Management, Germantown, MD
P. Dirkmaat, USDOE, Idaho Operations Office, Idaho Falls, ID
R. S. Dyer, Yucca Mountain Project Office, Las Vegas, NV
R. E. Erickson, USDOE, Office of Environmental Management, Germantown, MD
R. C. Ewing, University of New Mexico, Albuquerque, NM
R. Fish, B&W Fuel Company, Las Vegas, NV
C. W. Frank, USDOE, Office of Science and Technology, Washington, DC
T. J. Gerding, Plainfield, IL
C. Interrante, U. S. Nuclear Regulatory Commission, Washington, DC
V. J. Jain, West Valley Nuclear Services, West Valley, NY

C. Jantzen, Westinghouse Savannah River Company, Aiken, SC
L. J. Jardine, Lawrence Livermore National Laboratory, Livermore, CA
W. S. Ketola, USDOE, West Valley Project Office, West Valley, NY
D. A. Knecht, Lockheed Idaho Technology Company, Idaho Falls, ID
J. Kolts, USDOE, Idaho Operations Office, Idaho Falls, ID
J. H. Lee, Intera, Las Vegas, NV
H. H. Loo, Lockheed Idaho Technology Company, Idaho Falls, ID
W. Lutze, University of New Mexico, Albuquerque, NM
J. M. Matuszek, JMM Consulting, Del Mar, NY
P. K. Nair, Southwest Research Institute, San Antonio, TX
R. Palmer, West Valley Nuclear Services, West Valley, NY
E. C. Pearcy, Southwest Research Institute, San Antonio, TX
W. G. Ramsey, Westinghouse Savannah River Company, Aiken, SC
R. Ramsey, USDOE, Office of Environmental Management, Washington, DC
C. G. Russomanno, USDOE, Office of Civilian Radioactive Waste Management, Washington, DC
A. Simmons, USDOE, Las Vegas, NV
J. Sproull, Westinghouse Savannah River Company, Aiken, SC
D. Stahl, M&O/B&W Fuel Company, Las Vegas, NV
R. B. Stout, Lawrence Livermore National Laboratory, Livermore, CA
M. Tomozawa, Rensselaer Polytechnic Institute, Troy, NY
J. C. Tseng, USDOE, Office of Environmental Management, Germantown, MD
T. Wichmann, USDOE, Idaho Operations Office, Idaho Falls, ID
B. Grambow, Kernforschungszentrum Karlsruhe, GERMANY
L. Johnson, Atomic Energy of Canada, Ltd., Pinawa, Manitoba, CANADA
J. Kim, Kernforschungszentrum Karlsruhe, GERMANY
P. Van Iseghem, Boeretang, BELGIUM
E. Vernaz, Centre d'Etudes Nucleares de la Valle du Rhone, Marcoule, FRANCE
L. Werme, Svensk Karnbranslehantering AB, Stockholm, SWEDEN